

**What do we know about the quark gluon plasma
from lattice gauge theory ?**

E.-M. Ilgenfritz

Veksler-Baldin LHEP, JINR Dubna

The 7th APCTP-BLTP JINR Joint Workshop
“Modern problems in nuclear and elementary particle physics”

July 14 - 19, Bolshye Koty, Irkutsk region, Russia

Outline :

1. Intro : Let the system tell the difference between the phases
2. Lattice formulation for QCD thermodynamics : some basic facts
3. The order parameters of two abstract phase structure problems
4. Searching for a transition along a line in the phase diagram
5. Phase transition and thermodynamics of twisted-mass fermions
6. A special aspect : Gluon and ghost propagators in Landau gauge
7. Scanning the full phase diagram : Finite baryonic density
8. Deep inside the phase diagram : Properties of dense matter
9. Outlook

1. Intro : Let the system tell the difference between the phases

Start from a fundamental theory that covers all phases !

We believe that this is **Quantum Chromodynamics**.

No other *a priori* knowledge should be necessary.

If we knew the relevant **Hilbert space** (which is expected to be **different in different parts of the phase diagram**), thermodynamics would be derived from thermal density matrix or partition function:

$$\rho = \exp^{-\frac{1}{T}(H - \mu_i N_i)}, \quad Z = \hat{\text{Tr}}\rho, \quad \hat{\text{Tr}}(\dots) = \sum_n \langle n | (\dots) | n \rangle$$

μ_i are chemical potentials for some conserved charges N_i

The quantum mechanical trace is a sum over an Hilbert space, e. g. over the colorblue *a priori* unknown energy eigenstates $|n\rangle$ of the Hamiltonian (**no matter whether they are single or many-particle eigenstates !**).

If we knew the partition function $Z(T, \mu_i)$, we could obtain

$$\begin{aligned}
 F &= -T \ln Z, & \bar{N}_i &= \frac{\partial(T \ln Z)}{\partial \mu_i} \\
 p &= \frac{\partial(T \ln Z)}{\partial V}, & E &= -pV + TS + \mu_i \bar{N}_i \\
 S &= \frac{\partial(T \ln Z)}{\partial T},
 \end{aligned}$$

Since the free energy is extensive, $F = fV$, in the thermodynamic limit it is more convenient to deal with the corresponding densities:

$$f = \frac{F}{V}, \quad p = -f, \quad s = \frac{S}{V}, \quad n_i = \frac{\bar{N}_i}{V}, \quad \epsilon = \frac{E}{V}$$

In particular, **pressure p and energy density ϵ** define together the trace anomaly, the entropy density, and the velocity of sound :

$$I(T) = T^{\mu\mu}(T) = T^5 \frac{\partial p(T)}{\partial T T^4} = \epsilon - 3p, \quad s = \frac{\epsilon + p}{T}, \quad c_s^2 = \frac{dp}{d\epsilon}$$

Since we do not know the **eigenstates (even not qualitatively !)**, we better use a formulation that does not presuppose that knowledge.

We believe to know the fundamental theory: take the **path integral over the fundamental fields (no matter whether they are confined or can be represented – asymptotically – as free particles !)**.

Neither quarks nor gluons are “physical” particles in this sense !

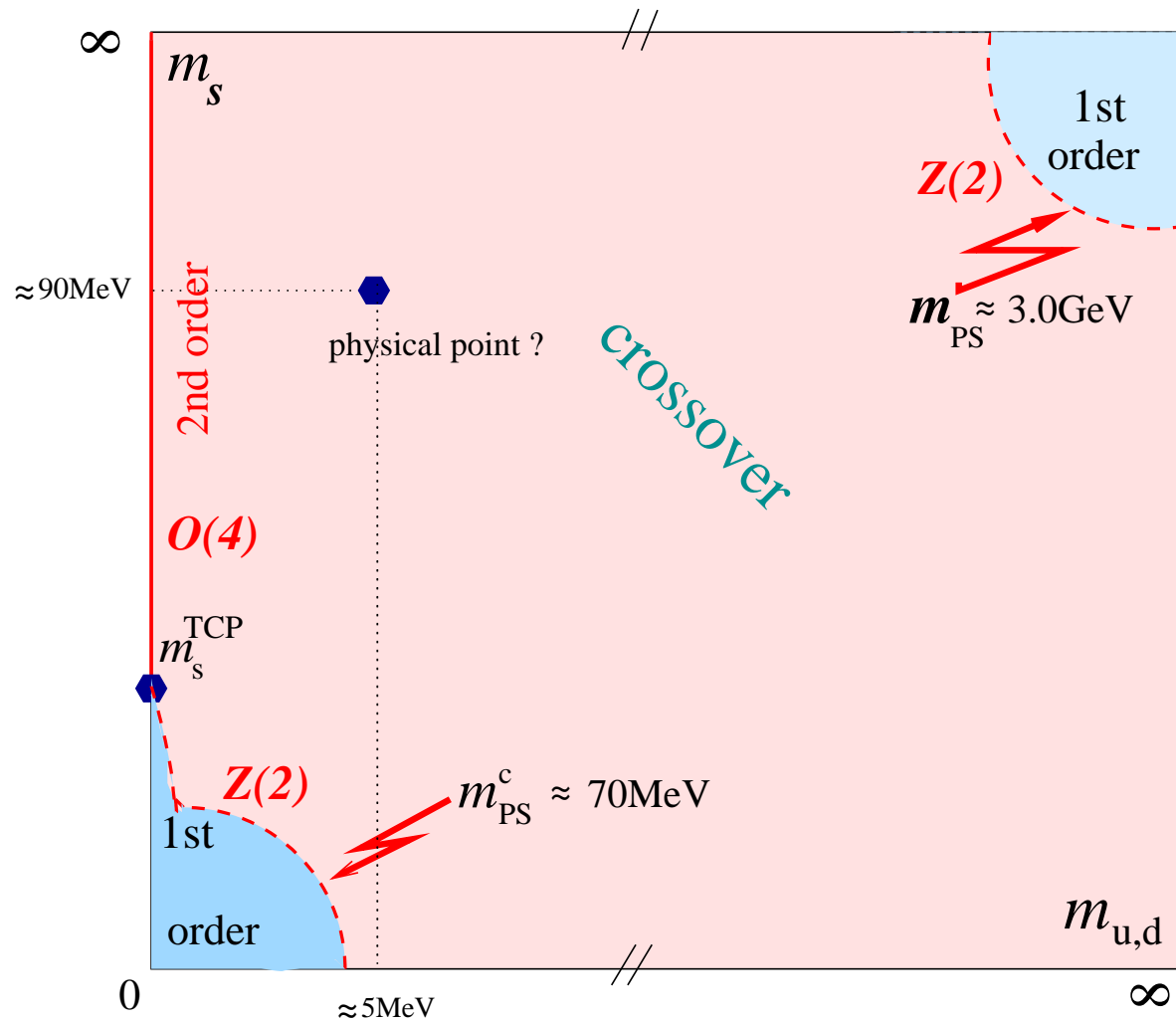
Their **lattice propagators** show it : **violation of spectral positivity !**

Analytical properties are **harder to extract** from lattice simulations.

Then, let's see in a simulation which phase is actually realized !

- **Thermodynamic functions** can witness only the sudden changes accompanying phase changes, cannot show structural details !
- To recognize structural changes, other observables are necessary (signals of symmetry breaking): **order parameters**.
- **Correlators are more general indicators of phase changes.**
Lifting a splitting between correlation lengths (masses) also may signal the restoration of symmetries.
- Change of **topological structure characterizes the different phases**.
- All symmetry-related signals will become **clearly visible only** in the corresponding limit $m_q \rightarrow \infty$ (**tantamount to gluodynamics**) or in the limit $m_q \rightarrow 0$ (**chiral limit of QCD**), not in real QCD !

The QCD transition at $\mu = 0$ as function of quark masses
 (Columbia plot) from arXiv:1203.5320 Petreczky



Some words about path integrals and partition functions :

If interactions are switched off (quadratic action), both for $T = 0$ and $T > 0$, a **path integral** can be presented in a more familiar form :

$$Z_0 = N \int D\phi e^{-S_0(\phi)} = N'(\det \Delta^{-1})^{-1/2}$$

$\Delta^{-1} = (\omega_n^2 + \omega^2)/T^2$ is the inverse propagator in momentum space.

This leads to the **more familiar expression** :

$$\lim_{V \rightarrow \infty} \ln Z_0 = V \int \frac{d^3p}{(2\pi)^3} \left[\frac{-\omega}{2T} - \ln \left(1 - e^{-\frac{\omega}{T}} \right) \right]$$

The integral over the first term diverges in the UV since $\omega \sim |\mathbf{p}|$.

Invoke the **renormalisation condition** : vacuum has zero pressure

$$p_{\text{phys}}(T) = p(T) - p(T = 0)$$

Partition function for a free gas of spinless bosons

$$\ln Z_0 = -V \int \frac{d^3p}{(2\pi)^3} \ln \left(1 - e^{-\frac{\omega}{T}} \right)$$

For the $m = 0$ case, the momentum integral can be done exactly.

Pressure per bosonic degree of freedom (no chemical potential, $\mu = 0$)

$$p = \frac{\pi^2}{90} T^4$$

For **non-abelian gauge fields** A_μ^a , each field component corresponds to one bosonic mode, i.e. sum over $a = 1, \dots, N^2 - 1$ and $\mu = 1 \dots 4$. This yields a **factor of** $4(N^2 - 1)$.

For gauge theories **gauge fixing is necessary** in order to invert the two-point function. For the free photon or Yang-Mills gas, two of the four bosonic Lorentz degrees of freedom get **cancelled by the corresponding ghost contributions**.

Thus a **factor of** $2(N^2 - 1)$ instead of $4(N^2 - 1)$ (with two polarisation states per massless vector particle) results.

Similar steps for a free Dirac field lead to the result

$$\ln Z_0 = 2V \int \frac{d^3p}{(2\pi)^3} \left[\ln \left(1 + e^{-\frac{\omega-\mu}{T}} \right) + \log \left(1 + e^{-\frac{\omega+\mu}{T}} \right) \right]$$

Factor of two : represents the **two spin states** of a fermion.

The two log-terms (with $\pm\mu$) are coming from **fermion and anti-fermion**.

Momentum integration for **one massless fermionic degree of freedom** (with $\mu = 0$) gives the **fermionic pressure per d.o.f.**

$$p = \frac{7\pi^2}{890} T^4$$

Stefan-Boltzmann pressure of N_f flavors of quarks and antiquarks (counting their N colors) plus corresponding gluons :

$$\frac{p}{T^4} = \left(2(N^2 - 1) + 4NN_f \frac{7}{8} \right) \frac{\pi^2}{90}$$

This can be summarised by the one-particle partition functions for arbitrary masses m_i ($\omega_i^2 = m_i^2 + \vec{p}^2$)

$$\ln Z_i^1(V, T) = \eta V \nu_i \int \frac{d^3p}{(2\pi)^3} \ln(1 + \eta e^{-(\omega_i - \mu_i)/T})$$

$\eta = -1$ for bosons and $\eta = 1$ for fermions, while ν_i gives the degree of degeneracy (spin) for the particle of type i .

The general form of $\ln Z_i^1(V, T)$ is applicable also for non-interacting (composite) particles, if and only if there are no internal d. o. f.

Hadron Gas Model (HG model, applicable for the confined phase) :

The general form of $\ln Z_i^1(V, T)$ is applicable also for non-interacting hadrons, **mesons = bosons and (anti-)baryons = fermions.**

The confinement phase is **interpreted as gas of individual hadrons.**

This is reasonable **as long as the energy density is not very high.**

The **deconfinement transition** then seems to be **not more** than a **sudden proliferation of degrees of freedom** at some temperature T_{dec} .

These new d.o.f. **remain “frozen” in the confinement phase** (i.e. quarks inside hadrons, gluons in glueballs/usual hadrons).

Freezing (confinement) and deconfinement **cannot be “explained” just by these thermodynamic formulae.**

The “bag pressure” B is merely a trick to make the two pressure functions (hadron gas vs. quark-gluon gas) intersecting at some T_{dec} , by downshifting of the steeper one (first order transition) :

$$p_{\text{hadron}}(T_{\text{dec}}) = p_{\text{plasma}}(T_{\text{dec}}) - B .$$

Hadron Resonance Gas Model (HRG model) :

This is an attempt to take into account the **interactions between hadrons, increasing with increasing density**, by including more (and more massive) resonance states in the sum over $\ln Z_i^1(V, T)$ (including Particle Data Group table states up to ≈ 2 GeV).

The model **describes reasonably well the onset of the phase transition from the hadronic side** (by an increasing number of effective degrees of freedom, of hadron species becoming “active”).

Hagedorn model :

exponential mass spectrum \rightarrow “maximal” hadronic temperature at singularities of the partition function:

such a spectrum was enforced by the selfconsistent “strong bootstrap” condition formulated by S. C. Frautschi in 1971

- “Statistical bootstrap model of hadrons”,
S. C. Frautschi, Phys. Rev. D3 (1971) 2821

replacing the earlier weak bootstrap condition of R. Hagedorn

- “Hadronic matter near the boiling point”,
R. Hagedorn, Nuovo Cim. A56 (1968) 1027

Alternative : instead of a maximal temperature, quark liberation !

Two important papers in 1975 : high temperature and high density

- “Exponential Hadronic Spectrum and Quark Liberation”,
N. Cabibbo and G. Parisi, Phys. Lett. B59 (1975) 67
- “Superdense Matter: Neutrons or Asymptotically Free Quarks?”,
John C. Collins and M.J. Perry, Phys. Rev. Lett. 34 (1975) 1353

Before this, Lattice Gauge Theory was invented in 1974 :

- “Confinement of Quarks”,
Kenneth G. Wilson, Phys. Rev. D10 (1974) 2445

Both developments demonstrate the “new thinking” after the
“November Revolution” (the J/ψ discovery) !

Application of LGT to the QCD transition :

The first real prediction of LGT : the **deconfinement transition**

- “A Monte Carlo Study of SU(2) Yang-Mills Theory at Finite Temperature”, L. D. McLerran and B. Svetitsky, Phys. Lett. B98 (1981) 195
- “Monte Carlo Study of SU(2) Gauge Theory at Finite Temperature”, J. Kuti, J. Polonyi, and K. Szlachanyi, Phys. Lett. B98 (1981) 199

Both discover deconfinement in the sense of center symmetry breaking (to be described later).

The first lattice publications from Dubna have been following soon :

- “SU(3) Gluon Condensate from Lattice MC Data”,
E.-M. Ilgenfritz and M. Müller-Preussker,
Phys. Lett. B119 (1982) 395
- “The Static Q Anti-Q Force from Instanton Gas and
Numerical Lattice Calculations”, E.-M. Ilgenfritz and
M. Müller-Preussker, Z. f. Phys. C16 (1983) 339
- “Phase Transitions in the Euclidean and Hamiltonian
Approaches in the Lattice Gauge Theories at Finite
Temperature”, V.P. Gerdt and V.K. Mitrjushkin,
JETP Lett. 37 (1983) 474

Especially encouraged by D. V. Shirkov and M. G. Meshcheryakov

2. Lattice formulation for QCD thermodynamics : some basic facts

Path integral expression for the partition function :

$$Z(V, \mu_f, T; g, m_f) = \hat{\text{Tr}} \left(e^{-(H - \mu_f Q_f)/T} \right) = \int DA D\bar{\psi} D\psi e^{-S_g[A_\mu]} e^{-S_f[\bar{\psi}, \psi, A_\mu]}$$

Euclidean formulation natural, not just a **trick (Wick rotation)**
to avoid the oscillating weight in Minkowski space (works for $\mu = 0$) !

Euclidean gauge and fermion actions :

$$S_g[A_\mu] = \int_0^{1/T} d\tau \int_V d^3x \frac{1}{2} \text{Tr} F_{\mu\nu}(x) F_{\mu\nu}(x),$$
$$S_f[\bar{\psi}, \psi, A_\mu] = \int_0^{1/T} d\tau \int_V d^3x \sum_{f=1}^{N_f} \bar{\psi}_f(x) (\gamma_\mu D_\mu + m_f - \mu_f \gamma_0) \psi_f(x)$$

Covariant derivative with A_μ field and gauge coupling g

$$D_\mu = (\partial_\mu - igA_\mu), \quad A_\mu = T^a A_\mu^a(x), \quad a = 1, \dots, N^2 - 1$$

Field strength, non-linear in A_μ (non-Abelian)

$$F_{\mu\nu}(x) = \frac{i}{g}[D_\mu, D_\nu] = \partial_\mu A_\nu - \partial_\nu A_\mu - ig[A_\mu, A_\nu]$$

Bosonic (commuting “c-numbers”) and **fermionic fields** (anticommuting, defined by Grassmann calculus) have **different temporal boundary conditions over the finite “time” interval of length $1/T$:**

$$A_\mu(\tau, \mathbf{x}) = A_\mu(\tau + \frac{1}{T}, \mathbf{x}), \quad \psi_f(\tau, \mathbf{x}) = -\psi_f(\tau + \frac{1}{T}, \mathbf{x})$$

In a finite volume $V = L^3$ and at temperature T

- allowed spatial momenta are $p_\mu = (2n_\mu\pi)/L$ for $\mu = 1, 2, 3$
- allowed “Matsubara” frequencies are
 $\omega = 2n_4\pi T$ for bosons (gluons) with periodic boundary conditions
 $\omega = (2n_4 + 1)\pi T$ for fermions (quarks) with antiperiodic b. c.

By discretizing space and time, a lattice $N_s^3 \times N_t$ is replacing the continuum, making it suitable for numerical simulation.

$$n_\mu = 0, \dots, N_s - 1 \text{ and } n_4 = 0, \dots, N_t - 1$$

The lattice spacing a relates this to the continuum box :

$$L = N_s a \quad V = L^3 \quad \text{and} \quad \frac{1}{T} = N_t a$$

What replaces the gluon field $A_\mu(x)$?

Fundamental degrees of freedom are links (“transporters”) between neighboring lattice sites :

$$U_\mu(x) = P \exp \left(\int_0^1 i a d\lambda A_\mu(x + (1 - \lambda)\hat{\mu}) \right)$$

The standard Wilson gauge action in terms of links

$$S_g[U] = \sum_x \sum_{1 \leq \mu < \nu \leq 4} \beta \left(1 - \frac{1}{3} \text{ReTr} U_p \right)$$

is expressed via elementary plaquettes (discrete version of curl !)

$$U_p = U_\mu(x) U_\nu(x + a\hat{\mu}) U_\mu^\dagger(x + a\hat{\nu}) U_\nu^\dagger(x)$$

β replaces the gauge coupling g through $\beta = 2N/g^2$.

The relation between a and β is set by **renormalisation group** :

$$a\Lambda_L = \left(\frac{6 b_0}{\beta}\right)^{-b_1/2b_0^2} e^{-\frac{\beta}{12b_0}}, \quad \text{for } N = 3 \text{ colors}$$

$$b_0 = \frac{1}{16\pi^2} \left(11 - \frac{2}{3}N_f\right), \quad b_1 = \left(\frac{1}{16\pi^2}\right)^2 \left[102 - \left(10 + \frac{2}{3}\right)N_f\right]$$

Λ_L characterizes the kind of lattice actions (mainly gluonic action).

Deviations from this “two-loop asymptotic scaling” formula

(are unavoidable at low β) can be fixed by ***ad hoc* calibration**

simulations at $T = 0$ (i.e. $N_s \leq N_t$), which are necessary to obtain

the function $a(\beta)$, by fixing either ...

Find the function $a(\beta)$ by fixing ...

- ... either the “**Sommer scale**” r_0 or its variant r_1 defined by

$$\left(r^2 \frac{dV_{\bar{Q}Q}(r)}{dr} \right)_{r=r_0} = 1.65 \quad \left(r^2 \frac{dV_{\bar{Q}Q}(r)}{dr} \right)_{r=r_1} = 1.00$$

to a generally agreed physical value, say $r_0 \approx 0.48$ fm.

- ... or a **measured vector meson mass**, say m_ρ , to the physical value.
- For most settings, the **measured pseudoscalar masses** m_π **etc.** then differ strongly from the physical values !
- The **ratio** m_π/m_ρ is an *a posteriori* **measure of quality**, describing how good the simulation approaches physical QCD.

- The simulation time behaves

$$\text{CPU time} \propto (N_s^3 N_t)^{\frac{5}{4}} \left(\frac{r_0}{a}\right)^7 \left(\frac{m_\rho}{m_\pi}\right)^{z_\pi}$$

with high exponent $z_\pi \approx 6$, the “Berlin wall” behavior !

- The limit $m_\pi \rightarrow m_\pi^{\text{physical}}$ is extremely costly !
Chiral perturbation theory (χ PT) may do the extrapolation.
- For all finite-temperature studies it is important to **record the would-be pion mass m_π to characterize the setting in use !**
- Typically, **many sets of simulations are done, with varying m_π ,** in order to get the corresponding crossover/transition temperatures T_χ and to find a suitable **chiral extrapolation.**

Hamiltonian and transfer matrix :

The definition of **transfer matrix in “coordinate U_i representation”**

$$T[U_i(\tau + 1), U_i(\tau)] = e^{-aH} = \int DU_0(\tau) \exp(-L[U_i(\tau + 1), U_0(\tau), U_i(\tau)])$$

includes the **integration over all timelike links linking 2 time slices.**

$$S_g = \sum_{\tau} L[U_i(\tau + 1), U_0(\tau), U_i(\tau)]$$

with

$$L[U_i(\tau + 1), U_0(\tau), U_i(\tau)] = \frac{1}{2}L_1[U_i(\tau + 1)] + L_2[U_i(\tau + 1), U_0(\tau), U_i(\tau)] \\ + \frac{1}{2}L_1[U_i(\tau)]$$

$$L_1[U_i(\tau)] = -\frac{\beta}{N} \sum_{p(\text{fixed } \tau)} \text{ReTr}U_p \quad (\text{spacelike at a single time})$$

$$L_2[U_i(\tau + 1), U_0(\tau), U_i(\tau)] = -\frac{\beta}{N} \sum_{p(\text{linking } \tau, \tau+1)} \text{ReTr}U_p \quad (\text{timelike only})$$

Partition function expressed as “matrix product” by multiple integration over spacelike links U_i (located within time slices) :

$$Z = \int \prod_{\tau} (DU_i(\tau, \mathbf{x}) T[U_i(\tau + 1), U_i(\tau)]) = \hat{\text{Tr}}(T^{N_{\tau}}) = \hat{\text{Tr}}(e^{-N_{\tau}aH})$$

A time slice $\{U_i(\tau)\}$ encodes **all possible states of the Hilbert space**. Importance sampling exhibits the differences between phases. Vanishing overlap between the Hilbert spaces in the limit $V \rightarrow \infty$?

Qualitative changes are physically recognizable (not only !) in equal-time correlators !

For Z , taking the trace, i.e. periodicity, requires :

$$U_i(\tau = 1) = U_i(\tau = N_{\tau} + 1)$$

Including “dynamical fermions” means inclusion of a bilinear fermion action in terms of Grassmann fields (interacting only through the gauge field !)

$$S_f = \sum_{x,y} \bar{\psi}(x) D_{xy}^f(\{U\}; m_f) \psi(y)$$

into the total action. D is the Dirac operator.

The **Grassmann Gauss integral can be done (only !) formally.**

In observables which contain ψ and $\bar{\psi}$, these can be **contracted by inserting everywhere fermion propagators** $(D^f)^{-1}(\{U\})$ (supposed to be known for the given gauge field background).

The full partition function contains the “fermion determinants” coming from Grassmann Gaussian integration :

$$Z(N_s, N_t; \beta, m_f) = \int \prod_{\tau=1}^{N_t} \prod_{\mathbf{x}, \mu} dU_\mu(\tau, \mathbf{x}) \prod_f \det D^f(\{U\}; m_f) e^{-S_g[U]}$$

with thermal (timelike) boundary conditions

$$\begin{aligned} U_\mu(\tau, \mathbf{x}) &= U_\mu(\tau + N_t, \mathbf{x}) \\ \psi(\tau, \mathbf{x}) &= -\psi(\tau + N_t, \mathbf{x}) \end{aligned}$$

and with the integration measure

$$dU = \text{Haar measure on the compact Lie group } SU(N)$$

For example, N_f degenerate Wilson fermions described by

$$\begin{aligned}
 S_f^W &= \sum_{x,y,f} a^4 \bar{\psi}_f(x) D_{xy}^f(\{U\}; m_f) \psi_f(y) \\
 &= \frac{1}{2a} \sum_{x,\mu,f} a^4 \bar{\psi}_f(x) [(\gamma_\mu - r) U_\mu(x) \psi_f(x + \hat{\mu}) \\
 &\quad - (\gamma_\mu + r) U_\mu^\dagger(x - \hat{\mu}) \psi_f(x - \hat{\mu})] \\
 &\quad + \sum_{x,f} \left(m + 4\frac{r}{a}\right) a^4 \bar{\psi}_f(x) \psi_f(x)
 \end{aligned}$$

Effective action includes the determinants :

$$S_{\text{eff}}[U] = S_g[U] - \sum_f \ln \det D^f(\{U\}; m_f)$$

General terminology (for all kinds of lattice fermions)

- **Gluodynamics/Yang-Mills theory** : $N_f = 0$, no dynamical fermions; “quenched approximation” of QCD, feedback of quarks impossible
- $N_f = 2$ “**full QCD**” : $N_f = 2$ degenerate flavors of first generation (u and d quarks) made dynamical; chiral limit $m_u = m_d \rightarrow 0$
- $N_f = 2 + 1$ “**full QCD**” : one heavier flavor (s quark) added to the first generation
- $N_f = 3$ **QCD** : all three flavors taken mass-degenerate, eventually the chiral limit $m_u = m_d = m_s \rightarrow 0$ is intended
- $N_f = 2 + 1 + 1$ “**real QCD**” : inclusion of two generations of light (degenerate u and d) and heavy (non-degenerate s and c) quarks. c quarks contribute to EoS already at temperature $T > 200$ MeV.

Euclidean measure :

positive as long as $\mu_B = 0$, then fermion determinants are real-valued.

Great advantage : importance sampling is still possible !

- for pure gauge theories : local updates (heat bath or Metropolis)
- for theories with fermions : non-local, global “smart updates”
obtained by solving Hamilton’s equations of motion for $U_\mu(x)$
 (“trajectories” running in 5-th dimension time over $\tau = \mathcal{O}(1)$) with
 - “potential energy” $U_{\text{pot}} = S_{\text{eff}}[U]$
 - “kinetic energy” $T_{\text{kin}} = \frac{1}{2} \sum_{x,\mu} \text{tr} [\Pi_\mu(x)]^2$,

applying Metropolis acceptance check w.r.t. the positive measure

$$\text{weight} \propto \exp(-T_{\text{kin}} - U_{\text{pot}})$$

This is the Hybrid Monte Carlo algorithm (and derivatives of it)

Lattice fermions present a deeper theoretical problem, however :

In order to circumvent the **fermion doubling problem**, one has to sacrifice **chiral symmetry**, $\gamma_5 D + D \gamma_5 = 0$, of the (massless) action.

Chiral symmetry is - after that step - either

- reduced, as for staggered (Kogut-Susskind) fermions, or
- broken completely, as for Wilson fermions.

This renders the study of the behaviour in the chiral limit difficult.

Chiral symmetry is optimally realized on the lattice using

- overlap (Neuberger) fermions, with $\gamma_5 D + D \gamma_5 = \frac{a}{\rho} D \gamma_5 D$ (D as solution of this “Ginsparg-Wilson relation”) or
- domain wall (Kaplan) fermions (**in 4+1 dimensions**).

Ideal solution ! Reaches the principal limit for chiral symmetry imposed by discretization ! However, apart from other delicate algorithmic problems, present day computing capacity is not sufficient for mass production.

Chemical potential $\mu_B \neq 0$ presents another hard practical problem !

This “sign problem” is not restricted to fermionic field theories !

A chemical potential, counting any kind of **conserved charge**, is introduced by the **substitution** (Karsch and Hasenfratz, 1982)

$$\begin{aligned} U_0(\mathbf{x}, \tau) &\rightarrow U_0(\mathbf{x}, \tau) \exp(+\mu_q a) && \text{timelike forward link} \\ U_0^\dagger(\mathbf{x}, \tau) &\rightarrow U_0^\dagger(\mathbf{x}, \tau) \exp(-\mu_q a) && \text{timelike backward link} \end{aligned}$$

μ_q acts as **time component of an external imaginary Abelian gauge field**, while the same μ_q counts **quark-minus-antiquark (baryon charge)**.

Along a forward **Wilson line** a weight $\exp(\mu_q/T)$ is accumulated, for a **baryon loop** the weight factor is $\exp(\mu_B/T) = \exp(3\mu_q/T)$.

Complex valuedness of fermion determinants can be concluded from the **γ_5 -hermiticity of Dirac operators** (precisely, its violation) :

$$\gamma_5 D \gamma_5 = D^\dagger \quad \text{implies} \quad \det D = [\det D]^*$$

γ_5 -hermiticity is **spoiled for $\mu_q \neq 0$** , when one has instead

$$\gamma_5 D(\mu_q) \gamma_5 = D^\dagger(-\mu_q) \quad \rightarrow \quad \text{determinant is complex}$$

This is the **fermionic origin** of the **sign problem**. Doubling of flavors would not render the weight factor real. This is the generic case !

There exist **important exceptional cases without sign problem** :

A. Imaginary chemical potential : for $\mu_q = i\eta$ the determinant is real. Then (at least for two flavors) the weight is then positive.

Optimistic approach : **simulate at $\mu_q^2 < 0$ and extrapolate to $\mu_q^2 > 0$** .

Examples for analytic continuation : **transition temperature, screening lengths** etc. can be represented as analytic functions of μ^2

But no direct access available to gauge field configurations that would be corresponding to real $\mu_q \neq 0$! (the “no-overlap problem”)

B. Isospin chemical potential : if for two flavors, the species have opposite isospin charge, $\mu_u = \mu_I$ and $\mu_d = -\mu_I$.

The **Dirac operator of both flavors** has block-diagonal form

$$\begin{pmatrix} D(\mu_I) & 0 \\ 0 & D(-\mu_I) \end{pmatrix}$$

or

$$\begin{pmatrix} D(\mu_I) & 0 \\ 0 & \gamma_5 D^\dagger(\mu_I) \gamma_5 \end{pmatrix}$$

The **common determinant** is

$$\det[D(\mu_I)] \det[\gamma_5 D^\dagger(\mu_I) \gamma_5] = \det[D(\mu_I)] \det[D^\dagger(\mu_I)] = |\det[D(\mu_I)]|^2$$

Lesson :

“For finite isospin chemical potential, the determinantal weight factor in the presence of two flavors (opposite in isospin) is real and positive.”

C. Chiral (or axial) chemical potential μ_5

Creates an **imbalance between left handed and right handed matter** mimicking the presence of a topologically charged background field :

$$D(\mu_5) = \gamma_\mu D_\mu + m + \mu_5 \gamma_4 \gamma_5 \quad \text{in continuum}$$

in lattice notation like Karsch/Hasenfratz :

$$\begin{aligned} [D_W(\mu_5)]_{x,y} &= \delta_{x,y} - \kappa \sum_i \left[(1 - \gamma_i) U_i(x) \delta_{x+\hat{i},y} + (1 + \gamma_i) U_i^\dagger(x - \hat{i}) \delta_{x-\hat{i},y} \right] \\ &\quad - \kappa \left[(1 - \gamma_4 e^{a\mu_5 \gamma_5}) U_4(x) \delta_{x+\hat{4},y} + (1 + \gamma_4 e^{-a\mu_5 \gamma_5}) U_4^\dagger(x - \hat{4}) \delta_{x-\hat{4},y} \right] \end{aligned}$$

with

$$e^{\pm a\mu_5 \gamma_5} = \cosh(a\mu_5) \pm \gamma_5 \sinh(a\mu_5)$$

This again **satisfies γ_5 -hermiticity** : $\gamma_5 D(\mu_5) \gamma_5 = D^\dagger(\mu_5)$

Consequently, the determinant is real-valued !

Simulation result : **A current is induced through the chiral magnetic effect (CME)** in presence of an external magnetic field \vec{B} acting on electrical charges e :

$$\vec{j} = \frac{1}{2\pi^2} \mu_5 e \vec{B}$$

D. Other gauge groups :

For example, the gauge groups $SU(2)$, G_2 and $SO(N)$ do not have a sign problem !

3. The order parameters of two abstract phase structure problems

A. The quenched limit of QCD and $Z(N)$ -symmetry

quarks infinitely heavy \rightarrow pure gauge theory plus static quark fields
action invariant under standard gauge transformations

$$S_g[U^g] = S_g[U] \quad \text{with} \quad U_\mu^g(x) = g(x)U_\mu(x)g^{-1}(x + \hat{\mu}), \quad g(x) \in SU(N)$$

with **periodic boundary conditions** both for U and g :

$$U_\mu(\tau, \mathbf{x}) = U_\mu(\tau + N_\tau, \mathbf{x}), \quad g(\tau, \mathbf{x}) = g(\tau + N_\tau, \mathbf{x})$$

In fact, also gauge transformations $g'(x)$ of **“topologically non-trivial kind”**
are permitted, **which are periodic only up to a constant matrix h** :

$$g'(\tau + N_\tau, \mathbf{x}) = hg'(\tau, \mathbf{x}), \quad h \in SU(N)$$

Thus, $g'(x)$ picks up a **“twist” factor h** winding once around the torus.

The gauge links, after an extended gauge transformation, behave across the temporal boundary as

$$U_{\mu}^{g'}(\tau + N_{\tau}, \mathbf{x}) = h U_{\mu}^{g'}(N_{\tau}, \mathbf{x}) h^{-1}$$

This is **consistent with periodicity** if and only if $[h, U_i^{g'}] = 0$, i.e.

$$h = z\mathbf{1} \in Z(N), \quad \text{center of } SU(N) \quad z = \exp\left(i\frac{2\pi n}{N}\right), \quad n \in \{0, 1, 2, \dots, N-1\}.$$

Lesson :

“Pure gauge theory at finite temperature is invariant under gauge transformations with non-trivial winding, for any global twist factor $h \in Z(N)$, the center of the gauge group $SU(N)$.”

Gauge invariant observables are sensitive to twists if and only if they wind, too.

Example: “Wilson line” in the temporal direction closing onto itself, nowadays called (untraced) “Polyakov loop”:

$$L(\mathbf{x}) = \prod_{x_0}^{N_\tau} U_0(x) .$$

Physically, this is the “propagator” of a static quark.

Under gauge transformations of the two sorts, it behaves

$$\begin{aligned} L^g(\mathbf{x}) &= g(x)L(\mathbf{x})g^{-1}(x), \\ L^{g'}(\mathbf{x}) &= g'(1, \mathbf{x})L(\mathbf{x})g'^{-1}(1 + N_\tau, \mathbf{x}) = g'(1, \mathbf{x})L(\mathbf{x})g'^{-1}(1, \mathbf{x})h^{-1} . \end{aligned}$$

such that

$$\mathrm{Tr} L^g = \mathrm{Tr} L, \quad \mathrm{Tr} L^{g'} = z^* \mathrm{Tr} L .$$

We conclude that the **traced Polyakov loop**

- is gauge invariant w.r.t. topologically trivial gauge transformations,
- picks up a center element z^* when transformed with a non-trivial, winding gauge transformation,

The Polyakov loop emerges as observable in the **QCD path integral with heavy quarks** (to leading order in the hopping expansion).

Example: partition function for pure gauge theory with a single static quark sitting at \mathbf{x} :

$$Z_Q = \int DU \operatorname{Tr} L(\mathbf{x}) e^{-S_g[U]} .$$

Hence, the **expectation value** is:

$$\langle \operatorname{Tr} L \rangle = \frac{1}{Z} \int DU \operatorname{Tr} L e^{-S_g} = \frac{Z_Q}{Z} = e^{-(F_Q - F_0)/T} ,$$

Lesson :

“VEV of Polyakov loop = exponential of free energy difference between the Yang-Mills plasma with and without static quark inserted.”

Two limiting cases :

- For $T \rightarrow 0$ Yang-Mills theory is confining. It would cost infinite energy to place a single quark into the gluon plasma, $F_Q = \infty$ and

$$\langle \text{Tr } L \rangle = 0$$

Center symmetry is manifest !

- $T \rightarrow \infty$ corresponds to $\beta \rightarrow \infty$, for which $U_0 \rightarrow 1$ and

$$\langle \text{Tr } L \rangle \rightarrow \text{Tr } \mathbf{1} = N .$$

A non-zero expectation value is no longer invariant under center transformations \rightarrow “spontaneous breaking of center symmetry”.

Lesson :

“QCD in the quenched limit has a true (non-analytic) deconfinement phase transition, corresponding to the breaking of the global center symmetry. The average of the Polyakov loop is the corresponding order parameter.”

If **dynamical quark fields are added**, they will behave as

$$\psi^g(x) = g(x)\psi(x), \quad \psi(\tau + N_\tau, \mathbf{x}) = -\psi(\tau, \mathbf{x}), \quad \psi^{g'}(\tau + N_\tau, \mathbf{x}) = -h\psi(\tau, \mathbf{x})$$

Statistical mechanics requires anti-periodic boundary conditions for fermions, therefore **trivial $h = 1$ is the only permissible choice.**

There is no center symmetry in the presence of dynamical quarks !

- Physically, if there are dynamical quarks, their pair production screens the confining force (it leads to string breaking):
 F_Q is finite, and the $Q\bar{Q}$ potential stops rising at $R = R_{\text{string-breaking}}$.
- Correspondingly, $\langle \text{Tr } L \rangle \neq 0$ for all temperatures, and the Polyakov loop is no longer a true order parameter.
- In this case, a non-analytic phase transition as a function of temperature is not realized; confined and deconfined regions may be then analytically connected by a smooth crossover.

Example: With heavy quarks ($m_q = \mathcal{O}(3 \dots 10)$ GeV) the first order phase transition line of $SU(3)$ Yang-Mills theory terminates, going over into a crossover at some critical endpoint.

Would-be physics is governed by competition between explicit and spontaneous breaking of center symmetry.

B. The chiral limit of QCD

Classical QCD Lagrangian in the limit of zero quark masses is invariant under **global chiral symmetry transformations** with the symmetry group $U_A(1) \times SU_L(N_f) \times SU_R(N_f)$.

- **axial $U_A(1)$ is anomalous**, quantum corrections break it down to $Z(N_f)$
- remainder gets **spontaneously broken to the diagonal subgroup**, $SU_L(N_f) \times SU_R(N_f) \rightarrow SU_V(N_f)$, giving rise to $N_f^2 - 1$ massless **pseudoscalar Goldstone bosons** (pions, kaons etc.)
- the **order parameter of chiral symmetry** is the chiral condensate,

$$\langle \bar{\psi}\psi \rangle = \frac{1}{N_s^3 N_t} \frac{\partial}{\partial m_f} \ln Z = \frac{1}{N_s^3 N_t} \langle \text{tr} D_f^{-1} \rangle \propto \langle \rho(\lambda = 0) \rangle$$

This is the “**Banks-Casher relation**”, it holds since

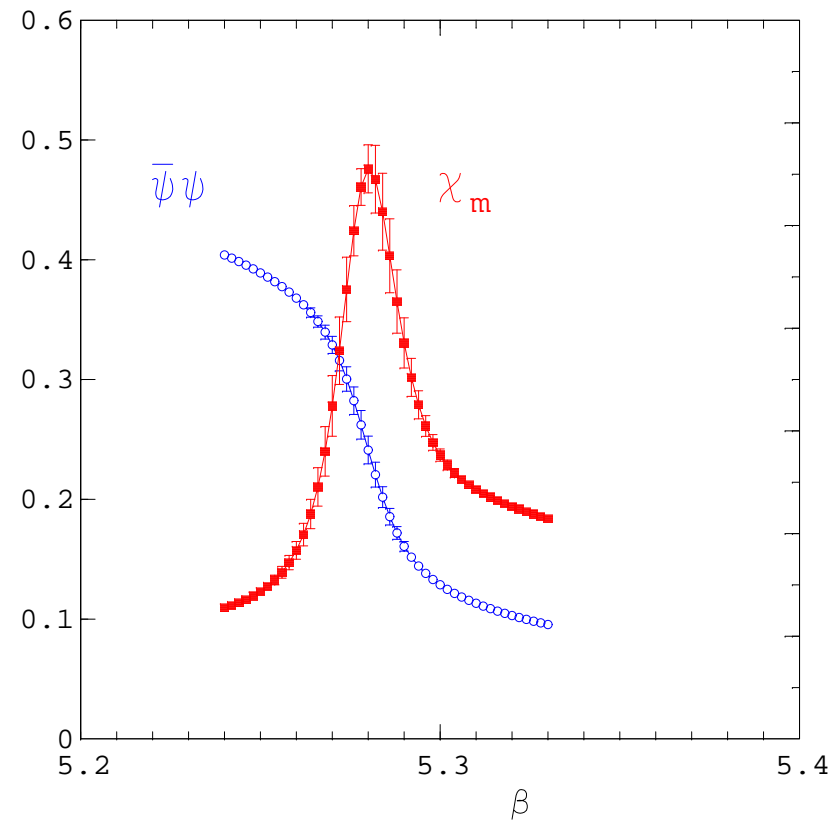
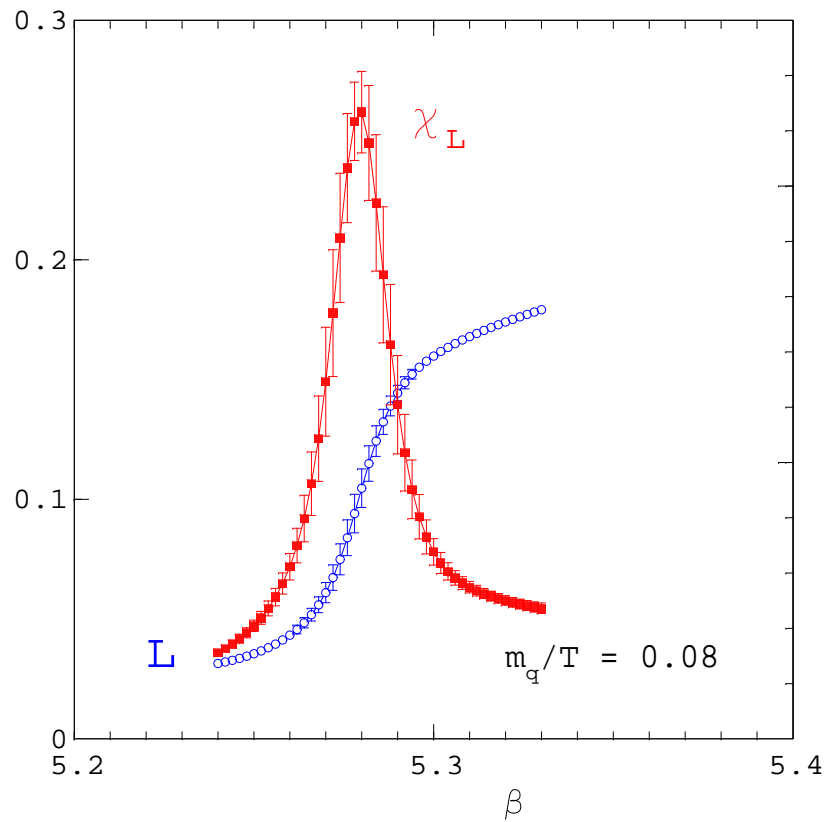
$$\langle \bar{\psi}\psi \rangle \propto \lim_{m \rightarrow 0} \left\langle \sum_{\text{eigenvalue } i} \frac{1}{i \lambda_i + m} \right\rangle = \lim_{m \rightarrow 0} \int d\lambda \langle \rho(\lambda) \rangle \frac{2m}{\lambda^2 + m^2} = \langle \rho(\lambda = 0) \rangle$$

- **A clear order parameter would mean :**
 $\langle \bar{\psi}\psi \rangle \neq 0$ for $T < T_\chi$ (chiral symmetry is **spontaneously broken**)
and $\langle \bar{\psi}\psi \rangle = 0$ for $T > T_\chi$ (when **chiral symmetry is restored**).
- for **zero quark mass** there is a **non-analytic finite temperature phase transition** corresponding to chiral symmetry restoration.
- For **non-zero quark masses**, chiral symmetry is broken explicitly.
The chiral condensate is then $\langle \bar{\psi}\psi \rangle \neq 0$ for all temperatures.
- Again, in this case a **non-analytic phase transition** related to **chiral symmetry** is not realized : **there is an analytical crossover.**

C. Physical QCD

- QCD with physical quark masses is **very different both from the chiral or quenched limit.**
- $Z(3)$ symmetry as well as **chiral symmetry** are explicitly broken.
- Still, physical QCD has **confinement (in the sense of absence of colored states, also of gluons)** as well as **three light pions** as “remnants” of **chiral symmetry (and its breaking).**
- In the presence of mass terms there is **no true order parameter.** The expectation values of Polyakov loop and chiral condensate are non-vanishing at any temperature.
- Hence, the deconfined or chirally symmetric phase is **analytically connected with the confined or chirally broken phase.**

Polyakov loop L (left) and chiral condensate $\langle \bar{\psi}\psi \rangle$ (right) together with their susceptibilities show both transitions in two flavour QCD.
from Karsch et al. 2001



However, center (a-)symmetry is intertwined with chiral symmetry breaking within quenched and real QCD !

see: E. Bilgici, F. Bruckmann, J. Danzer, C. Gattringer, C. Hagen, E.-M. I., A. Maas, Few Body Syst. 47 (2010) 125 , arXiv:0906.3957

Experiment : Calculate fermionic observables (chiral condensate etc.) with valence quarks, which may differ from sea quarks by **modified temporal boundary conditions** :

- for antisymmetric b. c. the standard result is reobtained;
- for periodic b. c. a fictive (valence) result is obtained;
- at which temperatures the results start to depend on b. c. ?
- how does the chiral condensate of valence quarks depend on their (continuously varied) boundary condition ?

We consider general b. c.

$$\psi(\mathbf{x}, N_t) = e^{i\phi} \psi(\mathbf{x}, 0)$$

Observation :

In the low-temperature phase the boundary condition applied to (valence) fermions does not play any role ! In the high-temperature phase various quantities (the spectral gap or - if it vanishes - the spectral density near zero eigenvalue $\rho(0)$) depend on ϕ !

Notice ! This is not real QCD. **For quenched QCD all fermions are valence quarks.** The observation applies also when **full QCD configurations are analysed by valence quarks !**

In other words : The way **how center symmetry is broken in the gauge system** can be **visualized by non-standard b. c. for fermions** (focussing at the same time on different types of topological excitations).

Define a **generalized quark condensate** :

$$S(\phi) = -\langle \bar{\psi}\psi \rangle|_{\phi} = \frac{1}{V} \sum_j \frac{1}{i \lambda_j(\phi) + m}$$

with Dirac eigenvalues $\lambda_j(\phi)$ depending on ϕ (modified temporal b. c.)

True quark condensate (quenched or dynamic) :

$$\Sigma^{(0)} = S(\phi = \pi) \quad \text{for antiperiodic b. c.}$$

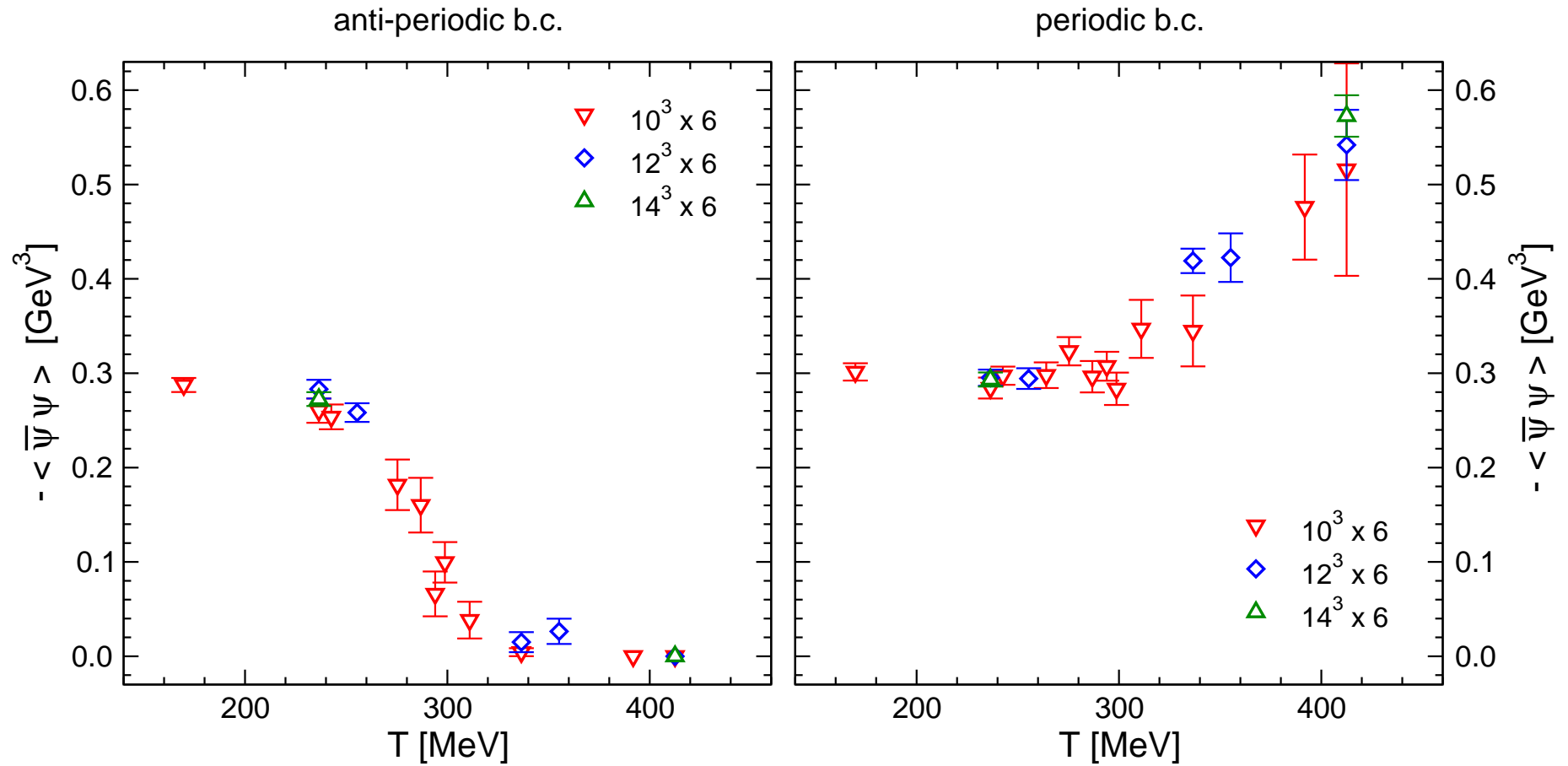
The **dual quark condensate** is the first Fourier component of $S(\phi)$:

$$\Sigma^{(1)} = \int_0^{2\pi} \frac{d\phi}{2\pi} S(\phi) e^{-i\phi}$$

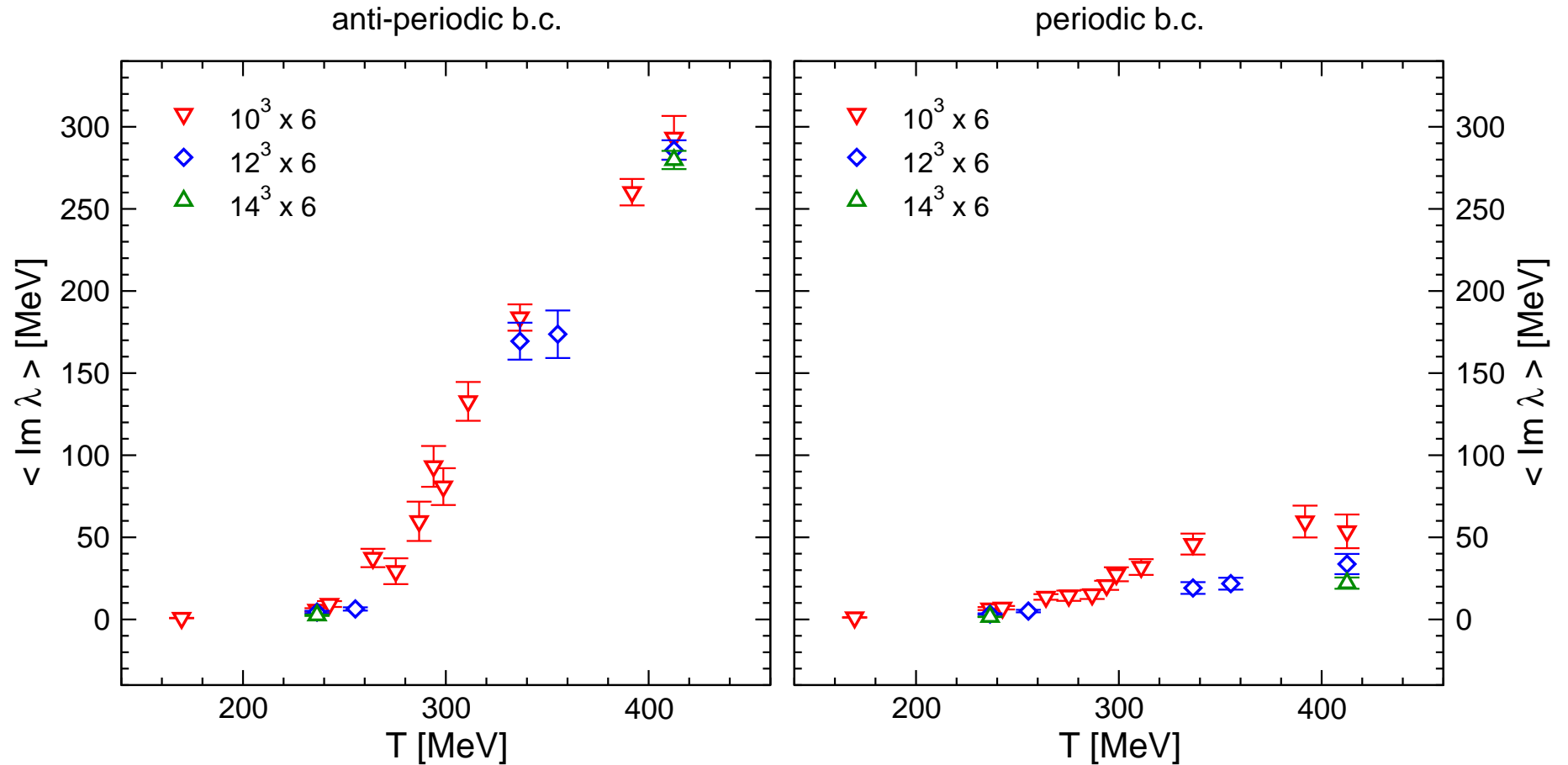
It behaves like the renormalized Polyakov loop. In literature:

“dual quark condensate” synonymous with “dressed Polyakov loop”

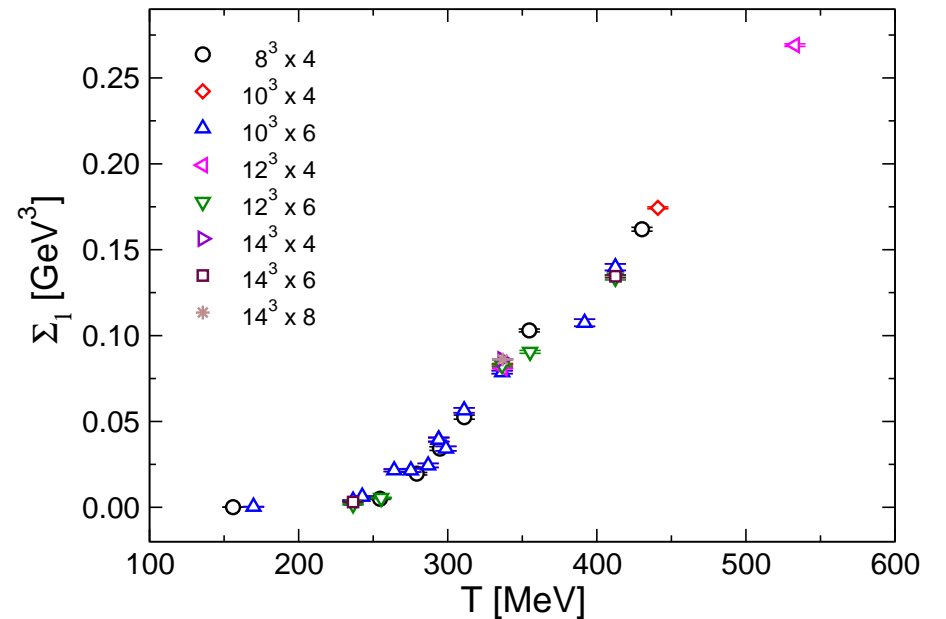
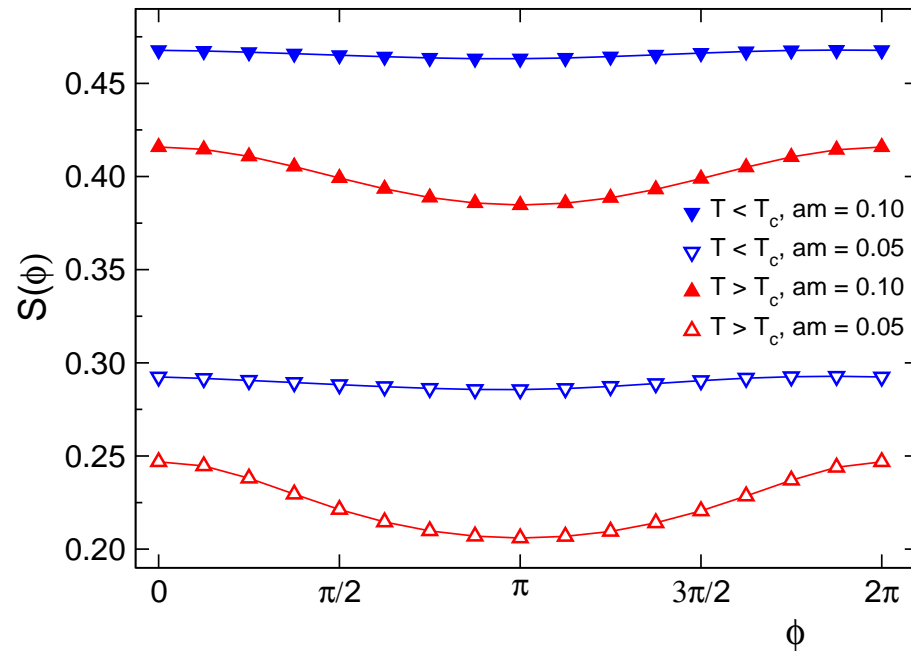
Quenched chiral condensate $-\langle\bar{\psi}\psi\rangle$ for anti-periodic (left) and periodic (right) temporal fermion boundary conditions as a function of temperature. (from arXiv:0906.3957)



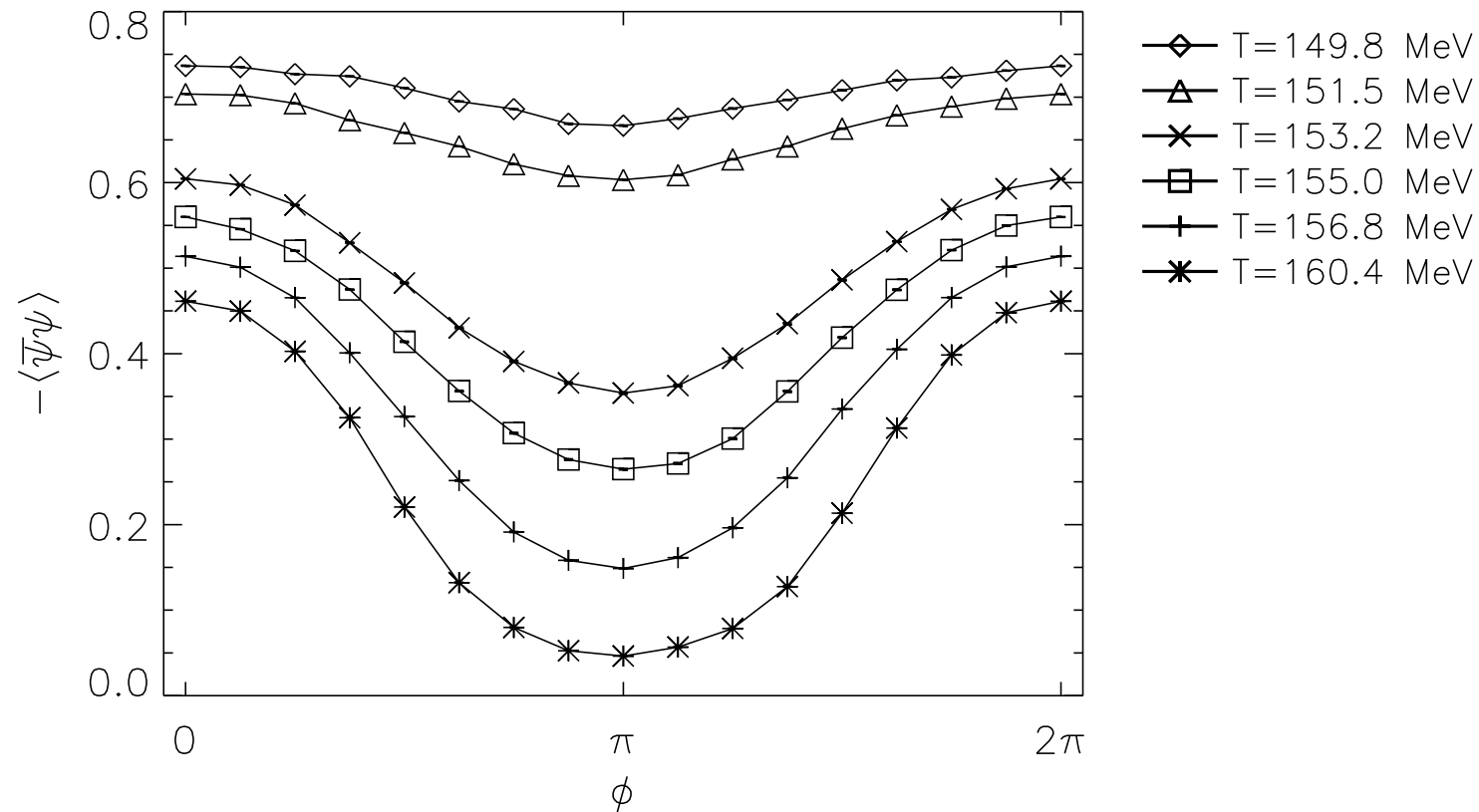
Quenched spectral gap for anti-periodic (left) and periodic (right) temporal fermion boundary conditions as a function of temperature.
(from arXiv:0906.3957)



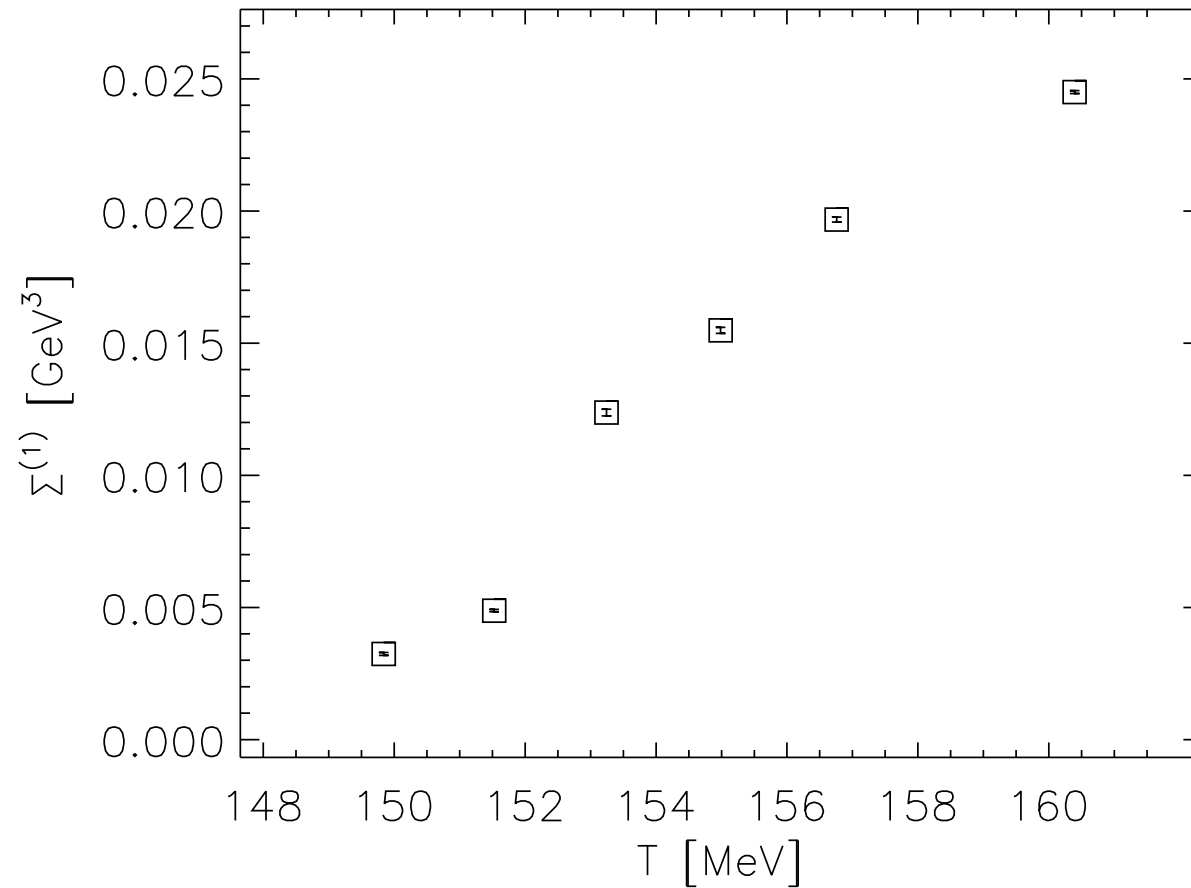
Left: the integrand $S(\phi)$ of the dual chiral condensate in the quenched case as function of the boundary angle ϕ . (two bare quark masses and two temperatures below and above T_{dec} . Right: the quenched dual chiral condensate as function of the temperature. (from arXiv:0906.3957)



The chiral condensate of the dynamical theory as function of the boundary angle ϕ for various temperatures. (from arXiv:0906.3957)



The bare dual chiral condensate $\Sigma^{(1)}$ for the dynamical theory as function of the temperature. (from arXiv:0906.3957)



The following qualitative features are left to numerical investigations :

- For which parameter values of QCD a **non-analytic phase transition** is recovered, and what is its order?
- Are confinement and chiral symmetry breaking disappearing at the **same single transition** or are there **different transitions** ?
Example : for **adjoint quarks**, $T_\chi(\text{adjoint}) \gg T_\chi(\text{fund}) \approx T_{\text{dec}}$!
- If there is just one transition, **what is the driving mechanism** ?
- If **topological objects** are responsible for the low-temperature properties, how is **topology restructured** at the crossover ?
- If there is only one smooth crossover, **how do the properties of matter change in the different regions of the phase diagram** ?
(precision results required !)

4. Searching for a transition along a line in the phase diagram

- Searching for the crossover/the crossovers by means of the Polyakov loop, the chiral condensate and the corresponding susceptibilities. For example, **varying T along the axis $\mu_q = 0$.**
- For **light quark masses and large N_t** the Polyakov loop loses **much of its analytic power** to describe “the (de)confinement side” of the transition. Polyakov loop is no derivative of $\ln Z$!
- Is the center symmetry really important for confinement, if the theory contains light quarks ? The dual condensate relates light quarks to center symmetry, as seen before !
- **What do we associate with “deconfinement” ?** The light quark number may start to fluctuate “freely”. Thus, the **quark number susceptibility supersedes the Polyakov loop** as deconfinement signal.

- **Renormalized Polyakov loop** (intention : removal of the finite- a effects)

$$\langle \text{Re}(L) \rangle_R = \langle \text{Re}(L) \rangle \exp(V(r_0)/2T)$$

$V(r_0)$ is the zero-temperature potential at distance r_0 .

Aim: search for inflection point and for a Gaussian peak of susceptibility above background.

- **Renormalized quark condensate** (aim : remove divergent part $\propto a^{-2}$)

$$\langle \bar{\psi}\psi \rangle_R = Z_p \left(\langle \bar{\psi}\psi \rangle + c(g_0) \frac{\mu_0}{a^2} \right)$$

practically used

$$R_{\bar{\psi}\psi} = \frac{\langle \bar{\psi}\psi \rangle(T, \mu_0) - \langle \bar{\psi}\psi \rangle(0, \mu_0) + \langle \bar{\psi}\psi \rangle(0, 0)}{\langle \bar{\psi}\psi \rangle(0, 0)}$$

The corresponding (disconnected) susceptibility of the quark condensate is obtained as the variance over the ensemble. It shows a maximum at the transition.

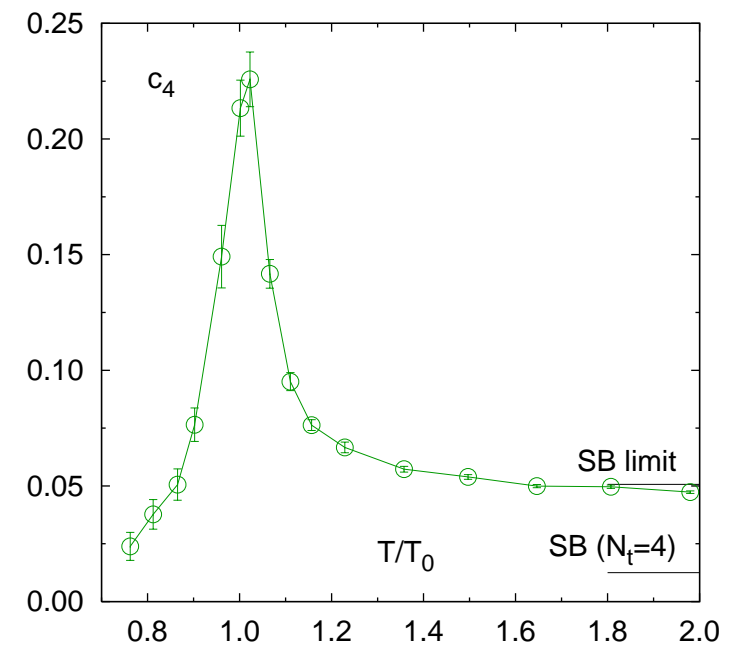
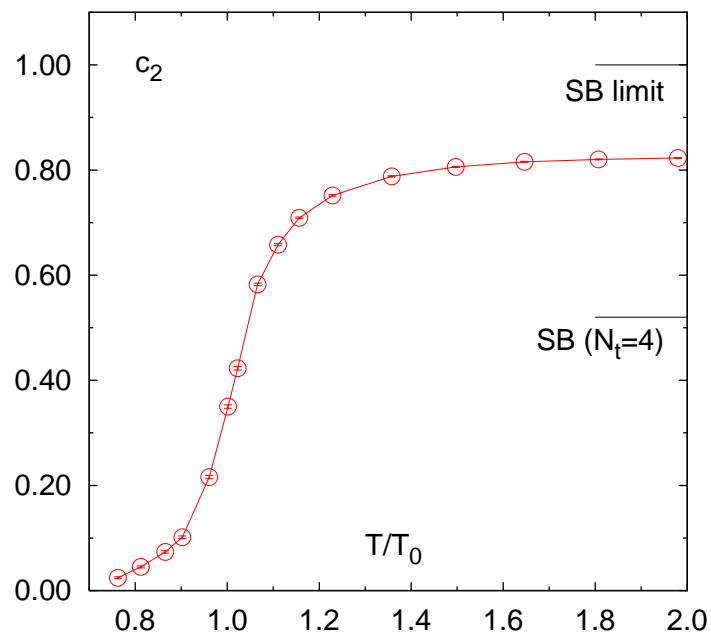
- **Quark number susceptibility** : second derivative w.r.t μ_q taken at $\mu_q = 0$
of $\ln \det D = \text{tr} \ln D$

$$c_2 = \frac{\partial^2 \ln \det D(\mu_q)}{\partial \mu_q^2} = -\text{tr} \left[D^{-1} \frac{\partial D}{\partial \mu_q} D^{-1} \frac{\partial D}{\partial \mu_q} \right] + \text{tr} \left[D^{-1} \frac{\partial^2 D}{\partial \mu_q^2} \right]$$

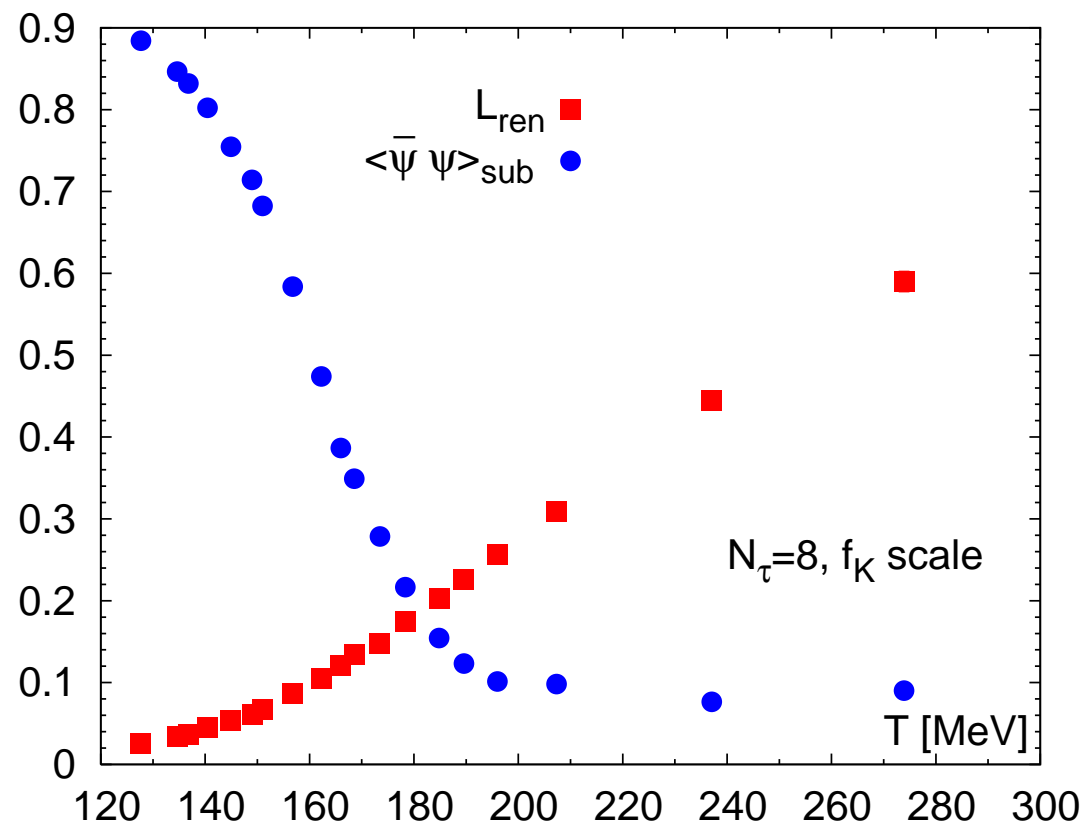
These expressions are standard for the Taylor expansion in μ_q used to explore the region of non-vanishing baryonic density.

Useful as an observable emphasizing the deconfinement at vanishing baryonic density !

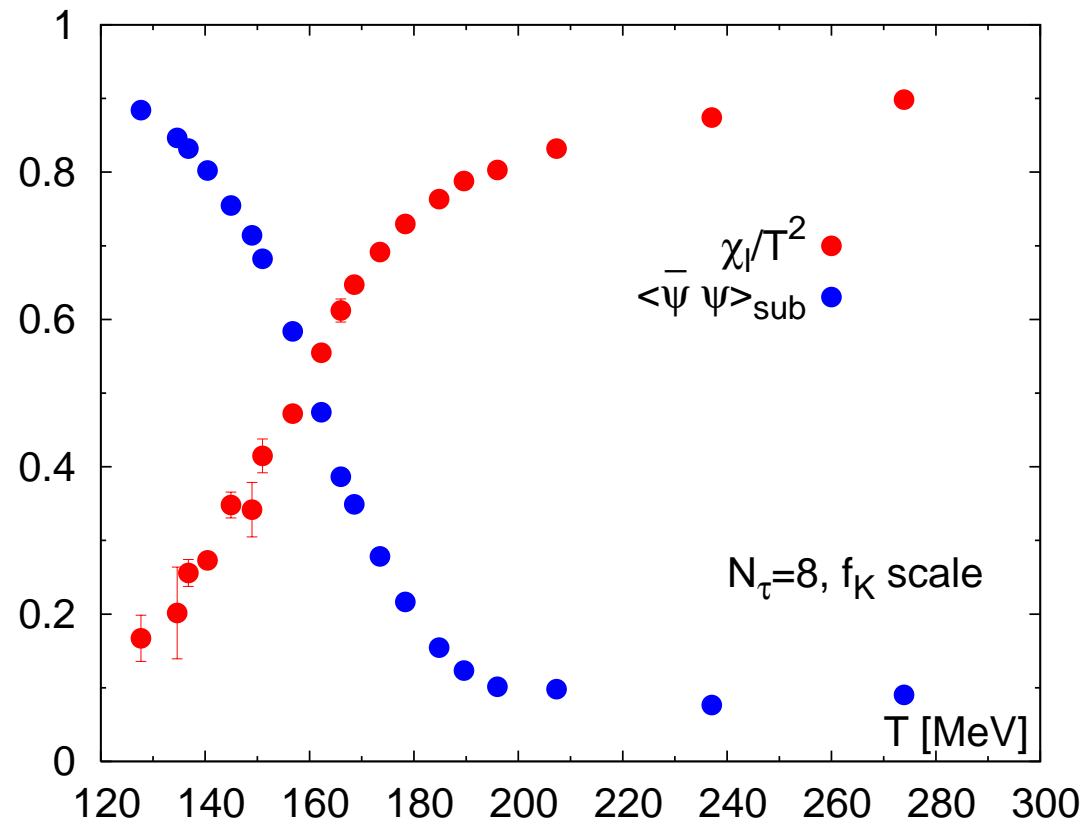
The second and fourth derivatives c_2 and c_4 as functions of temperature
Quark number susceptibility behaves like step function, the next higher
moment like a “usual” susceptibility. (from Ch. Schmidt hep-lat/0610116)



The chiral condensate compared to the renormalized Polyakov loop in full QCD from arXiv:1203.5320 Petreczky



The chiral condensate compared to the light quark number susceptibility in full QCD from arXiv:1203.5320 Petreczky



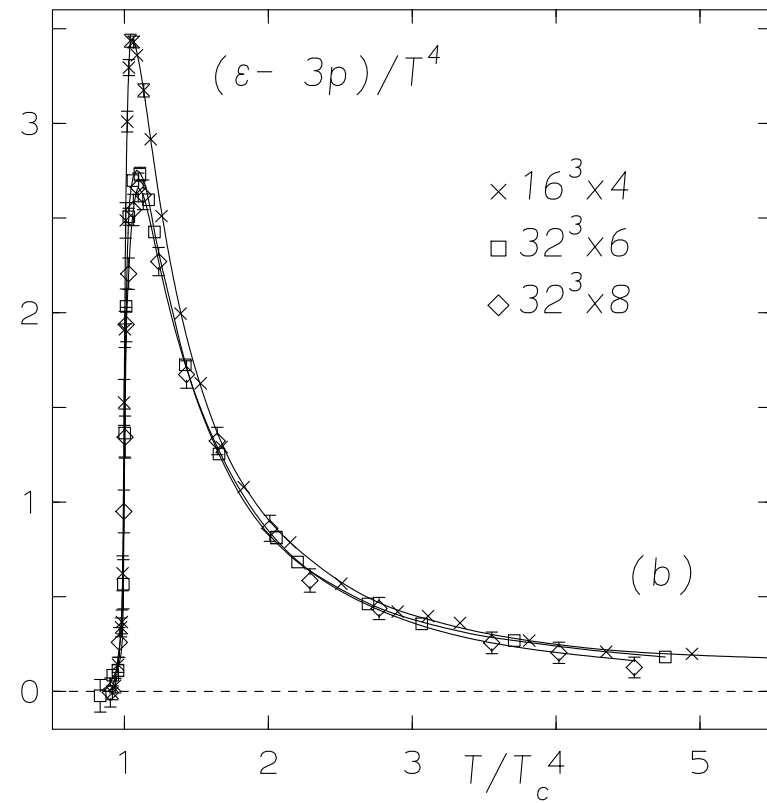
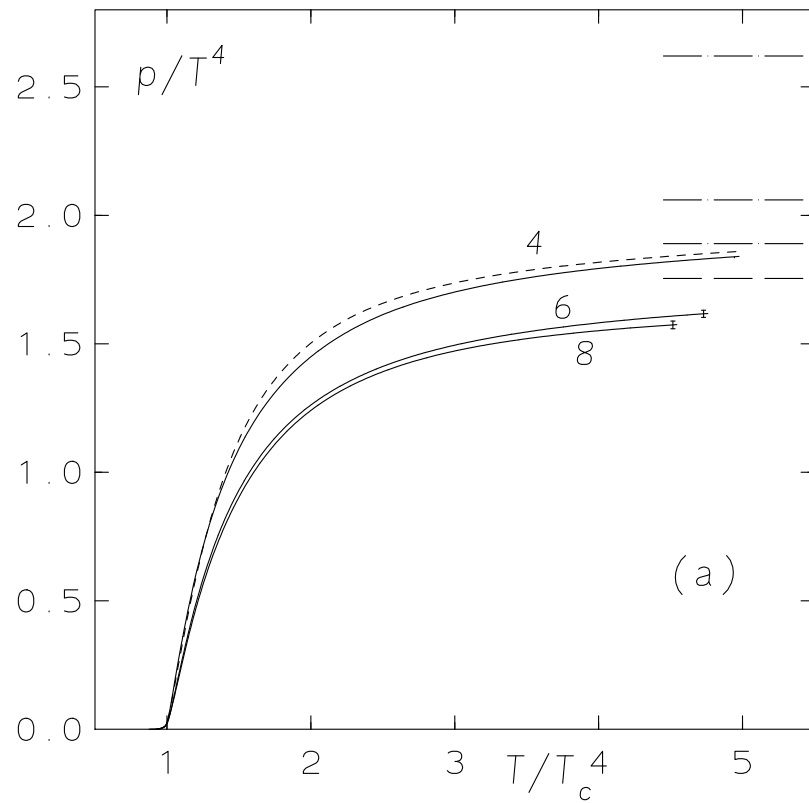
What comes behind the transition ?

What distinguishes high from low temperature in real QCD ?

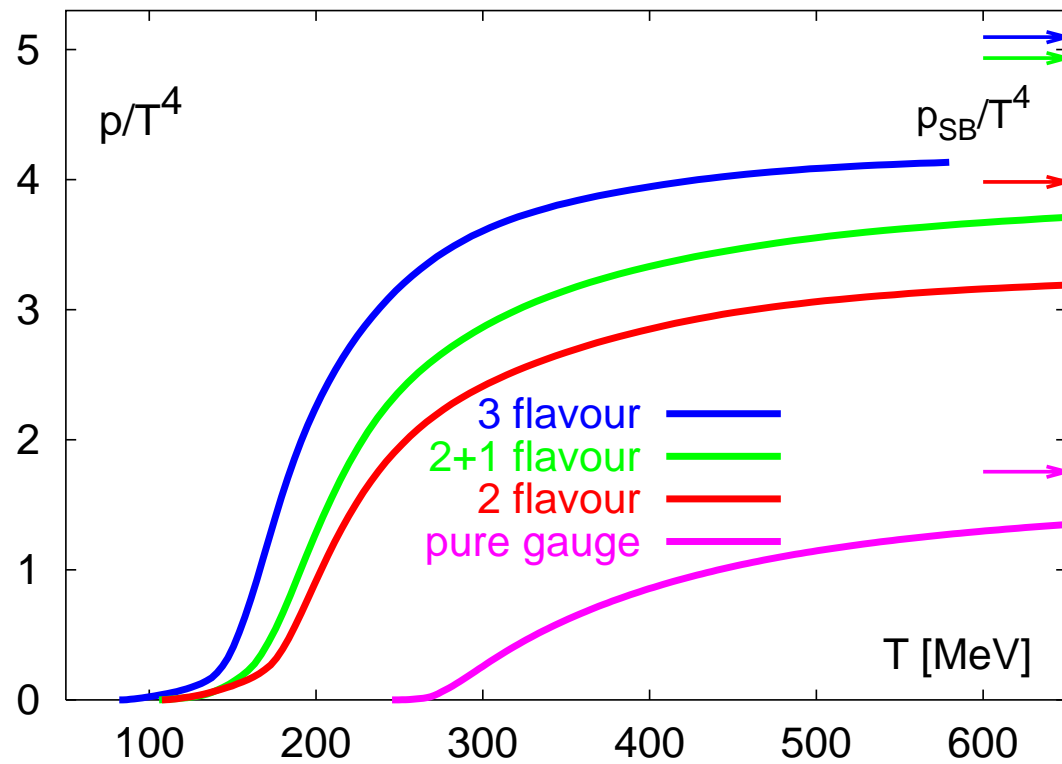
- The renormalized **Polyakov loop** is large.
- The renormalized **quark condensate** is small.
- The **quark number susceptibility** is large.
- The **pressure and the energy density** are large, however still far from the Stefan-Boltzmann limit.
- The **signal (driving force)** for the “liberation of degrees of freedom” is the **trace anomaly** (“interaction measure”).
- For pure Yang-Mills theory (no quarks) this is a **very sharp signal** !

The trace anomaly induces the rise of pressure and energy density.

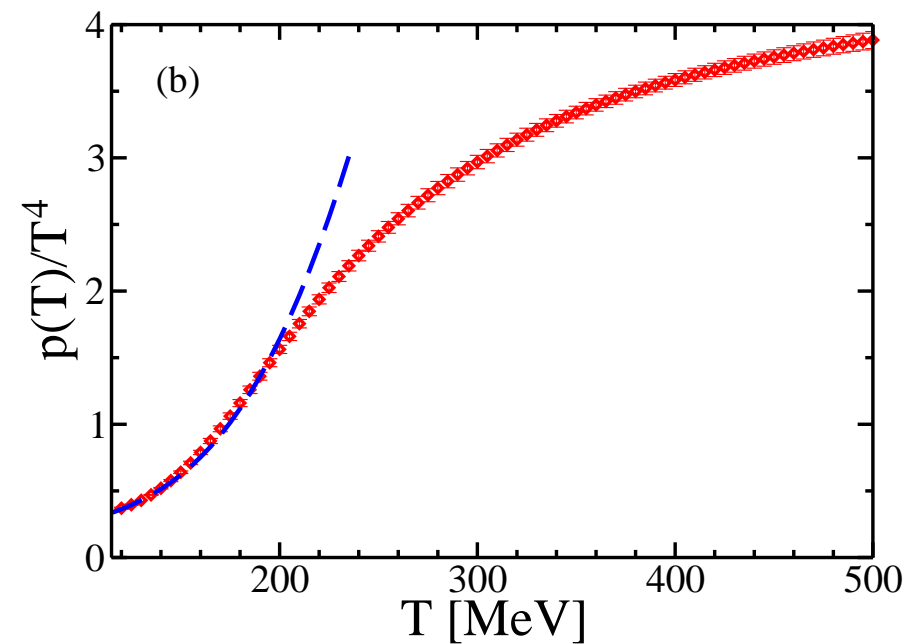
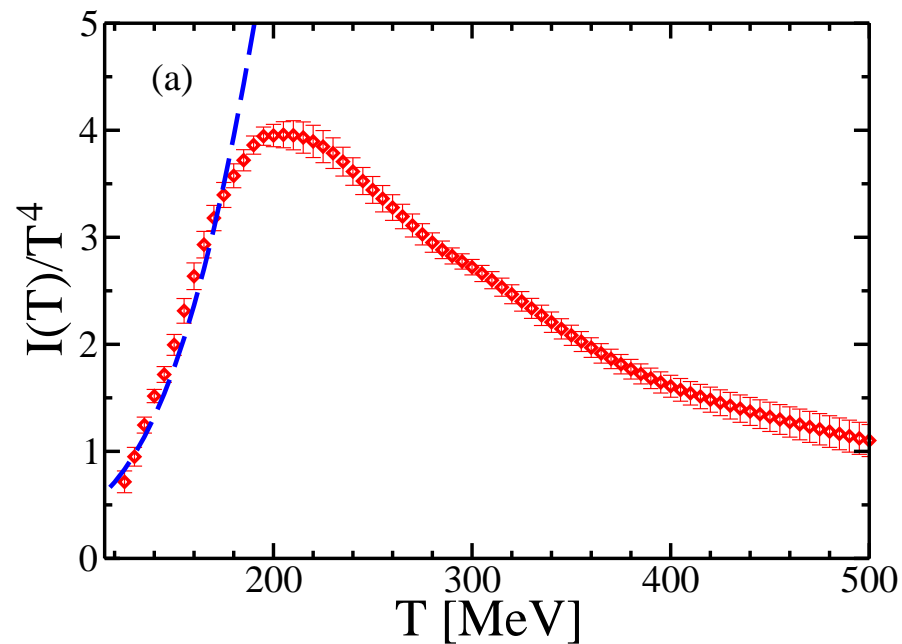
The pressure (left) versus T/T_c for $N_t = 4, 6$ and 8 in pure gluodynamics.
The interaction measure of gluons (trace anomaly) $(\epsilon - 3p)/T^4$ (right).
from Boyd et al. 1995



The pressure : gluons only, 2 light, 2 light + 1 heavy and 3 light flavors
from Karsch, Laermann and Peikert (2000)



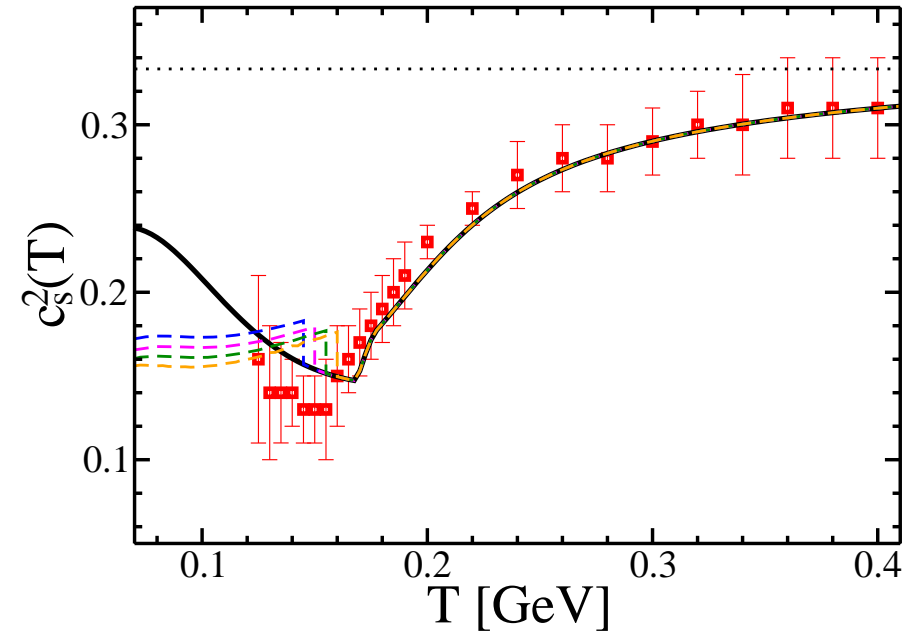
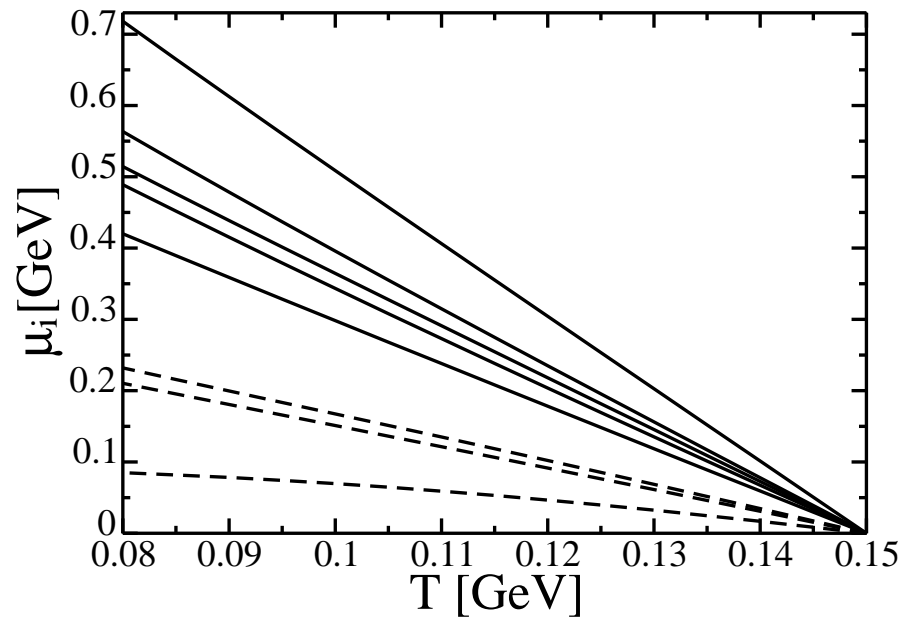
EoS recently obtained from lattice data at $n_B = 0$ and $N_f = 2 + 1$ flavors !
Interaction measure (left) and pressure (right) from $N_f = 2+1$ lattice data with physical quark masses (S. Borsanyi et al. Wuppertal-Budapest collaboration) from Bluhm, Alba, Alberico, Beraudo, Ratti, arXiv:1306.6188



Left: T -dependent effective chemical potential for freezeout at $T_{\text{freeze}} = 150$ MeV (solid: for baryons Ω^- , Ξ^- , Λ^0 and p ; dashed: for mesons η , K^- and π^+).

Right: speed of sound $c_s^2(T)$ (solid: HRG in equilibrium, dashed: partial chem. equilibrium in hadronic phase, symbols: equilibrium lattice data).

from Bluhm, Alba, Alberico, Beraudo, Ratti, arXiv:1306.6188



5. Phase transition and thermodynamics of twisted-mass fermions

For $\mu_q = 0$ lattice QCD importance sampling by Hybrid Monte Carlo works perfectly.

The problem here is only to control systematic effects of different fermion formulations.

Staggered (Kogut-Susskind) quarks

- Lattice thermodynamics is **dominated by staggered fermions** and improved variants of this (p4, asqtad, stout and HISQ).
This is computationally the cheapest method.
- The **improvements ameliorate problems** like taste symmetry breaking.
- The **fundamental problem, however, remains unanswered** : rooting, locality of the action Theoretically not completely clear !

- **Basic staggered action : 4 (degenerate) flavors, 16 d.o.f. per 2^4 cell.**
“Rooting” is the trick to get the action for N_f independent flavors :

$$\det D \text{ for } N_f \text{ flavors} = \left((\det D_{\text{staggered}})^{\frac{1}{4}} \right)^{N_f}$$

→ can make the flavors non-degenerate (different charges etc.)

Wilson fermions are the next-popular choice

- Advantage : **clear flavor interpretation.**
- **Breaks chiral symmetry completely**, hopefully restored in continuum.
- **Phase structure complicated, partly irrelevant** at finite a .
- **Considerably more CPU-intensive !**
- Twisting probes spontaneous parity-flavor breaking that leads to the **Aoiki phase at very strong coupling (keep away from this !!)**.

Two ways to improve Wilson fermion simulations to $\mathcal{O}(a)$:

- **Clover improvement** (adding a Pauli term, Sheikholeslami/Wohlert)
CP-PACS, WHOT, DIK (DESY-ITEP-Kanazawa) collaborations.
In this case, the hopping parameter κ drives the transition !
- **Twisted mass fermions** (chiral rotation within doublets, even number of flavors): ETMC, tmfT-Collaboration (HU Berlin, Frankfurt, INFN Frascati).

Advantage of twisted mass:

- **at maximal twist**, with κ set to $\kappa_c(\beta)$ (then β drives the transition !)
the twisted mass term takes the role of the mass term,
while **automatic $\mathcal{O}(a)$ improvement is guaranteed**.
Observed first by R. Frezzotti, G. C. Rossi, JHEP 0408 (2004) 007

What is twisted mass ?

Fermion action in the **physical basis** $\bar{\Psi}, \Psi$ written (see **Wilson's r -term**)

$$S_F[\Psi, \bar{\Psi}, U] = a^4 \sum_x \left[\bar{\Psi}(x) \left(\gamma_\mu \frac{1}{2a} (\nabla_\mu + \nabla_\mu^*) - \frac{ar}{2} e^{-i\omega\gamma_5\tau^3} \nabla_\mu^* \nabla_\mu + M_0 \right) \Psi(x) \right]$$

The **physical basis** $\bar{\Psi}, \Psi$ is related to the **twisted basis** $\bar{\psi}, \psi$ by the non-anomalous chiral rotation

$$\begin{aligned} \Psi &= \exp\left(i\frac{\omega}{2}\gamma_5\tau^3\right) \psi, \\ \bar{\Psi} &= \bar{\psi} \exp\left(i\frac{\omega}{2}\gamma_5\tau^3\right) \end{aligned}$$

with

$$M_0 = \sqrt{m_0^2 + \mu_0^2}, \quad \tan(\omega) = \mu_0/m_0,$$

(with M_0 , the bare polar quark mass and ω , the bare twist angle).

For maximal twist, both bases related through :

$$\Psi = \frac{1}{\sqrt{2}}(1 + i\gamma_5\tau^3)\psi \quad \text{and} \quad \bar{\Psi} = \bar{\psi}\frac{1}{\sqrt{2}}(1 + i\gamma_5\tau^3)$$

Introducing Wilson's **hopping parameter** $\kappa = 1/(2am_0 + 8r)$

and rescaling as usual $\sqrt{a^3/(2\kappa)}\psi \rightarrow \chi$ leads to the **standard form of the twisted fermion action (in the twisted basis) appearing in the simulation code :**

$$S_F[\chi, \bar{\chi}, U] = \sum_x \left[\bar{\chi}(x) (1 + i2\kappa a\mu_0\gamma_5\tau^3) \chi(x) - \kappa \sum_{\mu} \bar{\chi}(x) \left((r - \gamma_{\mu})U_{x,\mu}\chi(x + \hat{\mu}) + (r + \gamma_{\mu})U_{x-\hat{\mu},\mu}^{\dagger}\chi(x - \hat{\mu}) \right) \right]$$

This fermionic action is simulated together with **tree-level Symanzik improved gauge action** :

public code available, see <https://github.com/etmc/tmLQCD/>

$$S_G[U] = \beta \left[c_0 \sum_P \left(1 - \frac{1}{3} \text{Re} (\text{tr} [U(P)]) \right) + c_1 \sum_R \left(1 - \frac{1}{3} \text{Re} (\text{tr} [U(R)]) \right) \right]$$

where $\beta = 6/g_0^2$ and $U(P)$, $U(R)$ are **plaquette and rectangle loops**.

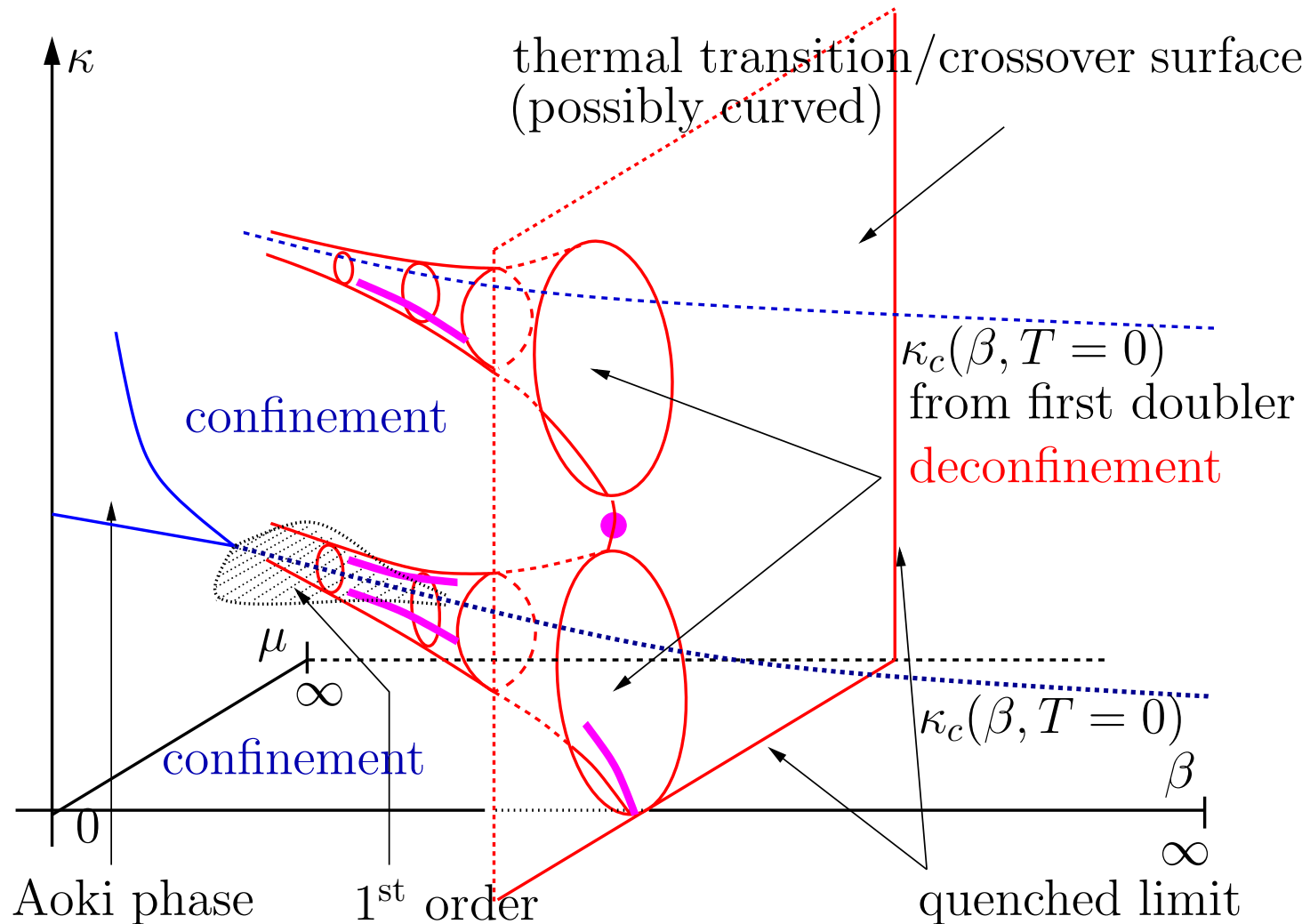
Tree-level improvement condition : $c_0 + 8c_1 = 1$, and $c_1 = -1/12$.

Outlook to future work of tmfT :

In order to describe $N_f = 2 + 1 + 1$ **flavors**, add a second, non-degenerate doublet:

$$S_F[\psi, \bar{\psi}, U] = a^4 \sum_x [\bar{\psi}_l(x) (D_W[U] + m_{0,l} + i\mu_l \gamma_5 \tau^3) \psi_l(x)] \\ + a^4 \sum_x [\bar{\psi}_h(x) (D_W[U] + m_{0,h} + i\mu_\sigma \gamma_5 \tau^1 + \mu_\delta \tau^3) \psi_h(x)]$$

Explorations of the full phase diagram for $N_f = 2$ summarized in a full 3-dimensional phase diagram (illustrating Creutz' "cone conjecture") :



What is the physically relevant branch ?

- Only the **lower cone is connected with the quenched limit !**
Varying the quark mass $\rightarrow \infty$, a **critical endpoint** is passed, at which the crossover goes over to a first order (under investigation).
The first order line ends in the **quenched endpoint** at $\kappa = 0$.
- How does a **line of constant physics (LCP)** pierce Creutz' cone ?
 - LCP **should run** at maximal twist !
 - LCP **must not run** at $\mu_0 = \text{const}$!

The details for this analysis rest on **calibration simulations at $T = 0$,**

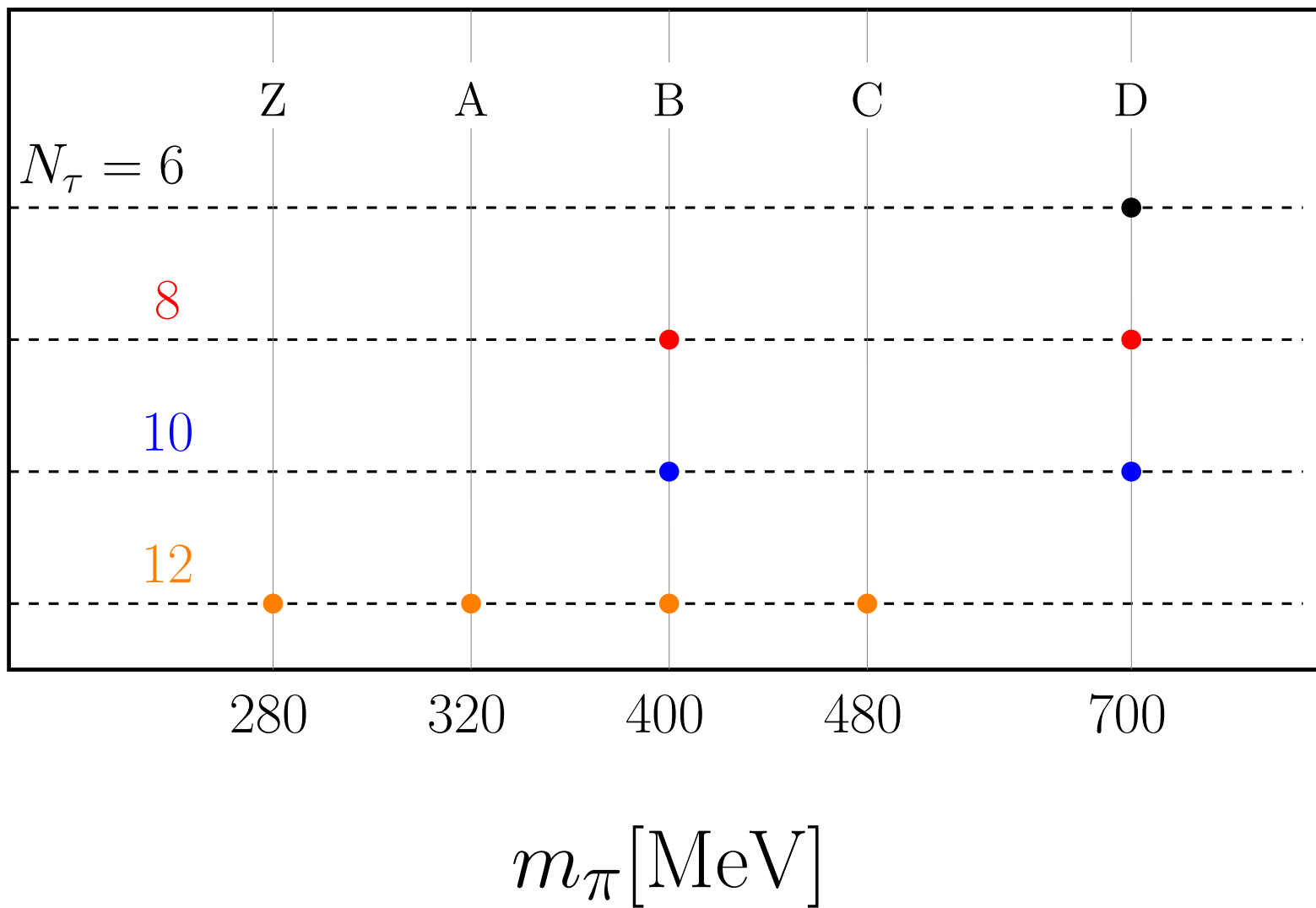
- done by the ETM Collaboration
- own simulations of the tmfT Collaboration

Locating the crossover

- Evaluated : **three families of ensembles** : A12, B12, C12
(one more becoming finished now : Z12)
- populate the **three-dimensional phase diagram** β, κ, μ_0
- a **β scan** should fix the position of the crossover line
- maximal twist: requires **tuning of** $\kappa = \kappa_c(T = 0, \beta)$
- fixed pion mass: requires **tuning of** $a\mu_0 = (a\mu_0)(\beta) = C \exp(-\beta/(12\beta_0))$

(obtained from a one-loop fit with $\beta_0 = \frac{11-2N_f/3}{(4\pi)^2}$ or from a two-loop fit)

- such **fits for various families of $T = 0$ simulations** based on data of the ETM-Collaboration exist [published JHEP 08 097 (2010)]



List of β -scans

- **A12:** $32^3 \times 12$, $3.84 \leq \beta \leq 3.99$,
 $m_\pi = 316(16)$ **MeV**, $r_0 m_\pi = 0.673(42)$
 $\beta_\chi = 3.89(3)$, $T_\chi = 202(7)$ **MeV**
- **B12:** $32^3 \times 12$, $3.86 \leq \beta \leq 4.35$,
 $m_\pi = 398(20)$ **MeV**, $r_0 m_\pi = 0.847(53)$
 $\beta_\chi = 3.93(2)$, $T_\chi = 217(5)$ **MeV**
 $\beta_{\text{deconf}} = 4.027(14)$, $T_{\text{deconf}} = 249(5)$ **MeV**
- **C12:** $32^3 \times 12$, $3.90 \leq \beta \leq 4.07$,
 $m_\pi = 469(24)$ **MeV**, $r_0 m_\pi = 0.998(62)$
 $\beta_\chi = 3.97(3)$, $T_\chi = 229(5)$ **MeV**
 $\beta_{\text{deconf}} = 4.050(15)$, $T_{\text{deconf}} = 258(5)$ **MeV**

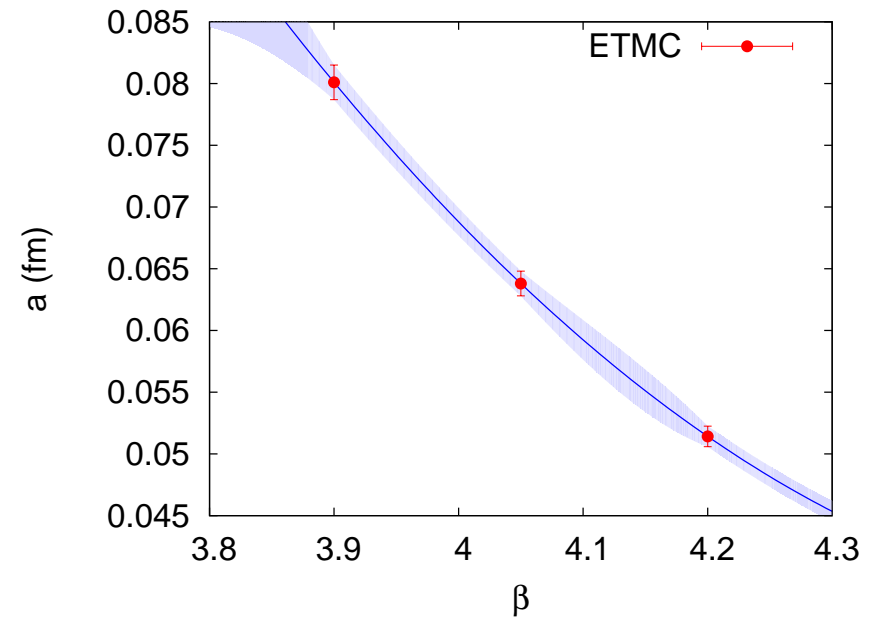
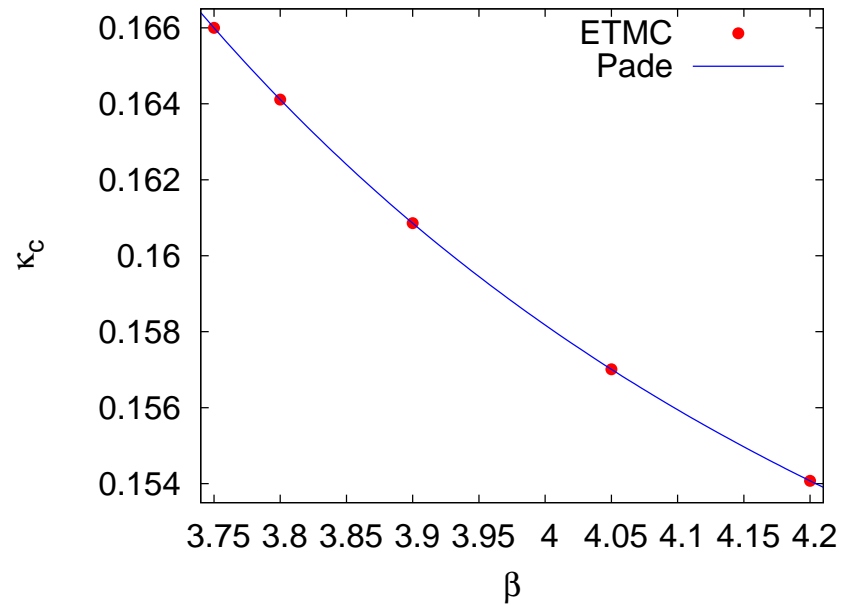
m_π -dependence and chiral extrapolations are discussed in papers :

- arXiv:1102.4530v2 (F. Burger et al.) Phys. Rev. D 87 (2013) 074508
- arXiv:1212.0982 (F. Burger at Lattice 2012)

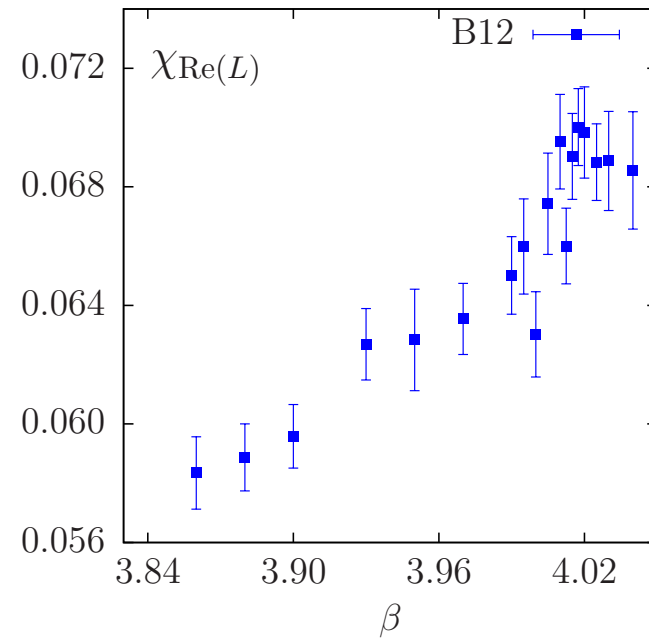
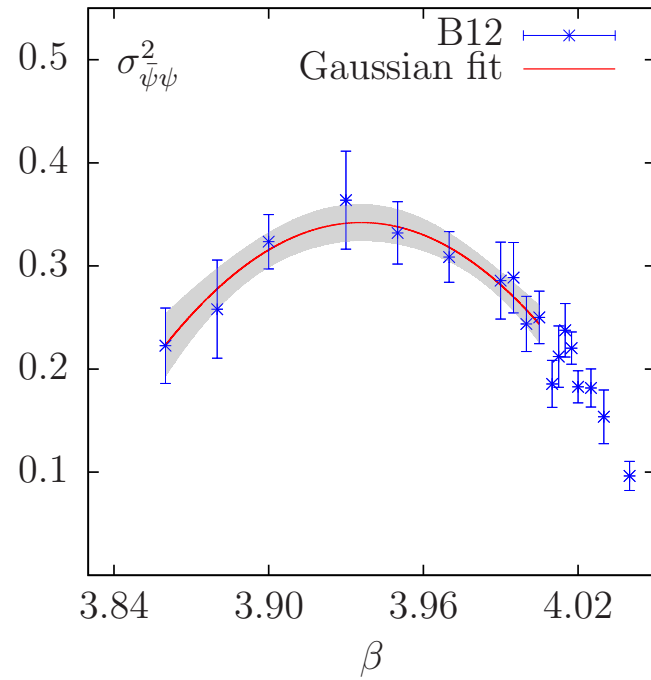
Global phase structure (for all β, κ, μ_0) had been discussed earlier in :

- arXiv:0905.3112 (E.-M. I., K. Jansen et al.) Phys. Rev. D 80 (2009) 094502

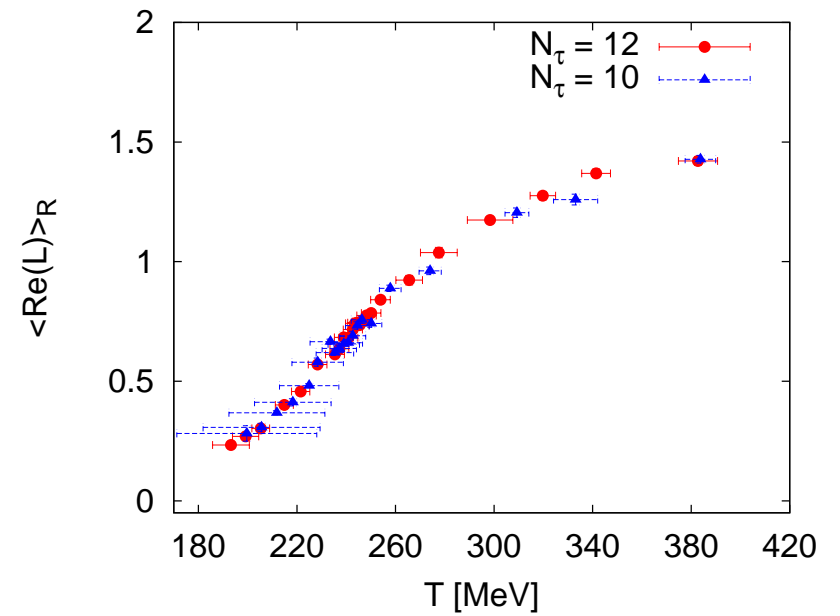
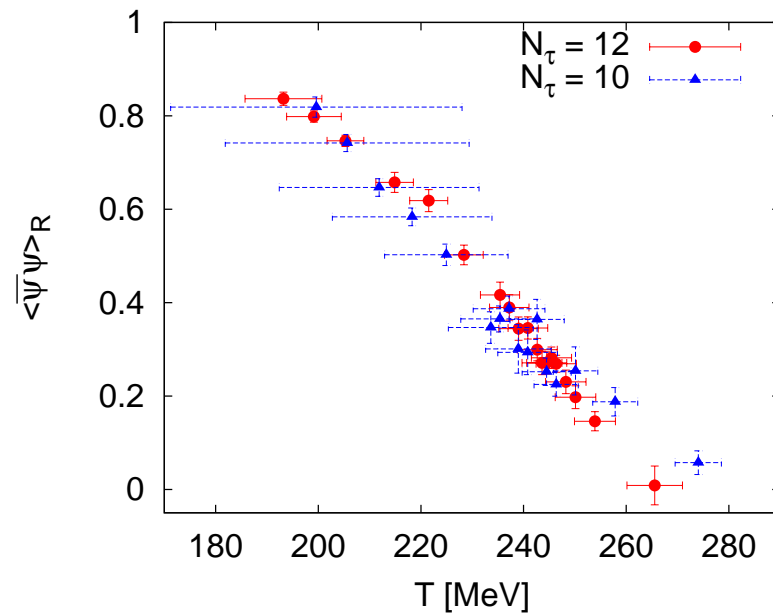
$\kappa_c(T=0, \beta)$ and the lattice spacing $a(\beta)$



Chiral susceptibility and Polyakov loop susceptibility for B12



Renormalized $\langle \bar{\psi}\psi \rangle_R$ and renormalized Polyakov loop $\langle \text{Re}(L) \rangle_R$
combining data from B12 and B10 ($N_t = 10$ and $N_t = 12$)



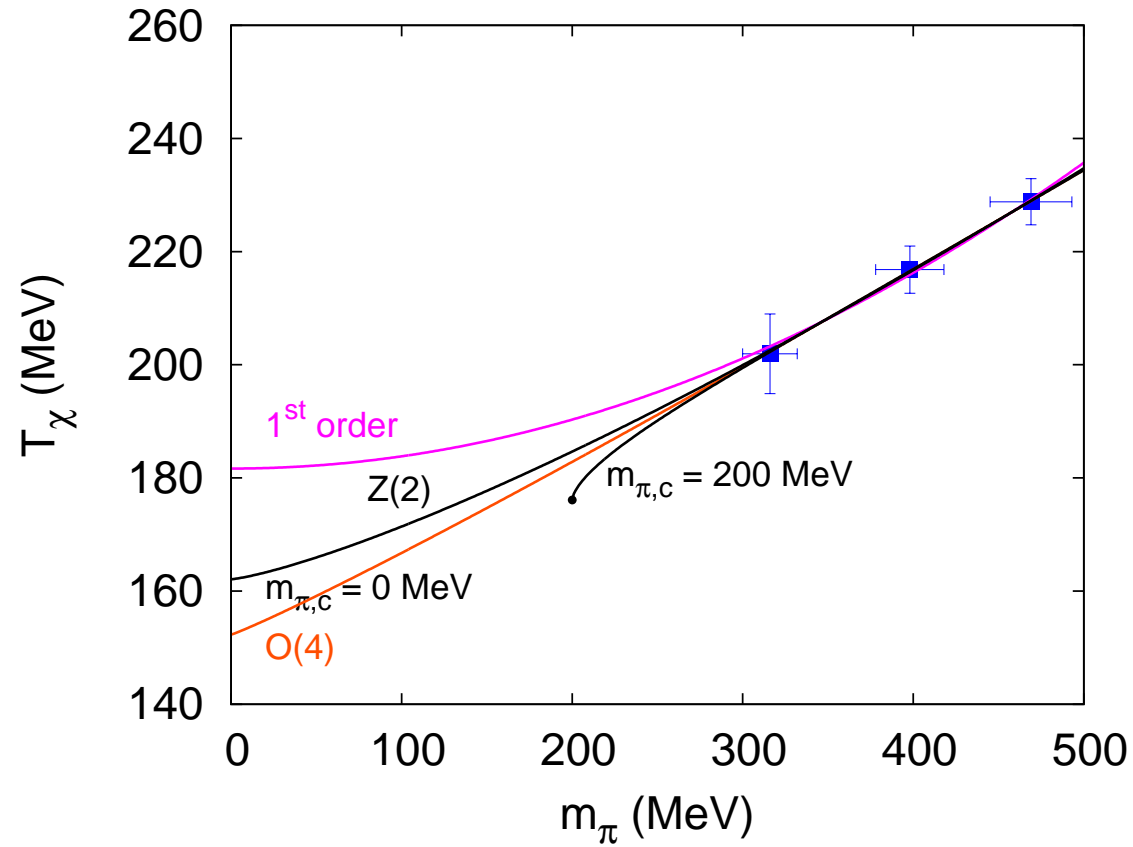
Chiral extrapolations for $T_\chi(m_\pi)$ for various scenarios (χ PT)

$$T_\chi(m_\pi) = T_\chi(m_\pi = 0) + A m_\pi^{2/(\tilde{\beta}\delta)}$$

with critical indices $\tilde{\beta}$, δ corresponding to the respective equivalence classes of **three-dimensional spin models**.

- $O(4)$: $2/(\tilde{\beta}\delta) = 1.08$ leads to $T_\chi(m_\pi = 0) = 152(26)$ MeV
- $Z(2)$: two cases $m_{\pi,c} = 0$ or $m_{\pi,c} \neq 0$;
lead to $T_\chi(m_\pi \rightarrow 0)$ **between $O(4)$ and 1-st order scenario**
- **first order** : in literature formally $2/(\tilde{\beta}\delta) = 2$ is taken;
leads to $T_\chi(m_\pi = 0) = 182(14)$ MeV
(applicability of these “critical indices” unclear !)

Chiral extrapolations for $T_\chi(m_\pi)$ for various scenarios



Towards the Equation of State (EoS)

The trace anomaly is the primary quantity on the lattice

$$\begin{aligned} \frac{I}{T^4} &= \frac{\epsilon - 3p}{T^4} = -\frac{T}{VT^4} \left\langle \frac{d \ln Z}{d \ln a} \right\rangle_{\text{sub}} \\ &= N_\tau^4 B_\beta \frac{1}{N_\sigma^3 N_\tau} \left\{ \begin{aligned} &\frac{c_0}{3} \langle \text{ReTr} \sum_P U_P \rangle_{\text{sub}} \\ &+ \frac{c_1}{3} \langle \text{ReTr} \sum_R U_R \rangle_{\text{sub}} \\ &+ B_\kappa \langle \bar{\chi} D_W[U] \chi \rangle_{\text{sub}} \\ &- [2(a\mu) B_\kappa + 2\kappa_c(a\mu) B_\mu] \langle \bar{\chi} i \gamma_5 \tau^3 \chi \rangle_{\text{sub}} \end{aligned} \right\} \end{aligned}$$

$\langle \dots \rangle_{\text{sub}} \equiv \langle \dots \rangle_{T>0} - \langle \dots \rangle_{T=0}$ denotes **subtraction of vacuum contributions.**

B_β , B_μ and B_κ are (related to) **derivatives of the bare parameters with respect to the lattice spacing :**

$$B_\beta = a \frac{d\beta}{da}, \quad B_\mu = \frac{1}{(a\mu)} \frac{\partial(a\mu)}{\partial\beta}, \quad B_\kappa = \frac{\partial\kappa_c}{\partial\beta}$$

Evaluation of the pressure by integrating the identity

$$\frac{I}{T^4} = T \frac{\partial}{\partial T} \left(\frac{p}{T^4} \right)$$

along the line of constant physics (LCP):

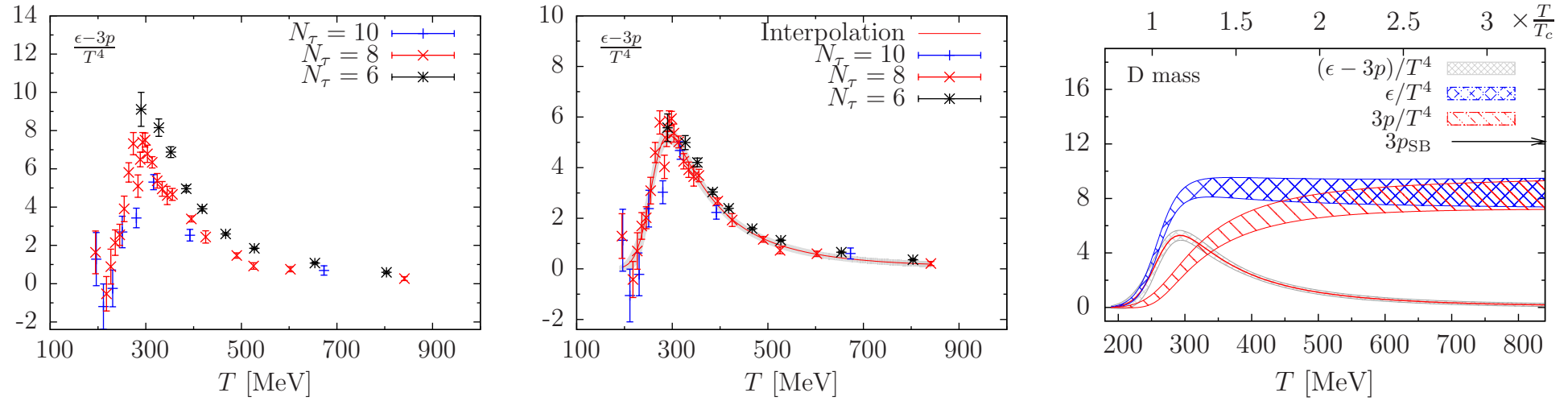
$$\frac{p}{T^4} - \frac{p_0}{T_0^4} = \int_{T_0}^T d\tau \frac{\epsilon - 3p}{\tau^5} \Big|_{\text{LCP}}$$

The available lattice data of $\frac{I}{T^4}$ have been fitted to the ansatz

$$\frac{I}{T^4} = \exp(-h_1 \bar{t} - h_2 \bar{t}^2) \cdot \left(h_0 + \frac{f_0 \{ \tanh(f_1 \bar{t} + f_2) \}}{1 + g_1 \bar{t} + g_2 \bar{t}^2} \right)$$

where $\bar{t} = T/T_0$ and T_0 is a free parameter in the fit.

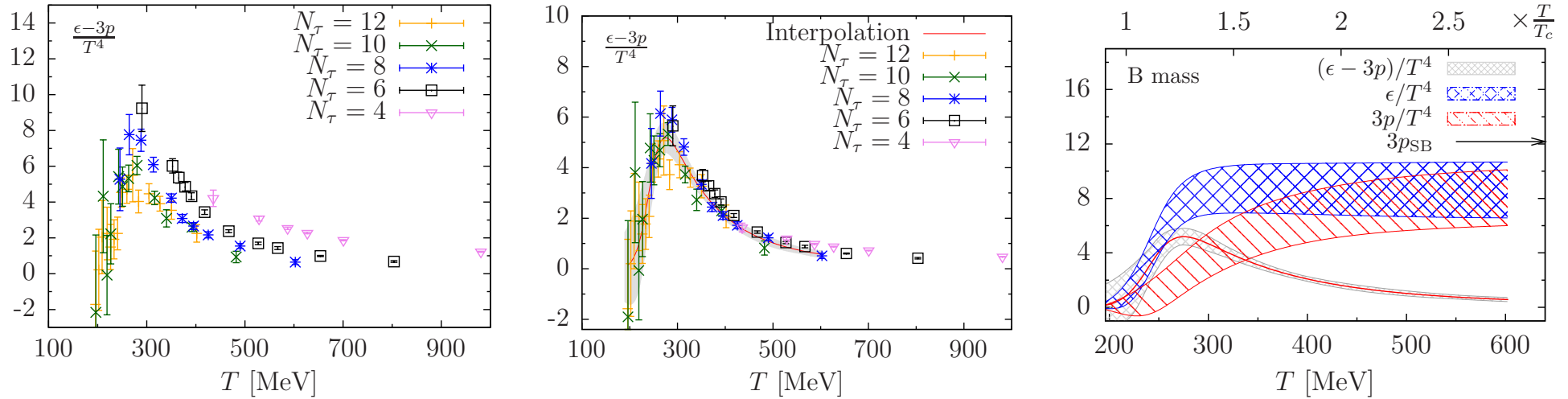
For the D ensembles data from $N_\tau = 8, 10$ have been fitted simultaneously.



Still preliminary : EoS for the D ensembles ($m_\pi \approx 700$ MeV)

Left: raw data for I , Middle: after tree-level corrections, Right: trace anomaly, pressure and energy density.

For the B ensembles data from $N_\tau = 8, 10$ and 12 have been fitted simultaneously.



Still preliminary : EoS for the B ensembles ($m_\pi \approx 400$ MeV)

Left: raw data for I , Middle: after tree-level corrections, Right: trace anomaly, pressure and energy density.

6. A special topic : Gluon and ghost propagators in Landau gauge

- Performing the Landau gauge fixing on a given ensemble of gauge field configurations gives the possibility to study gluon and ghost propagators in straightforward way. (Problem : Gribov ambiguity)
- We have done this for pure gluodynamics ($N_f = 0$) in the vicinity of the first order phase transition, and later for the relevant ensembles of full QCD configurations ($N_f = 2$) over the crossover region.
- Non-perturbative continuum techniques (DSE and FRG) are based on propagators and vertices : thermodynamics and various effective potentials, e.g. for the Polyakov loop, expressed through propagators.
- The propagators for gluodynamics and full QCD appear in Dyson-Schwinger equations (DSE). Lattice data allow crosschecks of the predictions by DSE relating quenched and non-quenched propagators.

Landau gauge

$$\nabla_\mu A_\mu(x) = \sum_\mu (A_\mu(x + \hat{\mu}/2) - A_\mu(x - \hat{\mu}/2)) = 0$$

where

$$A_\mu(x + \hat{\mu}/2) = \frac{1}{2ia g_0} (U_{x\mu} - U_{x\mu}^\dagger)_{|traceless}$$

can be enforced by **maximization** of the functional

$$F_U[g] = \frac{1}{3} \sum_{x,\mu} \text{Re tr} \left(g_x U_{x\mu} g_{x+\mu}^\dagger \right)$$

with suitable gauge transformations g_x (including twisted ones g'_x !).

- **Gauge fixing** is performed for relevant ensembles of Monte Carlo configurations, **irrespective of their origin** (quenched or dynamic).
- **Ghosts are not explicit, studied only algebraically**, by inversion of the Faddeev-Popov operator.

- We have studied the quark propagator for the gluon configurations generated with twisted mass fermions by the TMC : F. Burger et al., Phys.Rev. D 87 (2013) 034514, arXiv:1210.0838 [hep-lat]
- Our aim was to study the effect of the crossover on the gluon (and ghost) propagator in presence of quarks.
- For quenched $SU(3)$ gauge theory, the first order transition should lead to the strongest relative change of the propagator.
- To set a benchmark, we investigated first the finite T propagators for pure gauge theory !

Problem of Gribov copies turned out to be severe only in the **extreme infrared (IR) limit**, i.e. **practically irrelevant** for the following analyses !

The aim was to find a good **continuum parametrization** for the propagators,

- over a **relatively broad momentum interval**,
- for a **series of temperatures** around the transition/crossover temperature and **ranging up to $3 T_{\text{deconf}}$** ,

in order to provide this to the practitioners of continuum approaches (SDE and FRG) enabling crosschecks for their methods and approximations.

First step : quenched propagator study at finite T

R. Aouane et al., Phys. Rev. D 85 (2012) 034501

arXiv:1108.1735 [hep-lat] (with Wilson action, for various lattices)

Glue propagator in momentum space as ensemble average :

$$D_{\mu\nu}^{ab}(q) = \left\langle \tilde{A}_\mu^a(k) \tilde{A}_\nu^b(-k) \right\rangle$$
$$q_\mu(k_\mu) = \frac{2}{a} \sin\left(\frac{\pi k_\mu}{N_\mu}\right) \quad \text{for Matsubara frequency } q_4 = 0$$

For non-zero temperature, Euclidean invariance is broken,
useful to split $D_{\mu\nu}^{ab}(q)$ into two components, ($N_g = N_c^2 - 1$ and $N_c = 3$)

- **transversal D_T (“chromomagnetic”)** propagator
- **longitudinal D_L (“chromoelectric”)** propagator

$$D_{\mu\nu}^{ab}(q) = \delta^{ab} \left(P_{\mu\nu}^T D_T(q_4^2, \vec{q}^2) + P_{\mu\nu}^L D_L(q_4^2, \vec{q}^2) \right)$$

Propagators $D_{T,L}$ (or their respective dimensionless **dressing functions** $Z_{T,L}(q) = q^2 D_{T,L}(q)$) obtained from the Fourier transforms

$$D_T(q) = \frac{1}{2N_g} \left\langle \sum_{i=1}^3 \tilde{A}_i^a(k) \tilde{A}_i^a(-k) - \frac{q_4^2}{\vec{q}^2} \tilde{A}_4^a(k) \tilde{A}_4^a(-k) \right\rangle$$

and

$$D_L(q) = \frac{1}{N_g} \left(1 + \frac{q_4^2}{\vec{q}^2} \right) \left\langle \tilde{A}_4^a(k) \tilde{A}_4^a(-k) \right\rangle$$

The **corresponding renormalized functions**, in momentum subtraction (MOM) schemes, can be obtained from

$$\begin{aligned} Z_{T,L}^{ren}(q, \mu) &\equiv \tilde{Z}_{T,L}(\mu) Z_{T,L}(q) \\ J^{ren}(q, \mu) &\equiv \tilde{Z}_J(\mu) J(q) \end{aligned}$$

with the \tilde{Z} -factors being defined such that

$$\begin{aligned} Z_{T,L}^{ren}(\mu, \mu) &= 1 \\ J^{ren}(\mu, \mu) &= 1 \end{aligned}$$

Our main emphasis : Finite-volume and discretization studies, providing continuum parametrizations for various temperatures, as input (or benchmark) for finite- T continuum studies (within SDE and FRG), with eventual extensions to finite baryonic density !

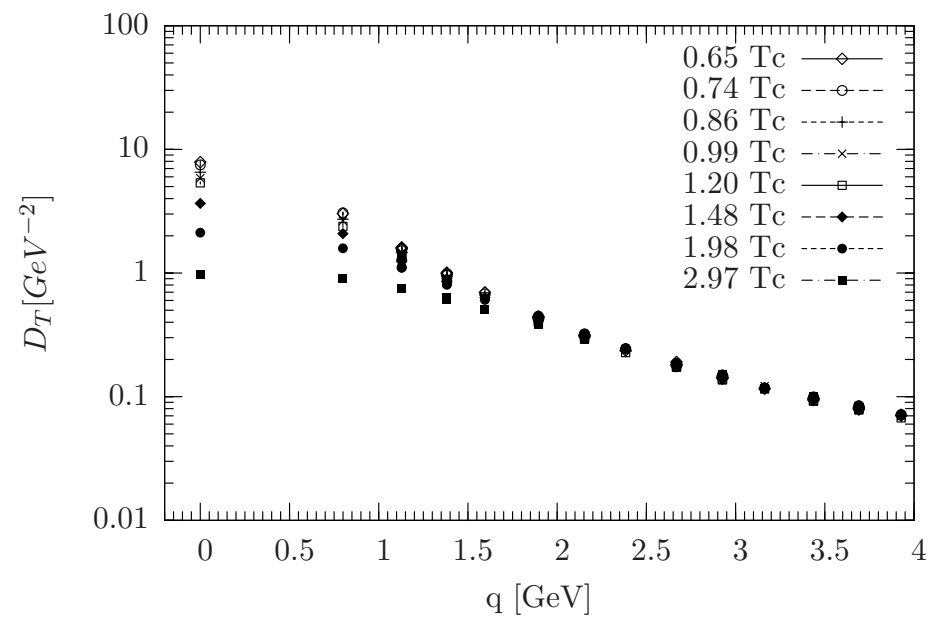
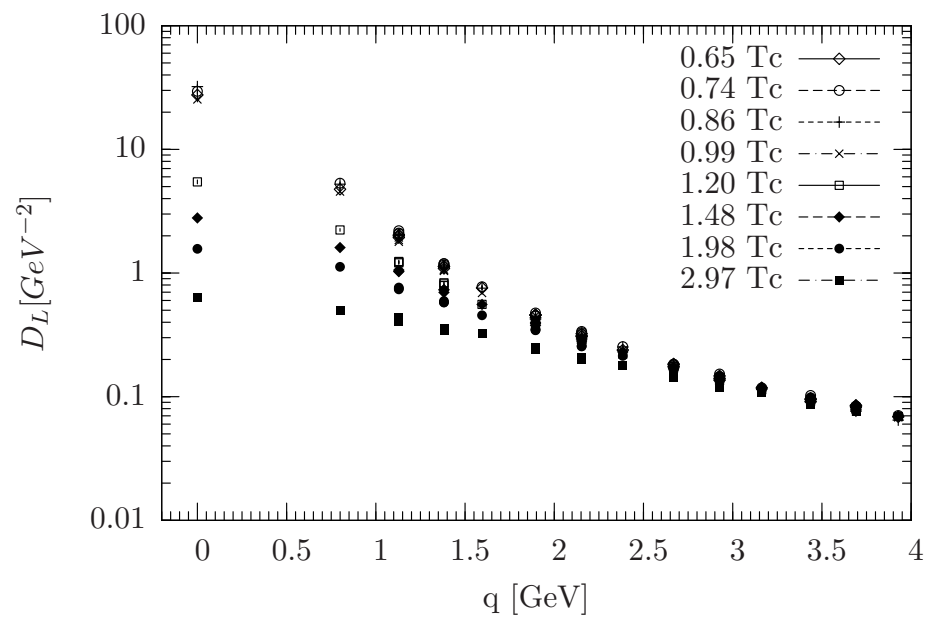
The gluon dressing function was fitted with the **Gribov-Stingl formula**

$$Z_{\text{fit}}(q) = q^2 \frac{c (1 + d q^{2n})}{(q^2 + r^2)^2 + b^2}$$

- fits of the momentum dependence of the propagators in the interval $0.6 \text{ GeV} < q < 3.0 \text{ GeV}$
- in the temperature range up to $3 T_{\text{dec}}$
 $0.65 < T/T_{\text{deconf}} < 2.97$
- Gribov copy and finite volume effects of minor importance in the momentum range under study

While the first order nature of the phase transition is obvious,
no abrupt changes have been found in the propagators !

q dependence of D_L and D_T for various temperatures



It is not difficult to reconcile the first order phase transition with these continuous changes of the propagators !

Our finite-temperature results for pure Yang-Mills theory have been used by [K. Fukushima and K. Kashiwa, arXiv:1206.0685v5 \[hep-ph\]](#)

- for the **effective potential for the Polyakov loop**
- for **reconstructing the Equation of State (EoS)**

In leading order of the 2PI-formalism, the **thermodynamical potential can be approximated** as follows in terms of the gluon and ghost propagators :

$$\frac{1}{T}\Omega_{\text{glue}} \simeq -\frac{1}{2}\text{tr} \ln D_{\text{gl}}^{-1} + \text{tr} \ln D_{\text{gh}}^{-1}$$

For example, the inverse gluon propagator has been extracted from our data for $T < 1.2 T_c$

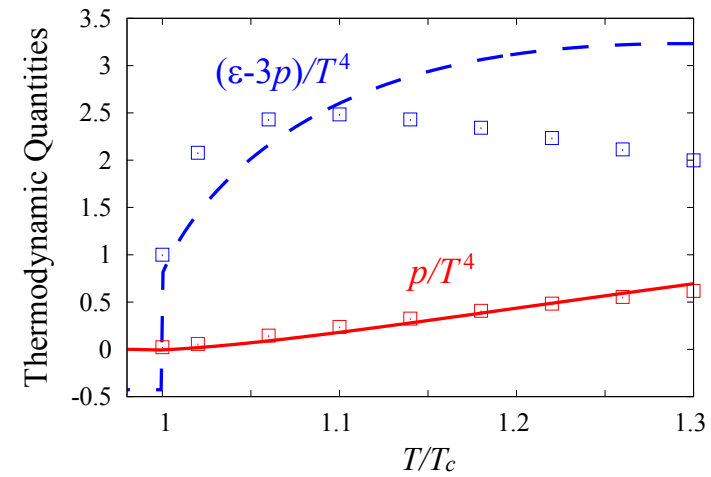
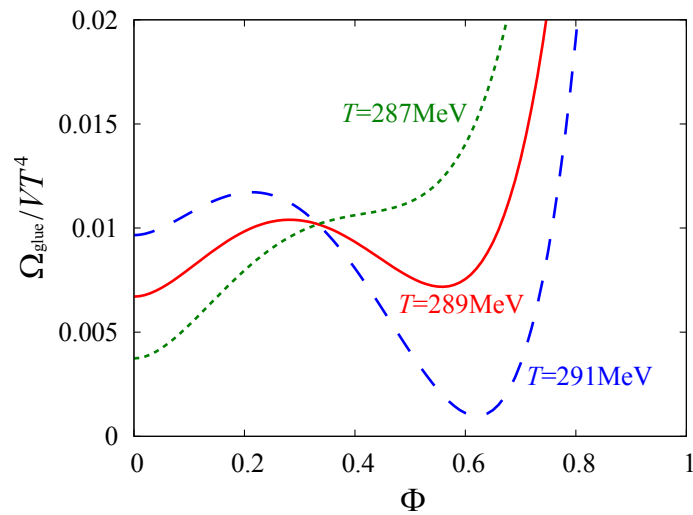
$$D_{\text{gl}}^{-1}(p^2) = \left[p^2 Z_T(p^2) T_{\mu\nu} + \xi^{-1} p^2 Z_L(p^2) L_{\mu\nu} \right] \delta^{ab}$$

Results :

- The transition temperature has been successfully reconstructed in terms of the Polyakov loop effective potential from the T -dependent propagator data.
- The pressure and trace anomaly are obtained, respectively, good and roughly correct.

Order parameter and EoS of pure Yang-Mills

Transition temperature and first rise of pressure successfully reconstructed from the T -dependent propagator data !



What about propagators from non-quenched simulations ?

How are non-quenched gluon propagators related to quenched ones ?

How good can SDE predict/postdict what will be/has been measured on the lattice ?

C. S. Fischer and J. Luecker, “Propagators and phase structure of $N_f = 2$ and $N_f = 2 + 1$ QCD”

Physics Letters B 718 (2013) 1036, arXiv:1206.5191,

also in: C. S. Fischer, L. Fister, J. Luecker, J. M. Pawłowski, “Polyakov loop potential at finite density”, arXiv:1306.6022

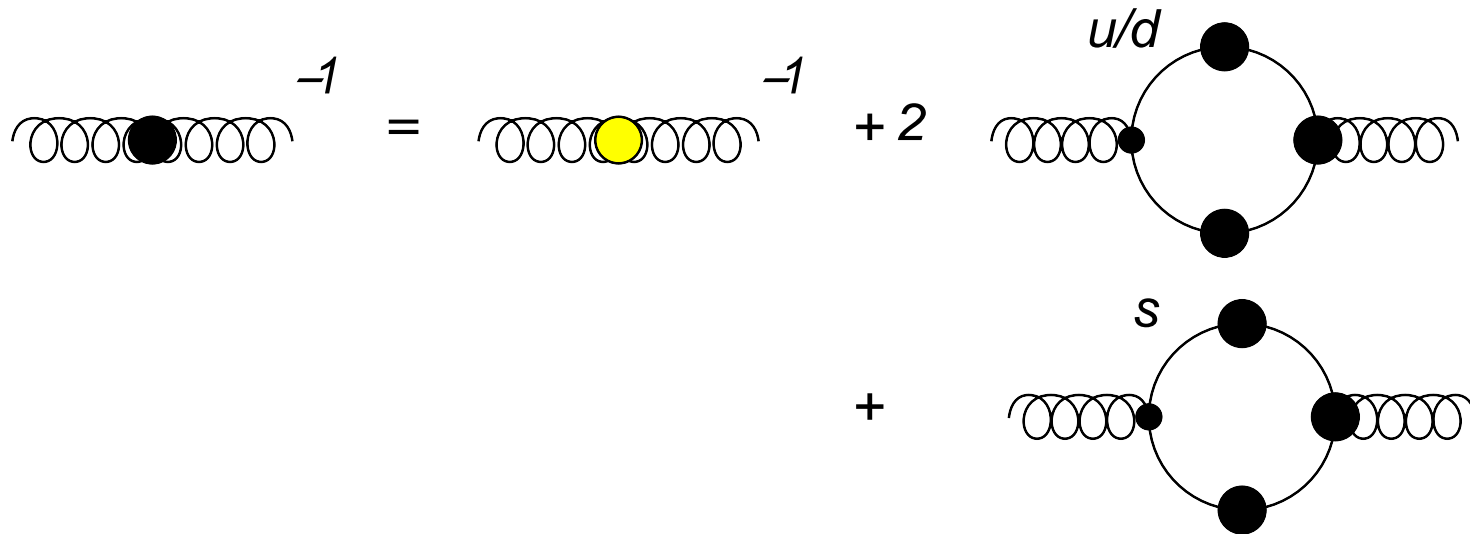
Full set of Schwinger-Dyson equations is used to predict the T dependence of full QCD propagators from the quenched ones, depending on m_π as a parameter to be measured in the non-quenched simulations (crossover).

Full Dyson-Schwinger equations for the quark and the gluon propagator

The diagram shows the Dyson-Schwinger equation for the quark propagator. On the left, a solid horizontal line with a black dot in the middle is followed by an equals sign and a superscript -1 . This is equal to a solid horizontal line with an arrow pointing to the right, followed by a plus sign and a superscript -1 . This is then followed by a plus sign and a diagram of a self-energy correction: a solid horizontal line with two black dots, with a semi-circular gluon loop (represented by a chain of small circles) connecting the two dots.

The diagram shows the Dyson-Schwinger equation for the gluon propagator. On the left, a wavy horizontal line with a black dot in the middle is followed by an equals sign and a superscript -1 . This is equal to a wavy horizontal line with a superscript -1 , followed by a plus sign and a diagram of a ghost loop (a dashed line forming a circle with two black dots), followed by a plus sign and a diagram of a quark loop (a solid line forming a circle with two black dots). Below this, there are two more rows of diagrams, each preceded by a plus sign. The first row contains two diagrams: a wavy line with a circular loop containing four black dots, and a wavy line with a circular loop containing two black dots. The second row contains two diagrams: a wavy line with a circular loop containing four black dots, and a wavy line with a circular loop containing two black dots.

Truncated gluon Dyson-Schwinger equation relating the quenched and the non-quenched gluon propagator (for u, d and evtl. s quarks)
 (yellow insert = quenched gluon propagator)



By-product of this study : quark propagator at $T \neq 0$
(was not yet studied by us for twisted mass at $T \neq 0$)

Would be interesting to compare !

More recently, [Phys. Rev. D 87 \(2013\) 114502](#), [arXiv:1212.1102](#)

“Landau gauge gluon and ghost propagators from lattice QCD with $N_f = 2$ twisted mass fermions at finite temperature”

R. Aouane, F. Burger, E.-M. I., M. Müller-Preussker, A. Sternbeck

has provided the unquenched propagators for twisted mass ensembles of the tmfT collaboration, leading to continuum parametrizations in the momentum ranges :

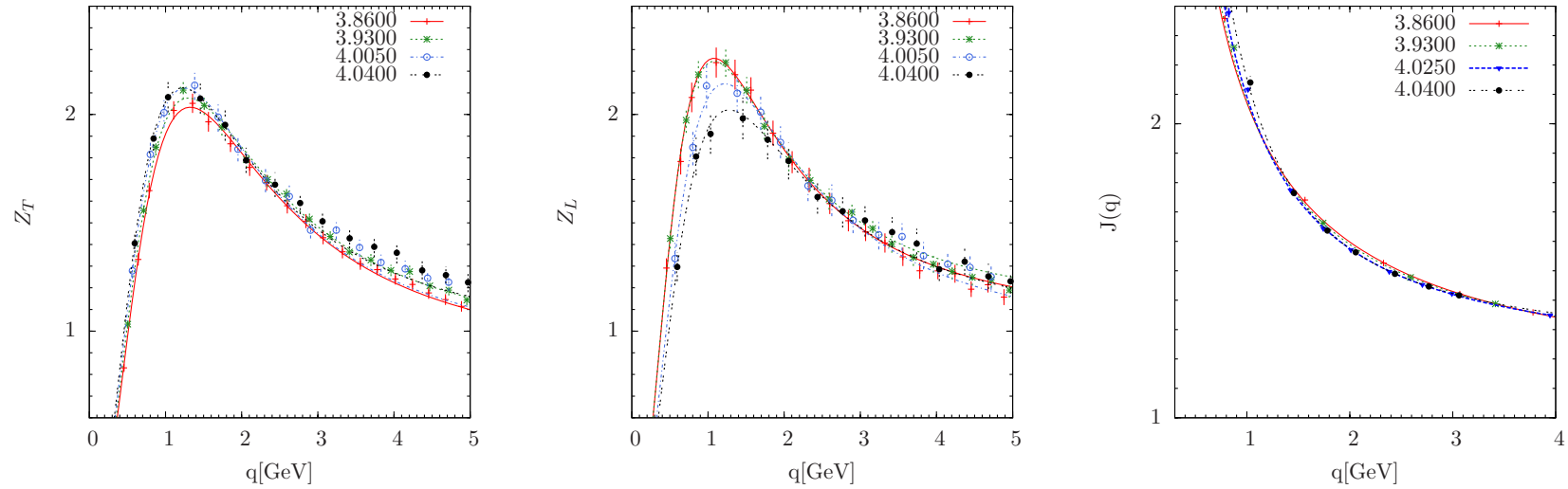
- $0.4 \text{ GeV} < q < 3.0 \text{ GeV}$ for the gluon propagators (perfect fit !)
fitting parameter b^2 in the Gribov-Stingl fit compatible with zero (no splitting in complex conjugate poles visible in this momentum range !)
- $0.4 \text{ GeV} < q < 4.0 \text{ GeV}$ for the ghost propagator (less good, fit correct within few percent, a mass term m_{gh} wouldn't help),

Temperature range :

- Done for various temperatures in the range $180 \text{ MeV} < T < 260 \text{ MeV}$ which were investigated in the “phase transition project”.

Renormalized propagators given for renormalization scale $\mu = 2.5 \text{ GeV}$.

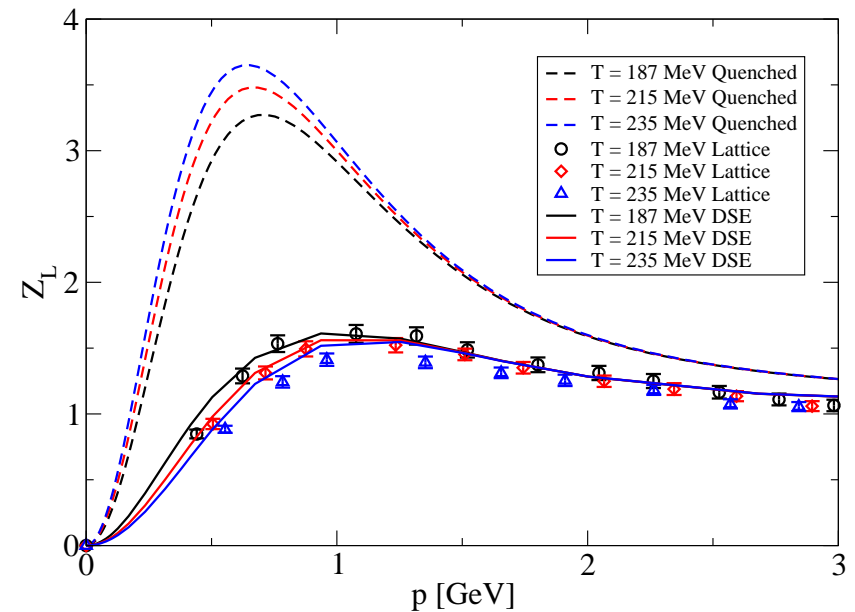
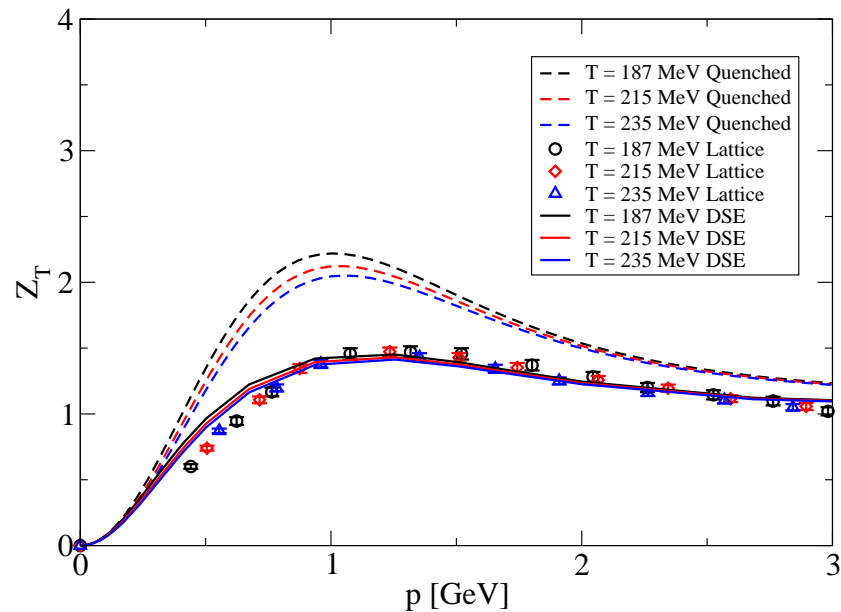
The unrenormalized dressing functions, Z_T (left panel), Z_L (middle panel) and for the ghost J (right panel) for various temperatures, B12 for $m_\pi = 398$ MeV



How are non-quenched gluon propagators related to quenched ones in the crossover region ?

C. S. Fischer, L. Fister, J. Luecker, J. M. Pawłowski,
“Polyakov loop potential at finite density”, arXiv:1306.6022

Dressing functions Z_T (left) and Z_L (right) with and without dynamical fermions from lattice and related through DSE



Conclusions concerning twisted mass at finite temperature

- The $N_f = 2$ **crossover structure** and the investigation of its chiral limit are **close to completion**.
- The results are in fair **agreement with** other results with **Wilson fermions** (DIK collaboration) and **other lattice fermions**.
- The **EoS** is will be presented **soon in full detail** (F. Burger).
- **Chiral crossover and deconfinement (hard to find) do not coincide**.
- The **effect of the crossover** on the gluon propagator is **visible**.
Masses too large ! Longitudinal gluon propagator most sensitive.
- Interesting **cross-checks with SDE** (Ch. Fischer et al.) !
- Future orientation of the **tmfT collaboration** ?
We will **turn to $N_f = 2 + 1 + 1$ simulations**.

- Strange and charmed quarks are less important for finding the chiral transition temperature. However, they are **important for the thermodynamics of the deconfined phase !**
- A **PRACE** (Partnership for Advanced Computing in Europe) **project** has been submitted by the tmfT collaboration.

7. Scanning the full phase diagram : Finite baryonic density

Let's next discuss the **generalization to non-zero baryon density**, the phase diagram in the $T - \mu_q$ plane. It is sufficient to consider $\mu_q \geq 0$.

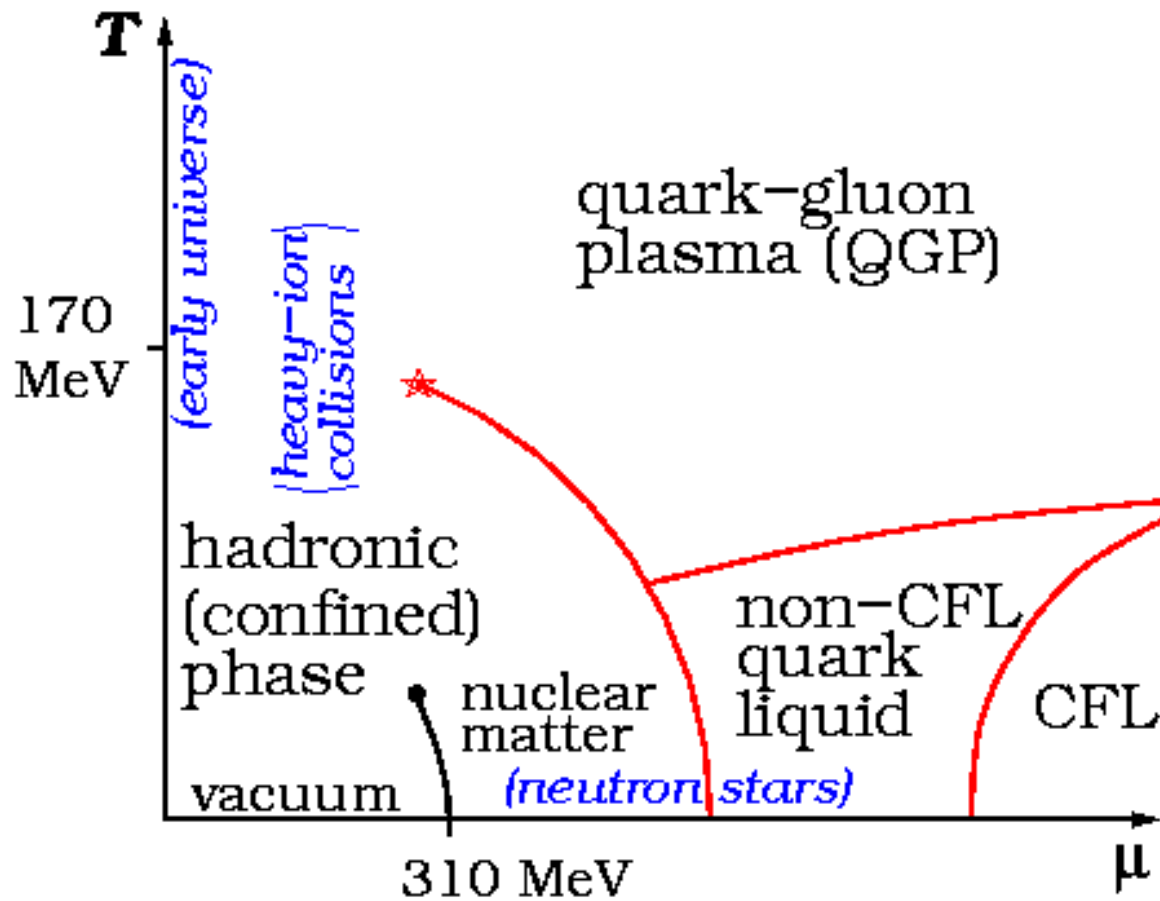
If one could simply simulate at any μ_q , one could map out the phase diagram by β -scans for all interesting μ_q or along fixed μ_q/T .

Unfortunately, **importance sampling simulation at $\mu_q \neq 0$ is impossible !**

Four main possibilities to fight the sign (complex weight) problem :

- Analytical continuation from imaginary $\mu_q = i\eta$ (for selected results)
- Phase quenching : neglecting the phase of the determinant during simulation, including it into the observable
- Reweighting across the β - μ_q plane
- Taylor expansion in μ_q in points along the β -axis

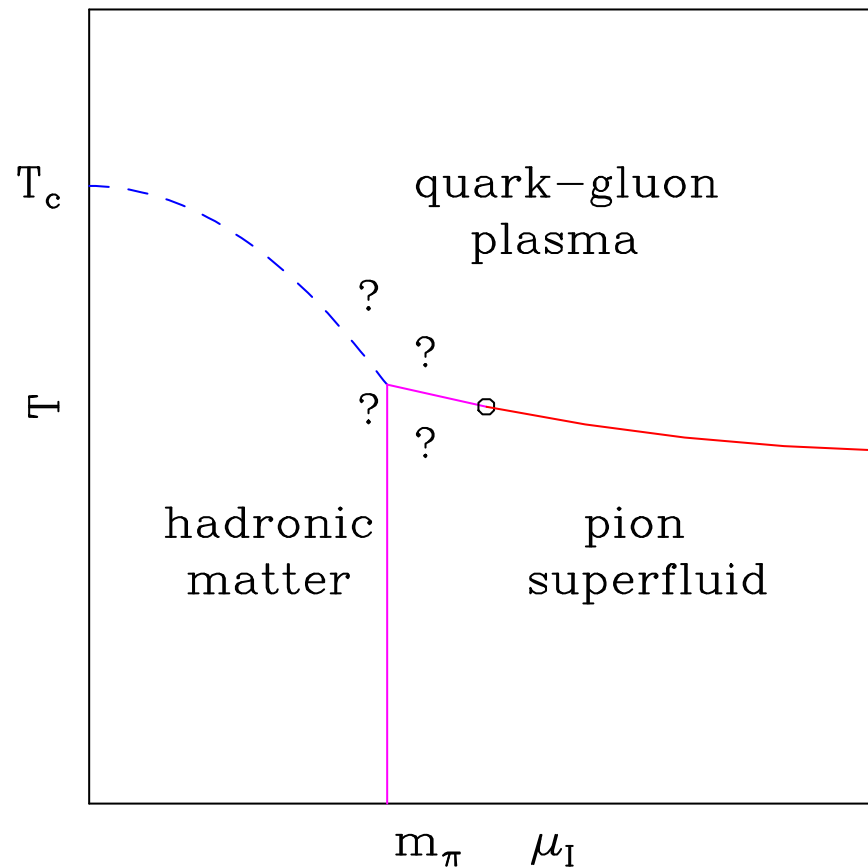
Hypothetic phase diagram of QCD (from Wikipedia)
after Ph. de Forcrand arXiv:1005.0539



What if one ignores the phase of the fermion determinant ?

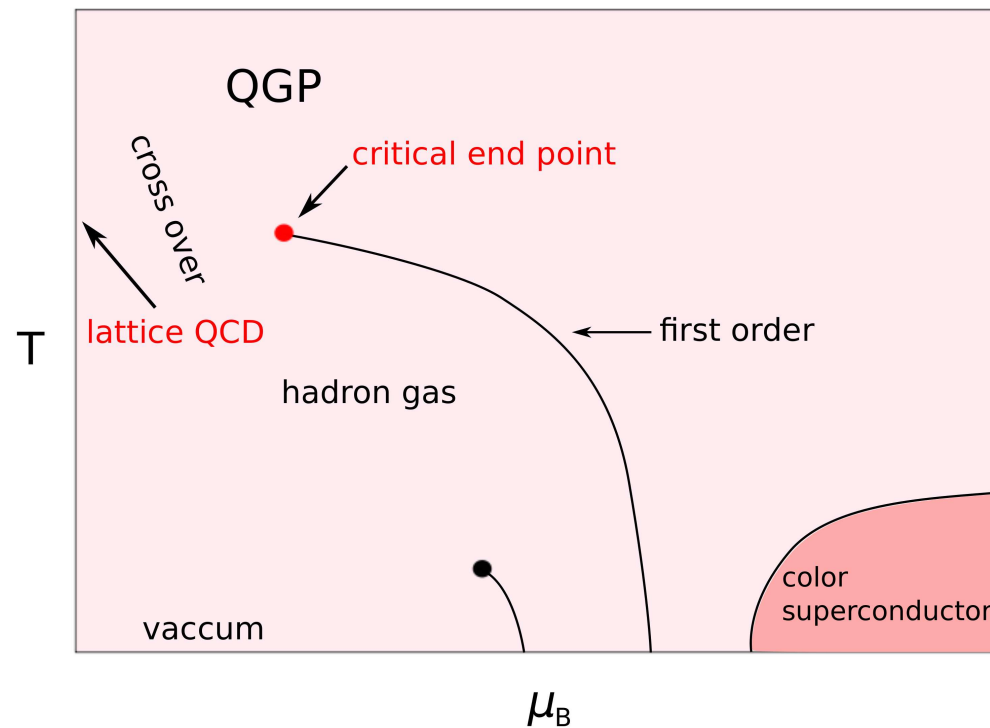
This would give the phase diagram for QCD at finite isospin density schematically, from Philipsen arXiv:1009.4089

$N_f=2$ QCD at finite isospin density

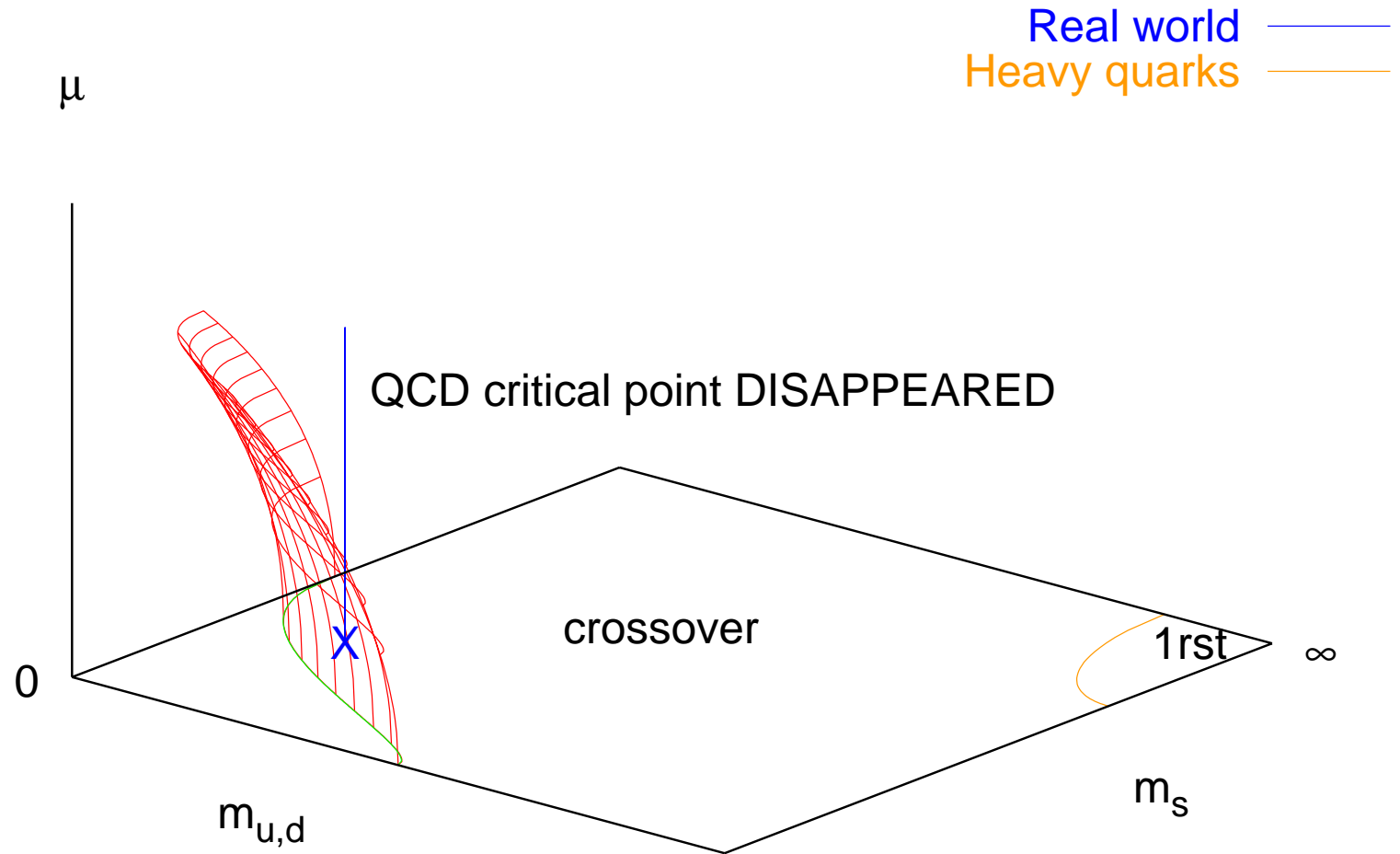


Crossover vs. First Order Transition in the Phase Diagram of QCD

from Anyi Li arXiv:1002:4459



The Columbia plot extended into a third direction μ : will there be a true phase transition (critical point) for physical quark masses ?
from Ph. de Forcrand and O. Philipsen hep-lat/0607017



Can we get the phase transition curve directly from experiment ?

From central Pb+Pb (Au+Au) collisions at SIS, AGS, SPS and RHIC the **collision energy dependence of temperature and baryonic chemical potential** (both obtained from particle yields, say via THERMUS) has been found

in the form (s_{NN} is the center of mass energy of a single nucleon pair) ;

$$\mu_B = \frac{1.308}{1 + 0.273\sqrt{s_{NN}}}$$

This μ_B enters the (chemical) “freeze-out” temperature $T_{\text{freeze}}(\mu_B)$ close to the phase transition (crossover) temperature at vanishing baryon density, $T_\chi(\mu = 0) = 0.166$ GeV parametrized as follows :

$$\frac{T_{\text{freeze}}(\mu)}{T_\chi(\mu = 0)} = 1 - 0.023 \left(\frac{\mu_B}{T}\right)^2 - \mathcal{O}\left(\left(\frac{\mu}{T}\right)^4\right)$$

J. Cleymans Phys. Rev. C 63 (2006) 034905

This has motivated the interest in lattice results for the μ dependence of the phase transition temperature $T_\chi(\mu)$ near $T_\chi(0)$ (it is not too hard).

$T_\chi(\mu)$ must be an even function of μ near $\mu = 0$.

$$\frac{T_\chi(\mu)}{T_\chi(\mu = 0)} = 1 - \sum_k t_{2k} \left(\frac{\mu}{T}\right)^{2k}$$

The curvature found on the lattice is much smaller than that of the freeze-out curve :

$$\frac{T_\chi(\mu)}{T_\chi(\mu = 0)} = 1 - 0.0066(7) \left(\frac{\mu}{T}\right)^2$$

Similarly

$$\frac{\beta_\chi(\mu)}{\beta_\chi(\mu = 0)} = 1 - \sum_k b_{2k} \left(\frac{\mu}{T}\right)^{2k}$$

The coefficients have been determined at imaginary $\mu = i\eta$.

A. Analytical continuation

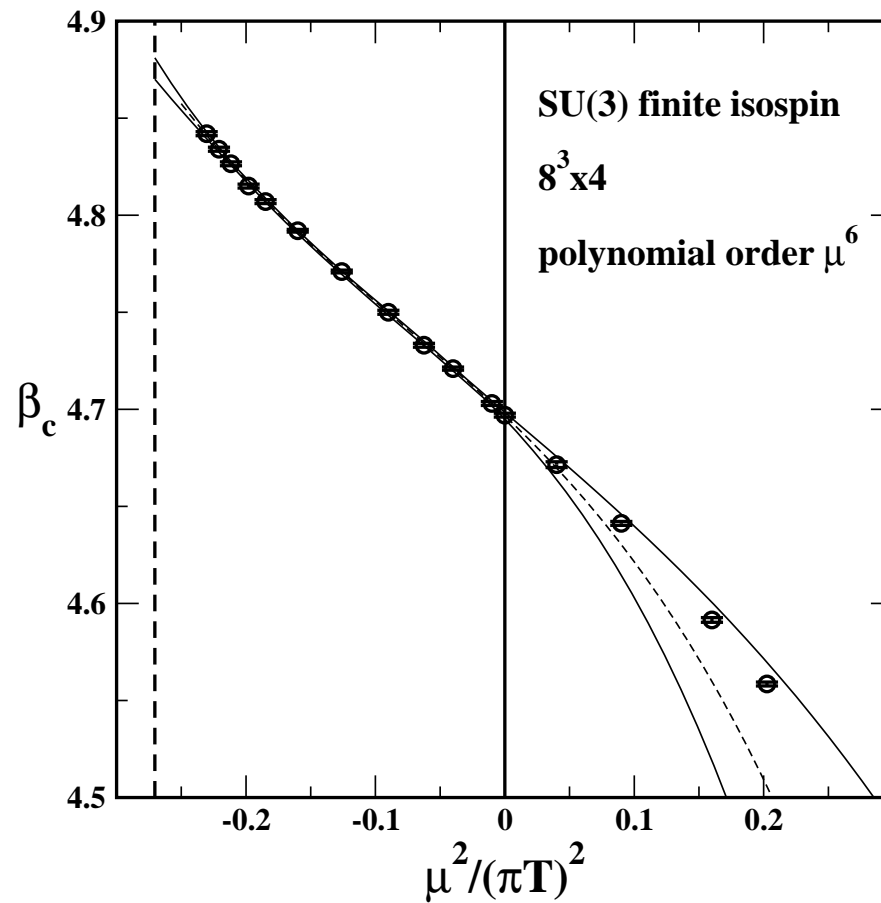
This is the first example for analytic continuation.

- It turns out, that the freeze-out temperature is three times more curved downward than $T_\chi(\mu)$.
- Moreover, the curvature seems to decrease in the continuum limit !
- However, the method is sensitive to the order of the series that is fitted to the imaginary- μ data :
The coefficients at imaginary μ are alternating in sign and can be determined only with large uncertainty.

Lesson :

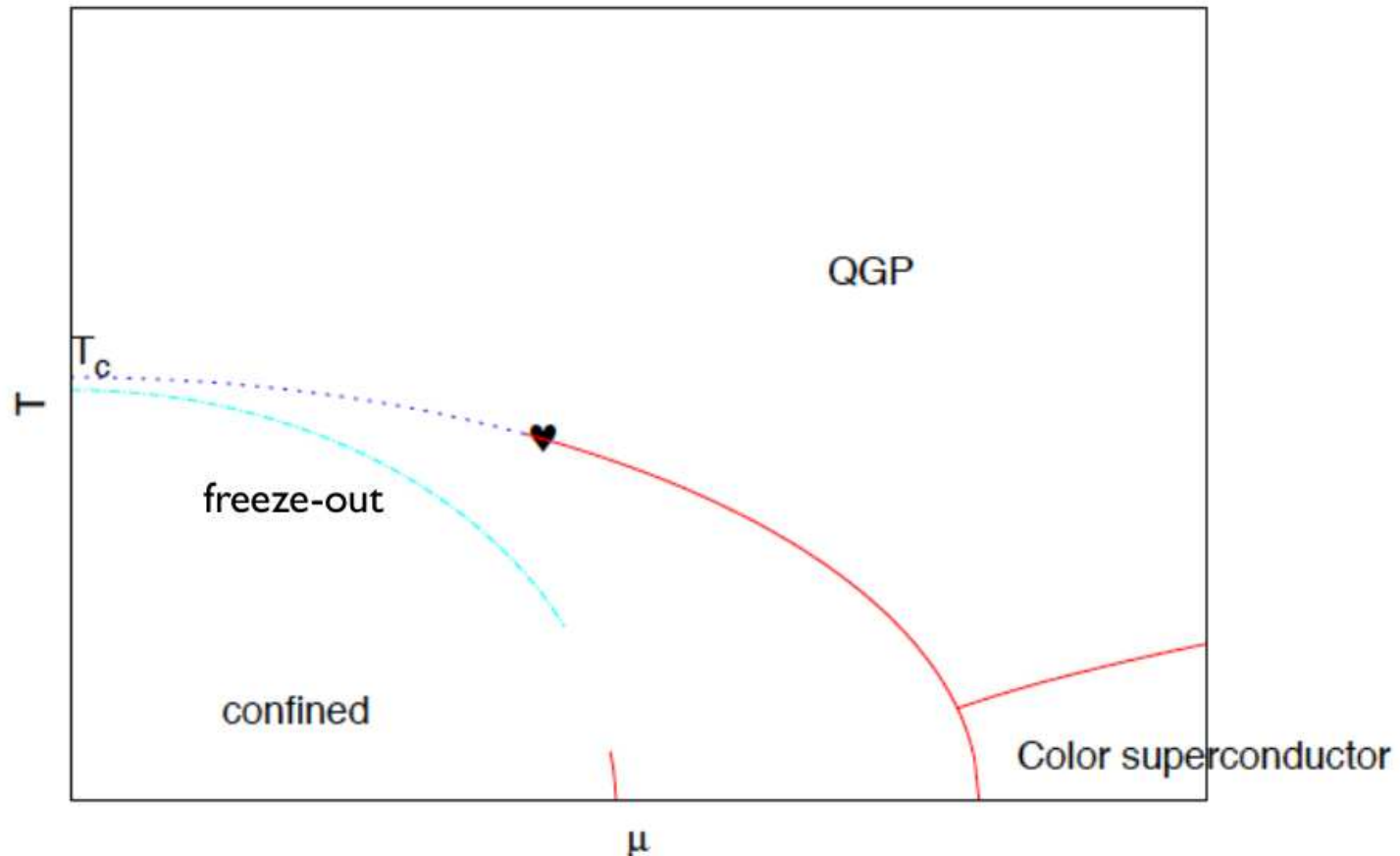
“The chemical freeze-out happens deep inside the hadronic phase and has no relation to the quark-gluon plasma.”

Continuation of β_c from negative μ^2 to positive μ^2
from Ph. de Forcrand arXiv:1005.0539



Sketch of the QCD crossover line $T_c(\mu)$ vs. the experimental freeze-out curve, which has a larger curvature, near $T_c(0)$.

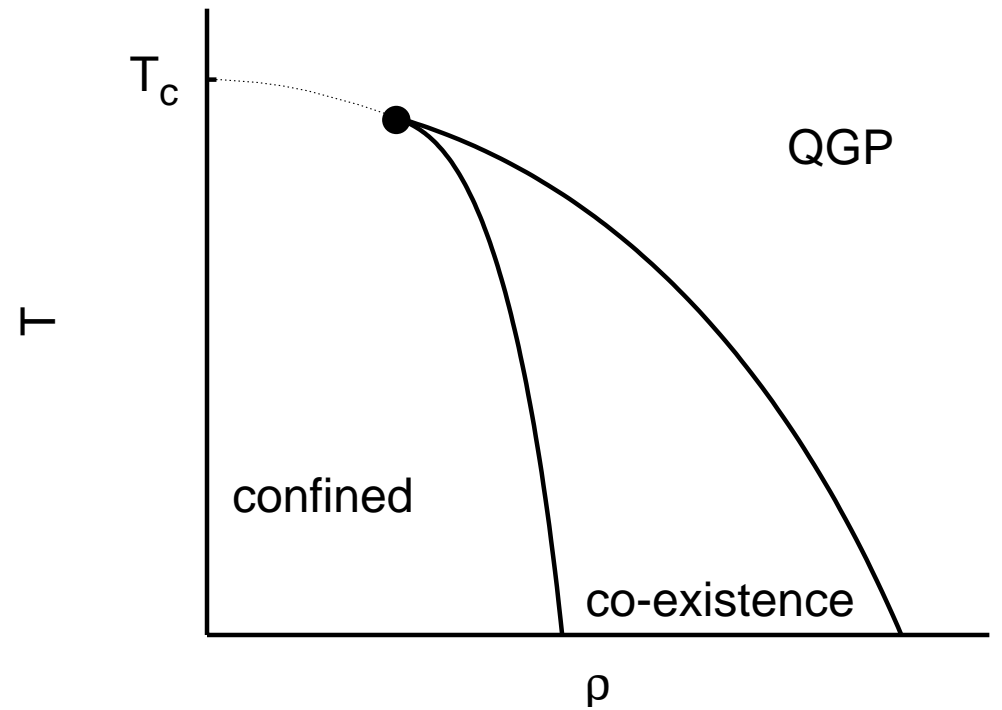
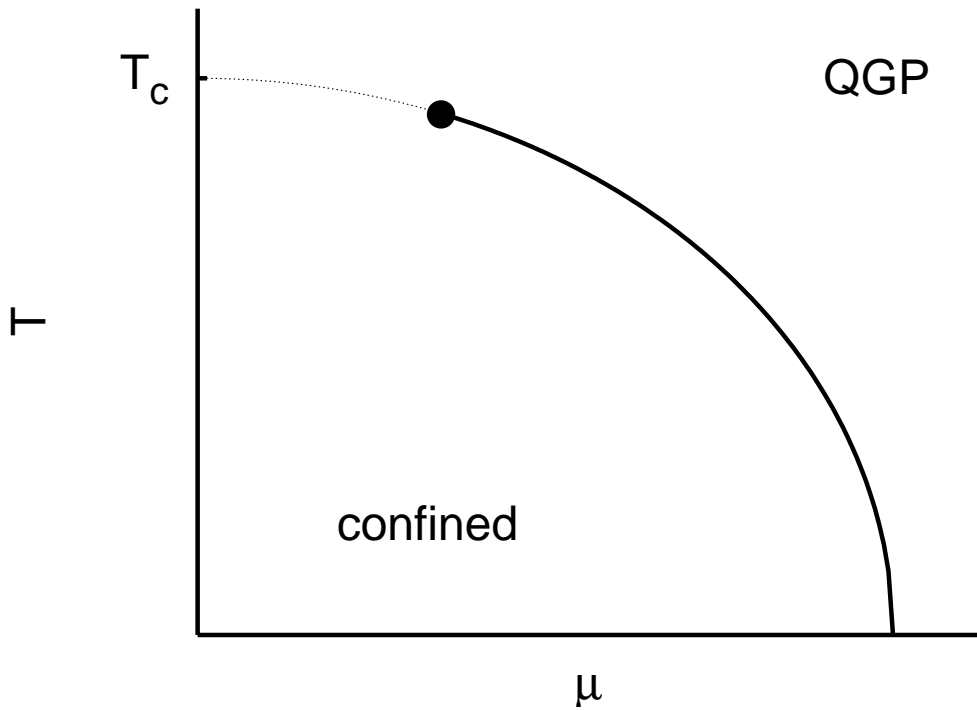
from Ph. de Forcrand arXiv:1005.0539



Much more could be said about imaginary chemical potential :

- full view of the phase diagram with imaginary chemical potential
- Roberge-Weiss periodicity : $\frac{\eta}{T} \rightarrow \frac{\eta}{T} + \frac{2\pi}{3}$
- construction of canonical ensembles for various numbers of baryons N_B
- phase diagram in the T - n_B (baryonic density) plane : mixed phases

The QCD Phase Diagram: Grand Canonical and Canonical View
from S. Kratochvila and Ph. de Forcrand hep-lat/0509143



Both thermodynamic ensembles should be equivalent in the infinite volume limit. However, this limit is difficult to achieve.

For large, **quasi-continuous baryon number** B , Z_C becomes a function of the baryon density ρ :

$$Z_C^{(q)}(V, T, n = NB) = Z_C^{(B)}(V, T, B) = Z_C^{(dens)}(V, T, \rho)$$

Then

$$\begin{aligned} Z(V, T, \mu) &= \int_{-\infty}^{+\infty} d\rho e^{VN\rho\mu/T} Z_C^{(dens)}(V, T, \rho) \\ &= \lim_{V \rightarrow \infty} \int_{-\infty}^{+\infty} d\rho e^{-\frac{V}{T}(f(\rho) - \mu\rho)} \end{aligned}$$

with $f(\rho)$ as the **free energy density in canonical ensemble**.

Finally, μ can be expressed as function of the baryon density ρ :

$$\mu(\rho) = \frac{1}{N} \frac{\partial f(\rho)}{\partial \rho}$$

This function shows a behavior resembling the van der Waals gas.

This approach has been pursued numerically :

S. Kratochvila and Ph. de Forcrand, hep-lat/0509143

$6^3 \times 4$ lattice, four degenerate staggered quarks, volume $(1.8 \text{ fm})^3$

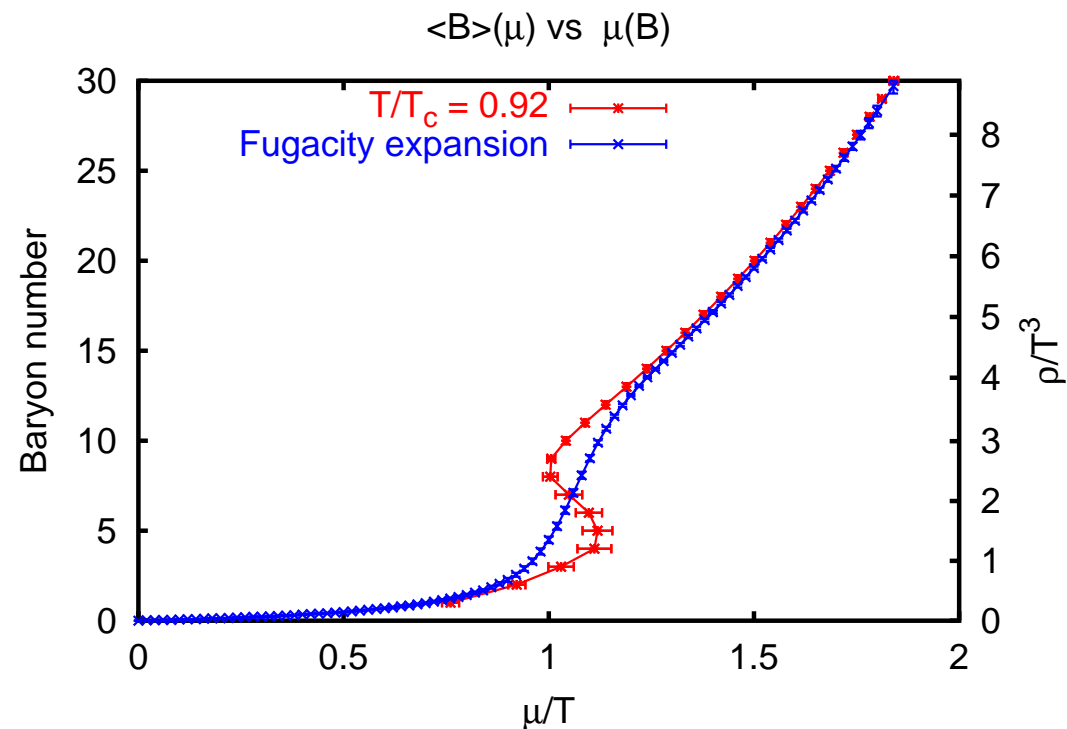
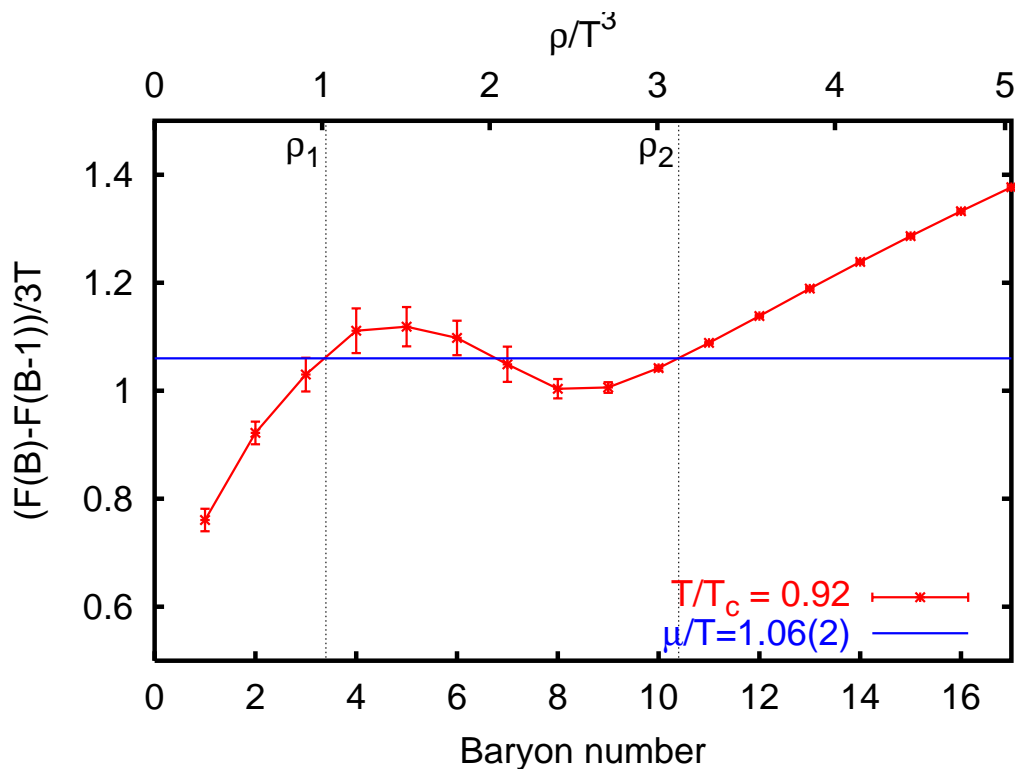
A. Alexandru, M. Faber, I. Horvath and K. F. Liu, hep-lat/0507020

Kentucky group :

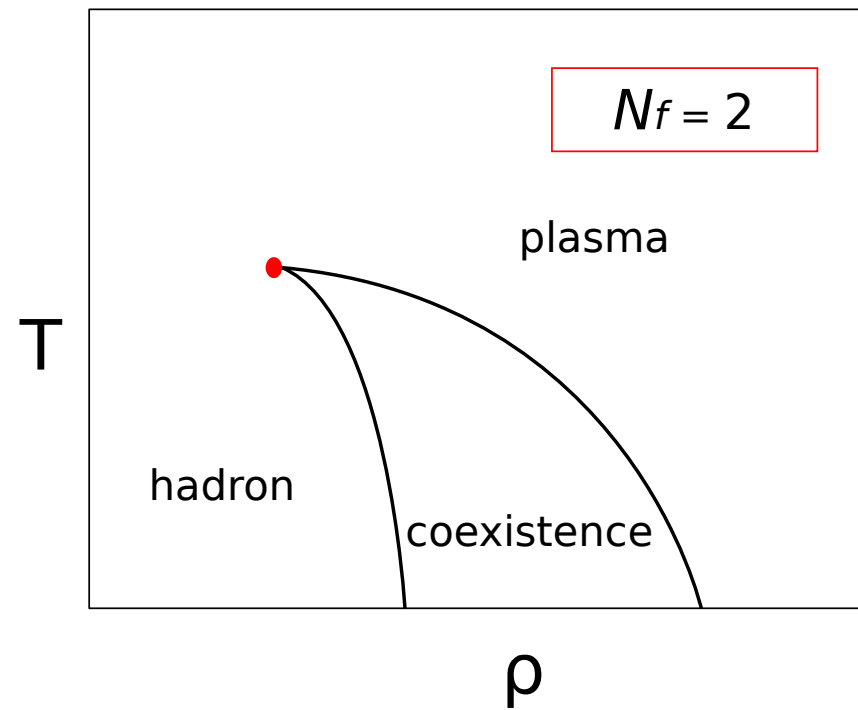
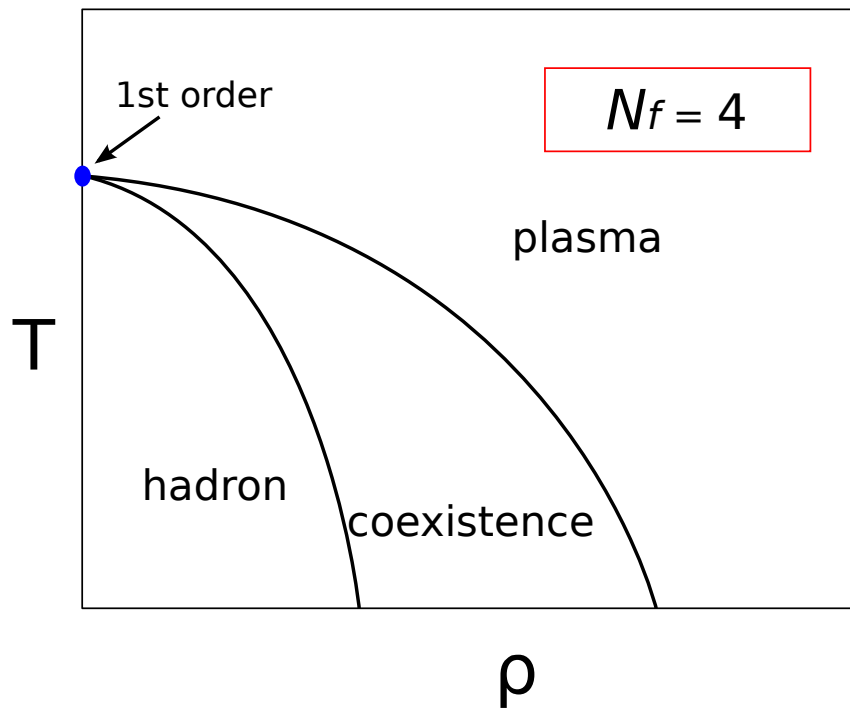
$6^3 \times 4$ lattice, clover-improved Wilson fermions $N_f = 2, 3$ and 4 .

Left: The Maxwell construction allows to extract the critical chemical potential and the boundaries of the co-existence region. Right: Comparing the saddle point approximation (red) with the fugacity expansion (blue). Strong finite-size effects in the latter obscure the first-order transition.

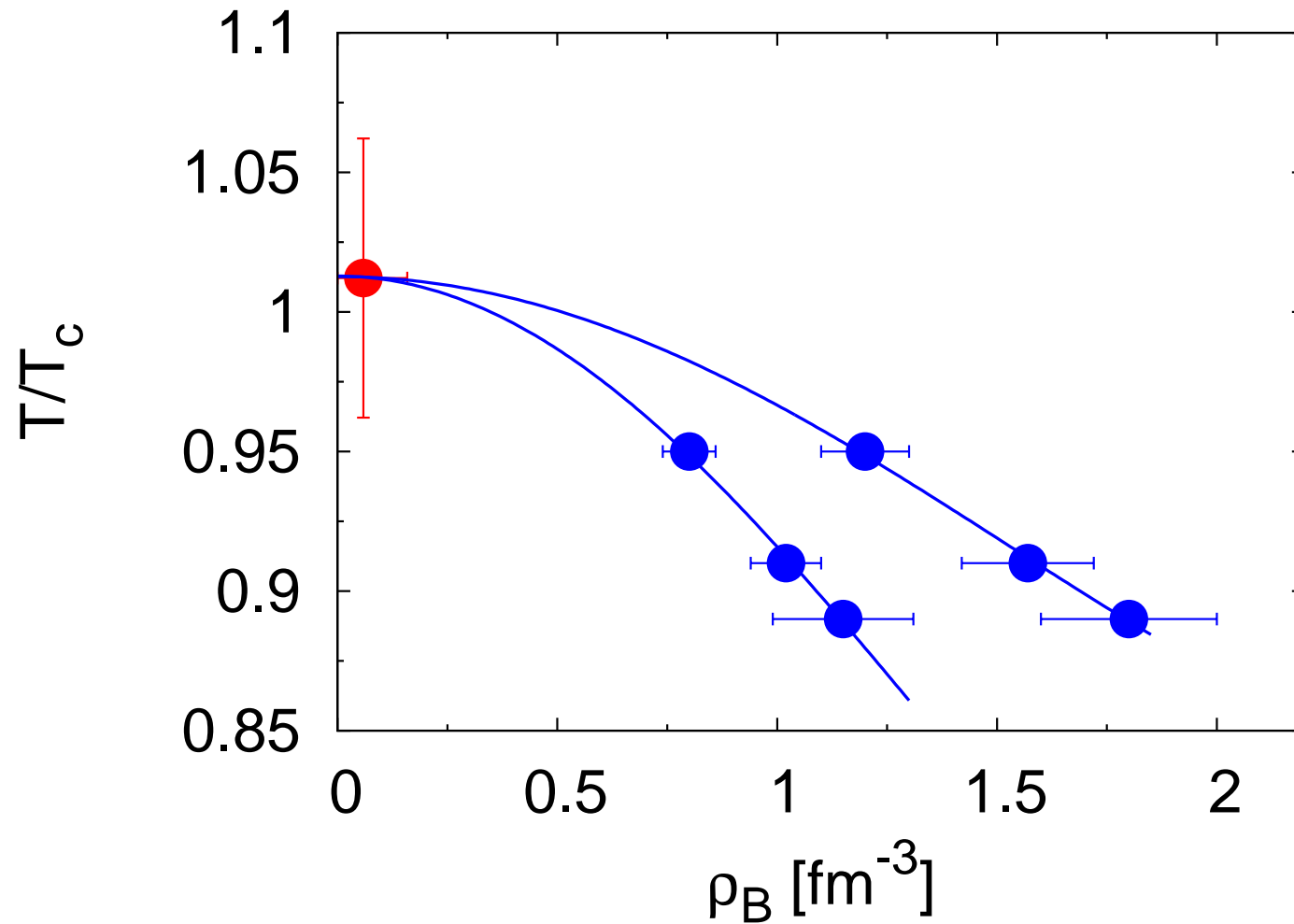
from S. Kratochvila and Ph. de Forcrand hep-lat/0509143



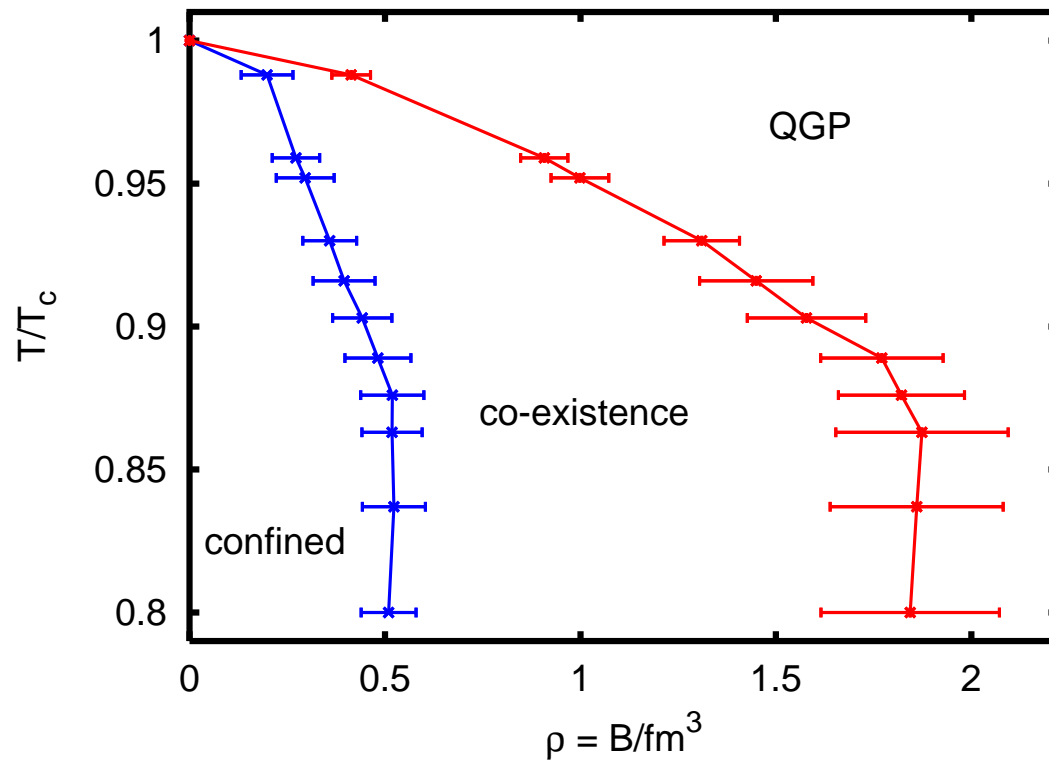
The number of flavors is extremely important : $N_f = 4$ vs. $N_f = 2$
from Anyi Li arXiv:1002:4459



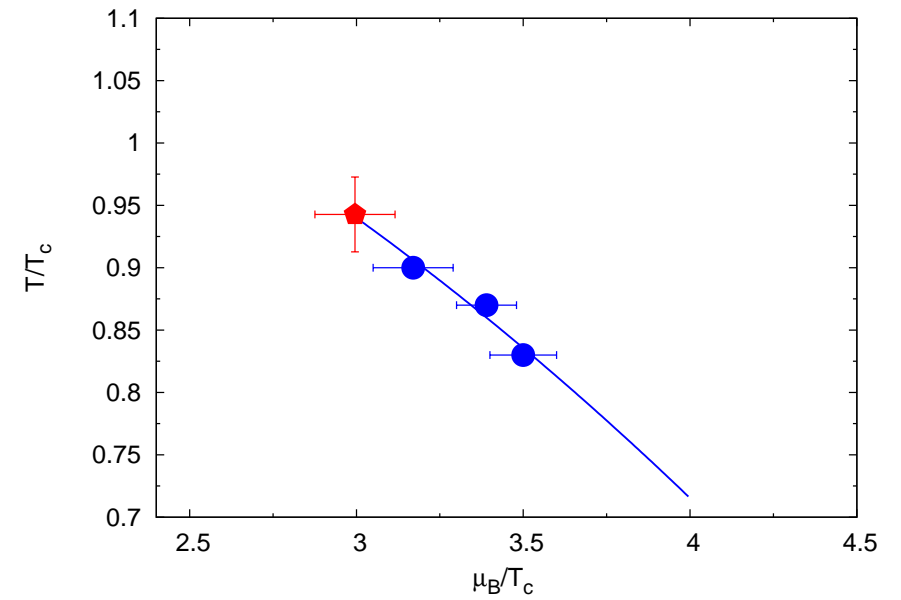
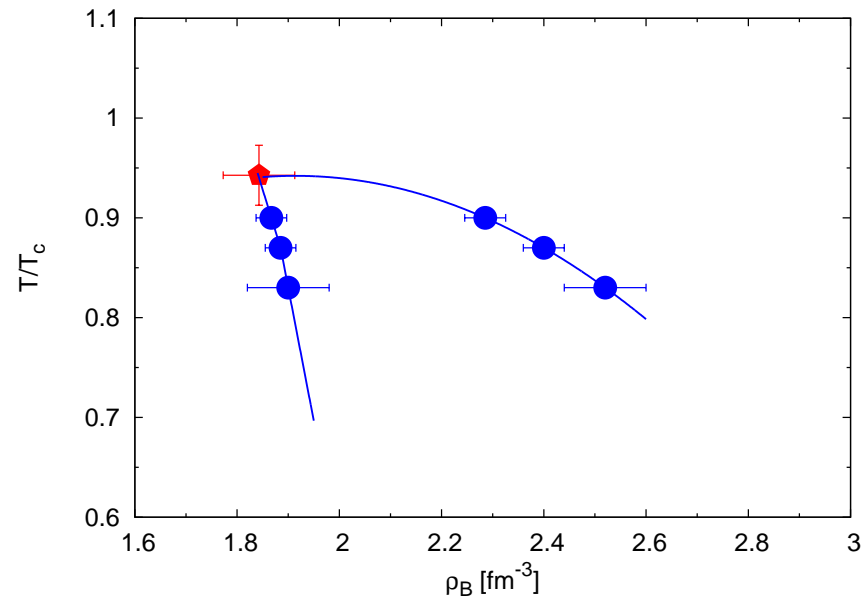
Phase boundaries in the temperature vs. density plot for $N_f = 4$.
from Anyi Li arXiv:1002:4459



Phase boundaries in the temperature vs. density plot for $N_f = 4$.
from S. Kratochvila and Ph. de Forcrand hep-lat/0509143



Left: Phase boundaries in the temperature vs. density plot for $N_f = 3$.
Right: Transition line in the temperature vs. chemical potential plot.
from Anyi Li arXiv:1002:4459



This looks rather systematic, however the lattices are too small.

There are possible systematic effects of the canonical ensemble method.

One would like to confirm this in a more robust way, that works also for large lattices (Taylor expansion), in order to verify the first order character of the transition.

B. Phase quenching

Consider the exact partition function with $n_B \neq 0$, i.e. $\mu_q \neq 0$:

$$Z_B(\beta, \mu_q) = \int D[U] (\det D(U, \mu_q))^{N_f} e^{-\beta S_G}$$

Factorize the complex determinant into **modulus and phase factor**

$$Z_B(\beta, \mu_q) = \int D[U] |\det D(U, \mu_q)|^{N_f} e^{i N_f \theta} e^{-\beta S_G}$$

Phase-quenched ensemble :

$$Z_{pq}(\beta, \mu_q) = \int D[U] |\det D(U, \mu_q)|^{N_f} e^{-\beta S_G}$$

Fortunately, this ensemble can also be sampled according to HMC, if one interpretes this as the **fixed-isospin ensemble** with $\mu_I = \mu_q$

$$Z_{pq}(\beta, \mu) = Z_I(\beta, \mu_I = \mu)$$

For even N_f

$$|\det D(U, \mu_q)^{N_f}| = \det D(U, +\mu_q)^{\frac{N_f}{2}} \det D(U, -\mu_q)^{\frac{N_f}{2}}$$

such that phase quenching is equivalent to fixed isospin with $\mu_I = \mu_q$.

For $N_f = 2$

$$(\det D(U, \mu_q))^2 = |\det D(U, \mu_q)|^2 e^{2i\theta}$$

For an observable \mathcal{O} we can consider **two expectation values**

$$\langle \mathcal{O} \rangle_I = \frac{1}{Z_I} \int D[U] \mathcal{O} |\det D(U, \mu_q)|^2 e^{-\beta S_G} \quad (\text{simulation possible})$$

$$\langle \mathcal{O} \rangle_B = \frac{1}{Z_B} \int D[U] \mathcal{O} (\det D(U, \mu_q))^2 e^{-\beta S_G} \quad (\text{simulation impossible})$$

Nevertheless, the last **average can be estimated** by including the missing phase factor into the observable : estimator

$$\langle \mathcal{O} \rangle_B = \frac{\langle \mathcal{O} e^{2i\theta} \rangle_I}{\langle e^{2i\theta} \rangle_I}$$

where the averages are taken w.r.t. the phase quenched (pq), i.e. fixed-isospin (I) ensemble. **Phase quenching is a more general trick !**

While the **Monte Carlo process is guided by the fixed isospin ensemble**, the global phase factor has to be evaluated only after the trajectory is finished, simultaneously with the observable \mathcal{O} on the configuration.

The smallness of the denominator (“average phase factor”) quantifies the severity of the sign problem !

When the denominator is small due to phase cancellations, the error of the numerator is also big, and the estimate not reliable.

The denominator decreases exponentially with volume and $1/T$

$$\langle e^{2i\theta} \rangle_I \propto e^{-\frac{V}{T}\Delta f}$$

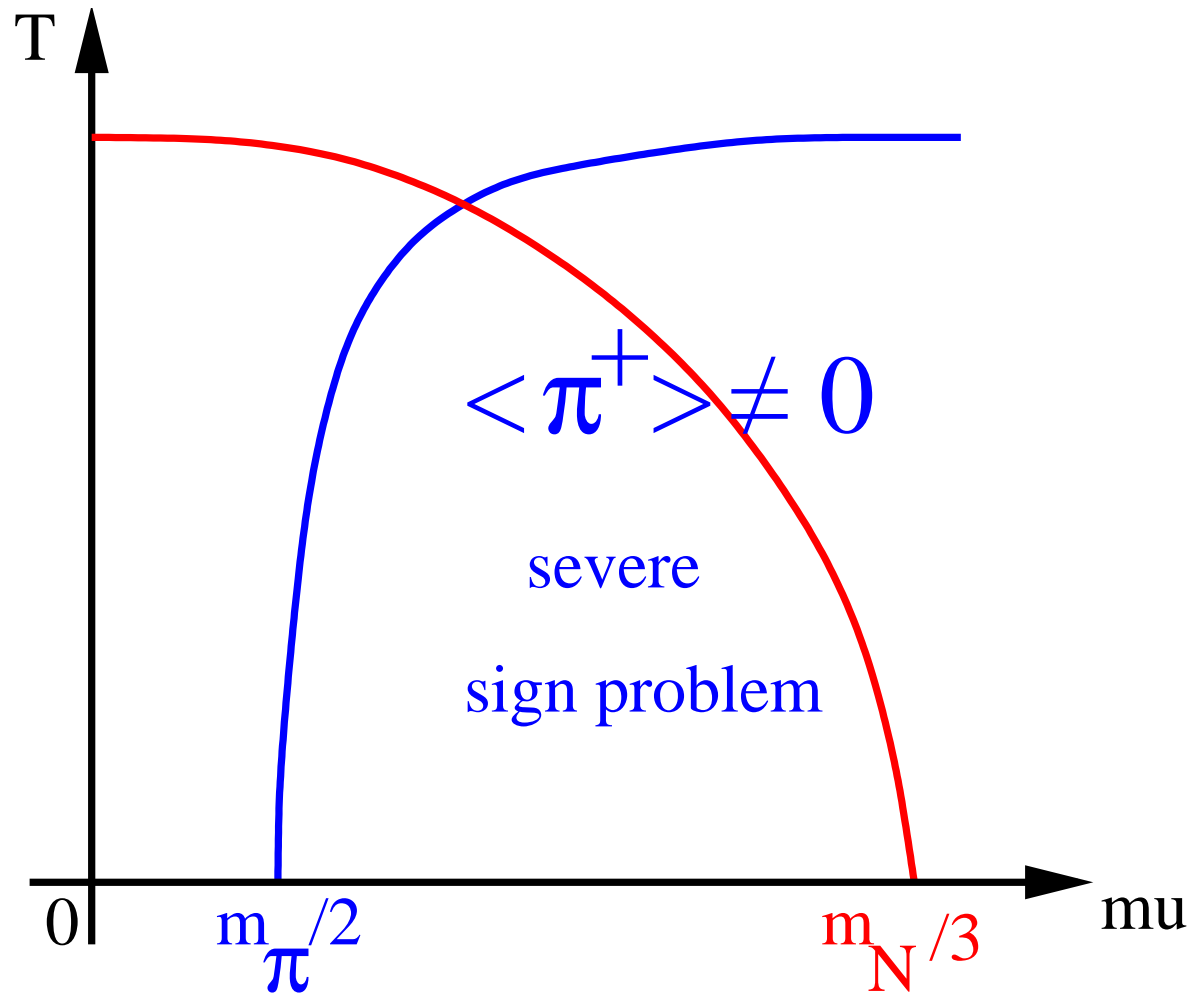
where Δf is the difference in free energy density between the systems described by Z_B and $Z_I = Z_{pq}$. This (intensive) difference Δf is non-uniform over the β - μ_q -plane ! This limits the reliable range there (low μ_q , high T).

Results of a systematic investigation of the average phase factor :

- The sign problem is not severe for $\mu_q < \frac{m_\pi}{2}$
- Large differences exist between the free energy densities of the phase-quenched and full theory for $\mu_q > \frac{m_\pi}{2}$.
- The method becomes problematic, anyway, for large volumes.
- For high temperature the average phase factor doesn't drop as fast with volume as for $T \leq T_\chi$

“Phase quenching is problematic at low temperature and high density !”

Where the phase-quenched simulation fails
from Ph. de Forcrand arXiv:1005.0539



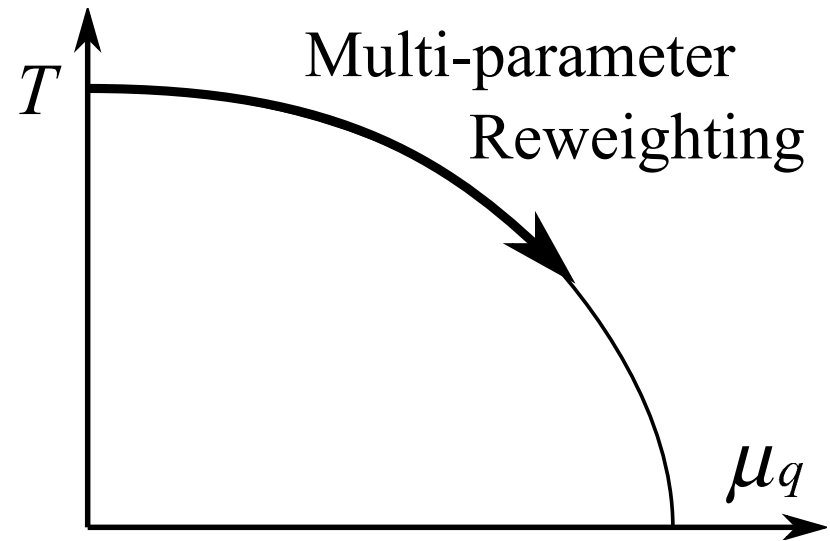
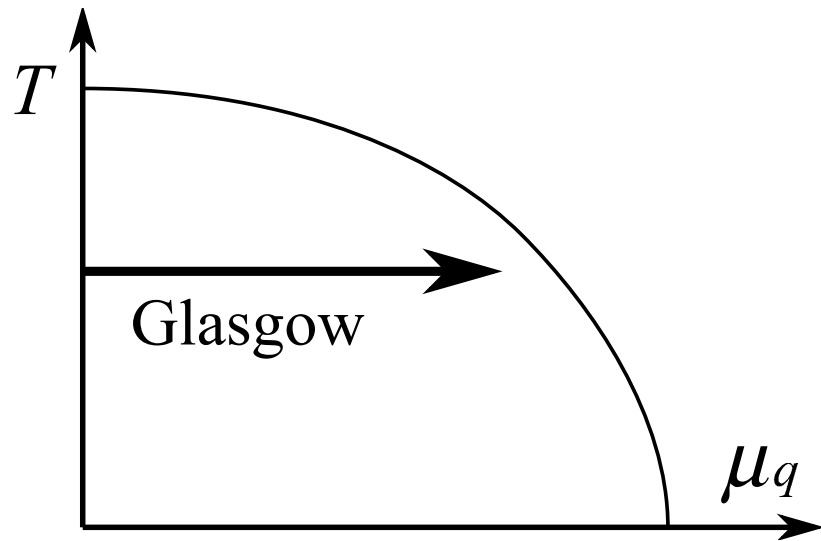
C. Reweighting across the β - μ_q plane

An attempt to find curvature and critical endpoint (Fodor, Katz et al.)

What is the best reference ensemble ?

1. Replace (β, μ_q) by $(\beta, 0)$! “horizontal reweighting”
“Glasgow method”, failed because of bad overlap between the simulated and the (unknown) target ensemble
2. Replace (β, μ_q) by $(\beta', 0)$ (with some suitable β') !
“multiparameter reweighting” or “Budapest method”, working successfully.
3. A convincing example for $\mu \rightarrow i \eta$: (accessible to direct simulation) condensate $\langle \bar{\psi} \psi \rangle$ should rise with η (as seen in direct simulation), opposite to real μ_q !

Glasgow (horizontal) vs. Budapest (multiparameter) reweighting



In both cases the reference ensemble is on the β axis, with real determinant.

The role of the “phase” above is played here by the reweighting factor

$$R = \frac{\det D(U, \mu_q) e^{-\beta S_G}}{\det D(U, 0) e^{-\beta' S_G}}$$

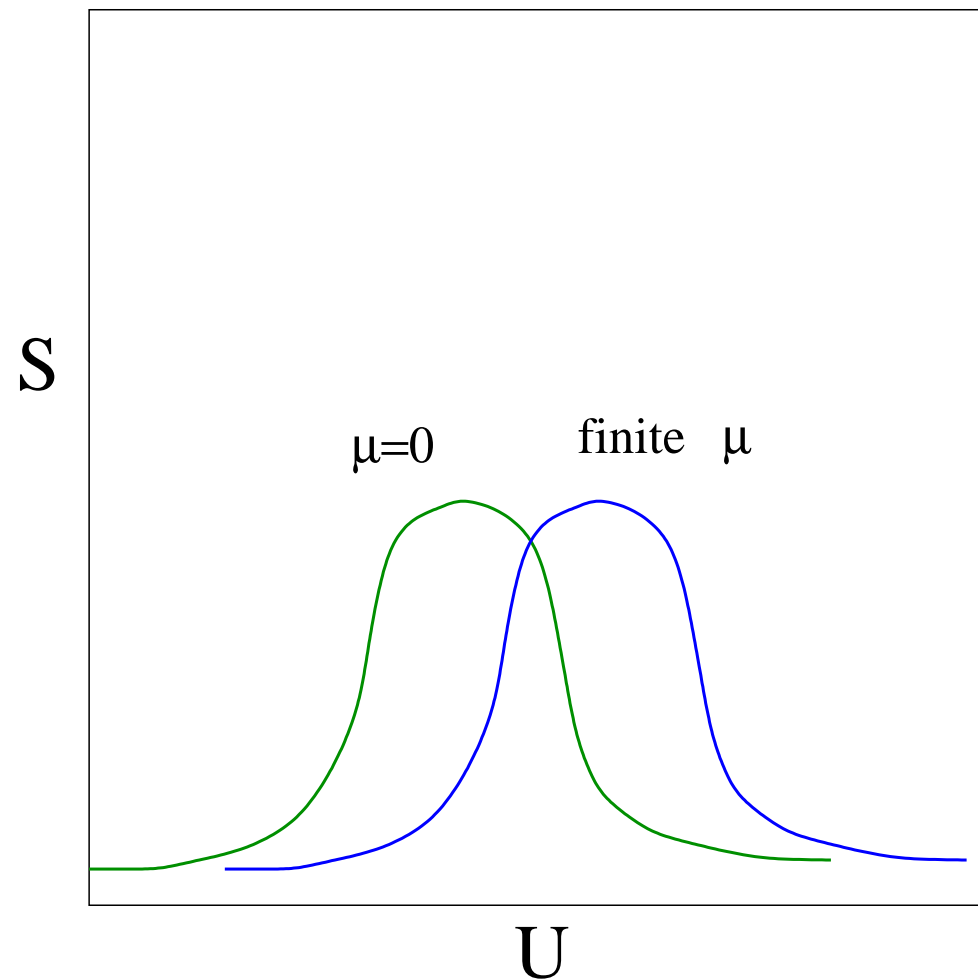
While the **Monte Carlo process is guided by the $(\beta', \mu = 0)$ ensemble** the global reweighting factor R has to be evaluated only after each trajectory is finished, simultaneously with the observable \mathcal{O} .

estimator :

$$\langle \mathcal{O} \rangle_B = \frac{\langle \mathcal{O} R \rangle_{\text{reference}}}{\langle R \rangle_{\text{reference}}}$$

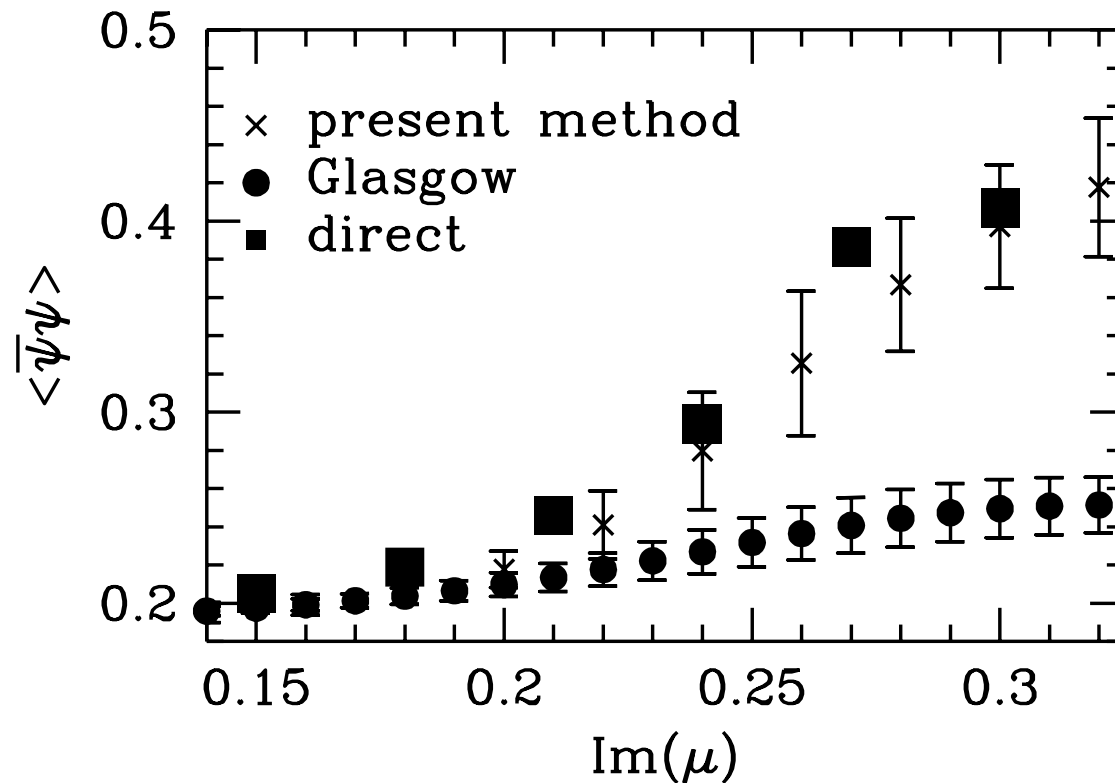
Hidden problem : “overlap problem” or better: “problem of insufficient overlap”

The “reference ensemble” might not contain enough configurations falling into the “target ensemble”, such that this bias cannot be corrected simply by reweighting.



Testing the methods at imaginary μ by comparison with direct simulation. Failure of the Glasgow method due to the overlap problem. (from Z. Fodor and S. D. Katz hep-lat/0111064)

Budapest method reproduces the exact result, Glasgow method not !



Special method of Fodor and Katz rapidly evaluating determinants :

- shift the μ -dependence into two time slices
- factorization of the μ_q -dependence

$$\det D(\mu_q) = e^{-3N_s^3 N_t \mu_q} \det (P - e^{N_t \mu_q})$$

P is the “reduced fermion matrix” (a $2NN_s^3 \times 2NN_s^3$ matrix) with two time slices.

When all $2NN_s^3$ eigenvalues λ_i of the reduced matrix are known,

$$\det D(\mu_q) = e^{-NN_s^3 N_t \mu_q} \prod_{i=1}^{2NN_s^3} (e^{N_t \mu_q} - \lambda_i)$$

Thus the reweighting factor is faster evaluated, while the sampling runs with real positive weight $\det D(\mu_q = 0)$ at $\beta' \neq \beta$!

The “reduced fermion matrix technique” is broadly applied.

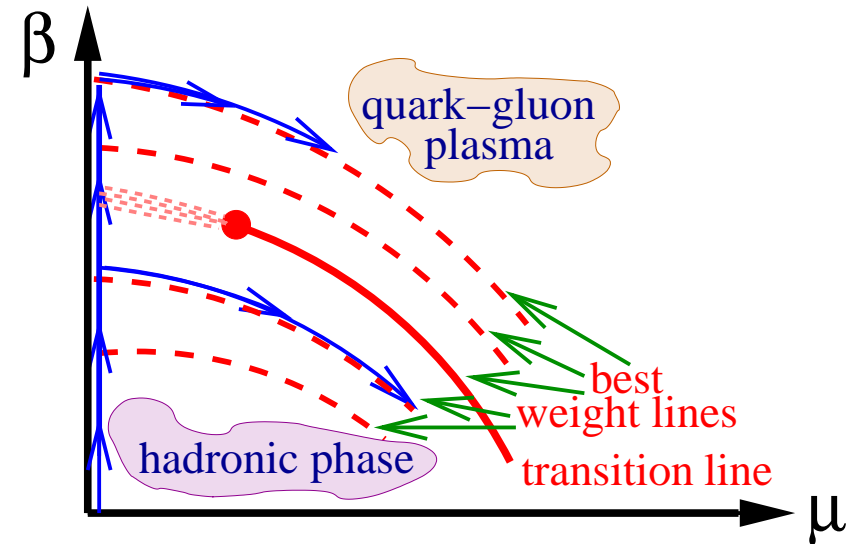
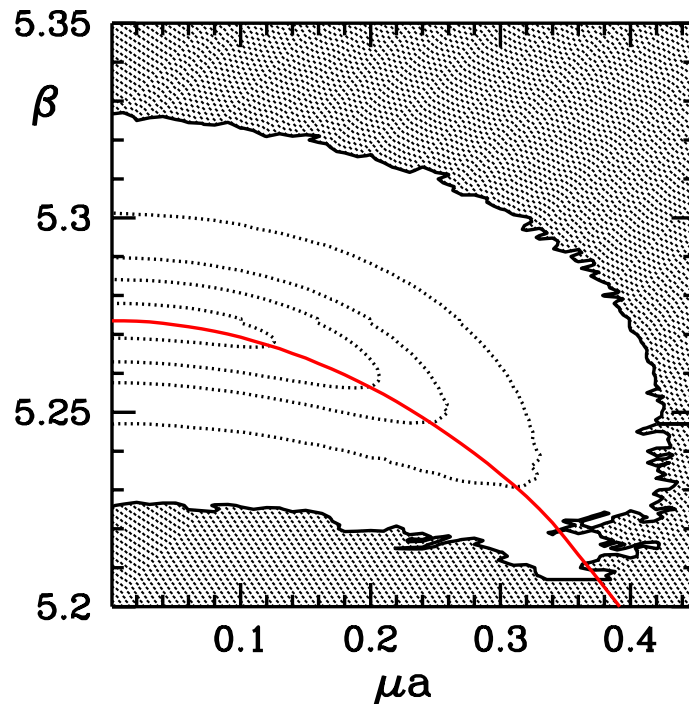
A useful tool for QA : one can define an “overlap measure” α :

Definition : “ α is the overlap measure, if a randomly selected fraction α of configurations of the “reference ensemble” (where they occur equally weighted) acquires a weight $1 - \alpha$ when taken as members of the “target ensemble” (where they are not equally weighted).”

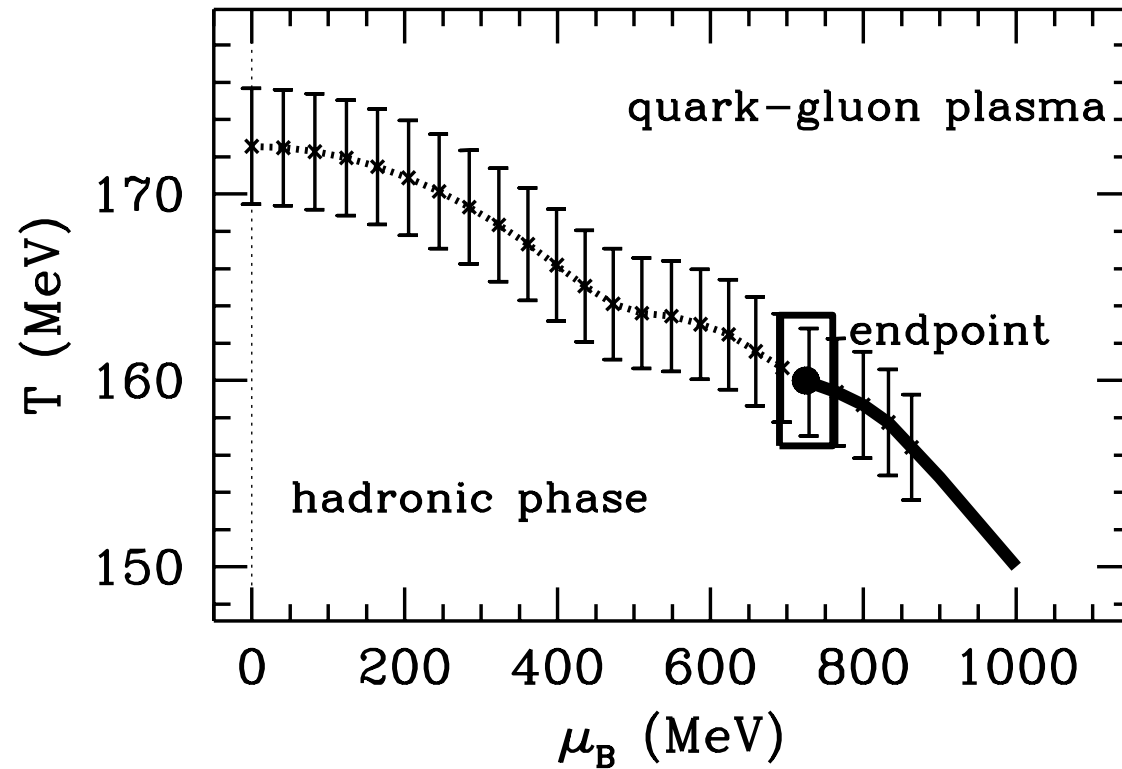
The optimal overlap is $\alpha = 50\%$

The grey area (next figure) is not accessible by reweighting from the reference point $(\beta', \mu_q = 0)$.

Left: Relief map of the overlap measure. The red line (the line of the crossover !) is determined by the peaks of susceptibility. (from F. Csikor et al. hep-lat/0401016) Right: Best pathes for reweighting in β - μ plane. (schematically from F. Csikor et al. hep-lat/0301027)



Finding the line of the crossover and the critical endpoint
from F. Csikor et al. hep-lat/0301027



The method of Lee-Yang zeroes :

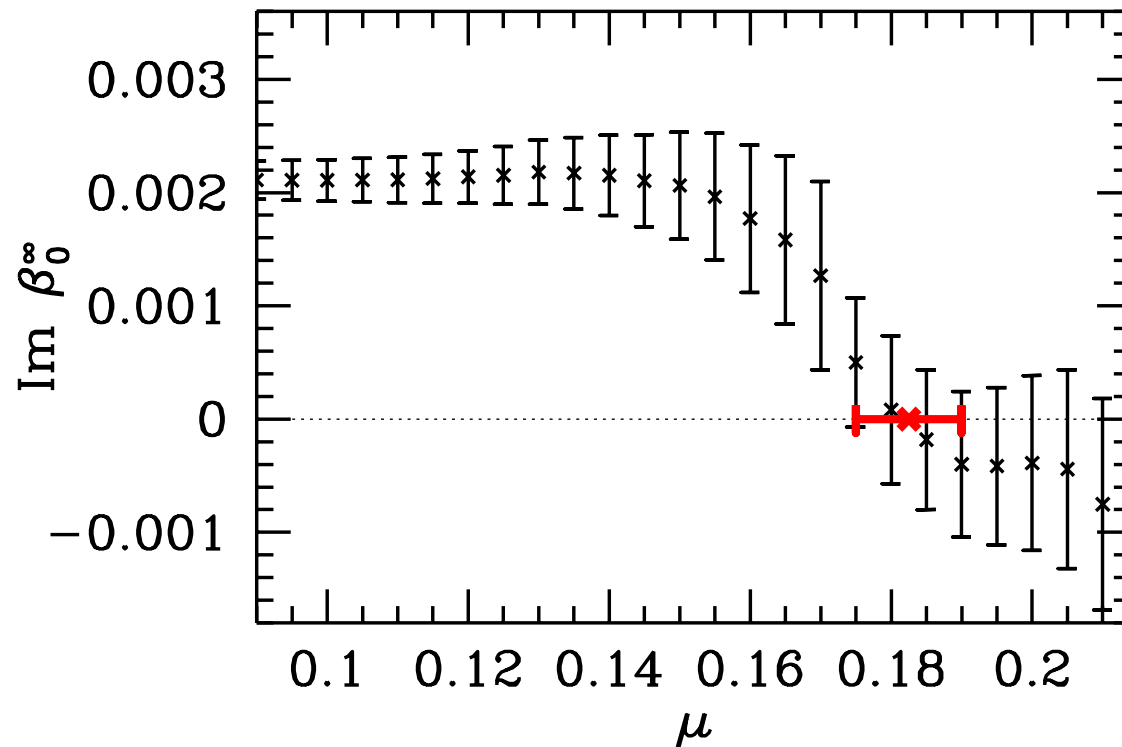
Adding an imaginary part to β allows to study the Lee-Yang zeroes of the theory : these are the zeroes of the partition function.

When the Lee-Yang zeroes in the limit $V \rightarrow \infty$ approach the real axis this signals that a real singularity (phase transition) appears.

At finite volume, the pattern of the n^{th} Lee-Yang zeroes β_{LY}^n is $\text{Im } \beta_{LY}^{(n)} = C(2n + 1)$.

When a crossover turns into a first order transition, the location of the (extrapolated) lowest Lee-Yang zero touches the real axis, $C \rightarrow 0$.

Locating the critical endpoint by the lowest Lee-Yang zero
(extrapolated to $V \rightarrow \infty$) ($\text{Im } \beta_{LY}^{(0)}$) in the complex β plane.
from Z. Fodor and S. D. Katz hep-lat/0111064



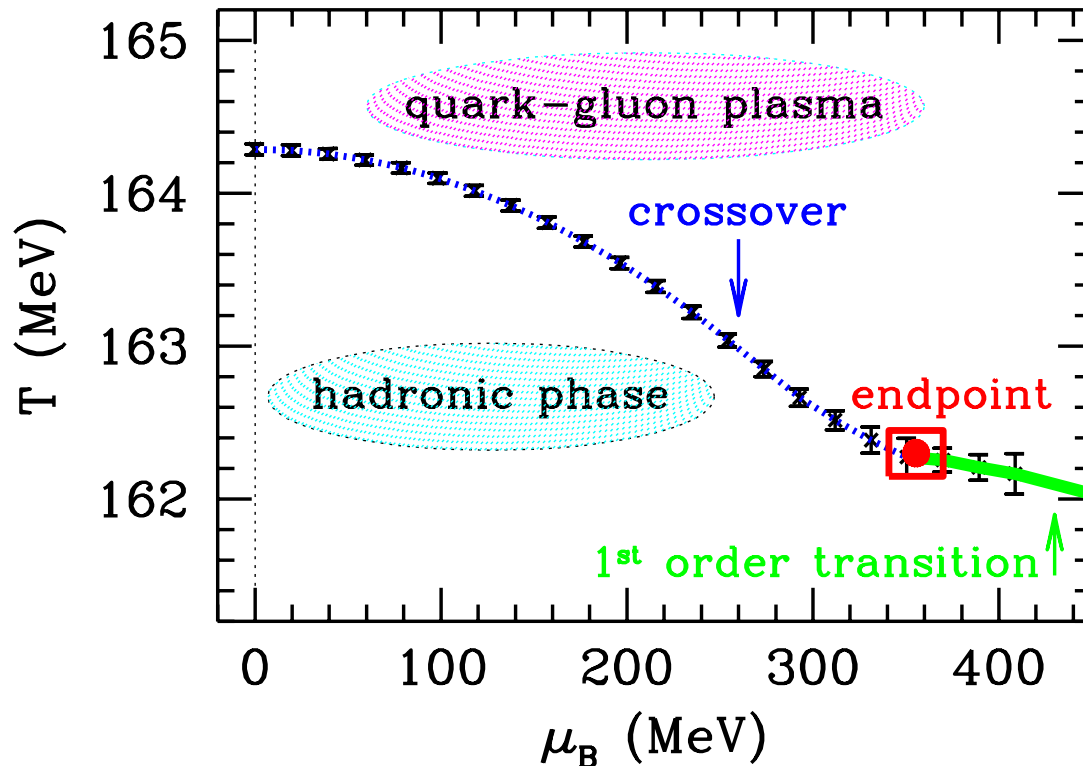
This fixes the critical endpoint : F. Csikor et al. hep-lat/0301027

For 2 + 1 flavors the Wuppertal-Budapest group has obtained

$$\mu_B^E = 725 \pm 35 \text{ MeV} \quad T^E \approx 160 \pm 3.5 \text{ MeV} \quad T_c(\mu = 0) = 172 \pm 3 \text{ MeV}$$

(has been later updated !)

Update of the critical point (small square) in physical units.
Dotted line for the crossover, solid line for the first order phase transition.
The small square shows the endpoint. Combining all uncertainties one obtains $T_E = 162 \pm 2$ MeV and $\mu_E = 360 \pm 40$ MeV.
from Z. Fodor and S. D. Katz hep-lat/0402006

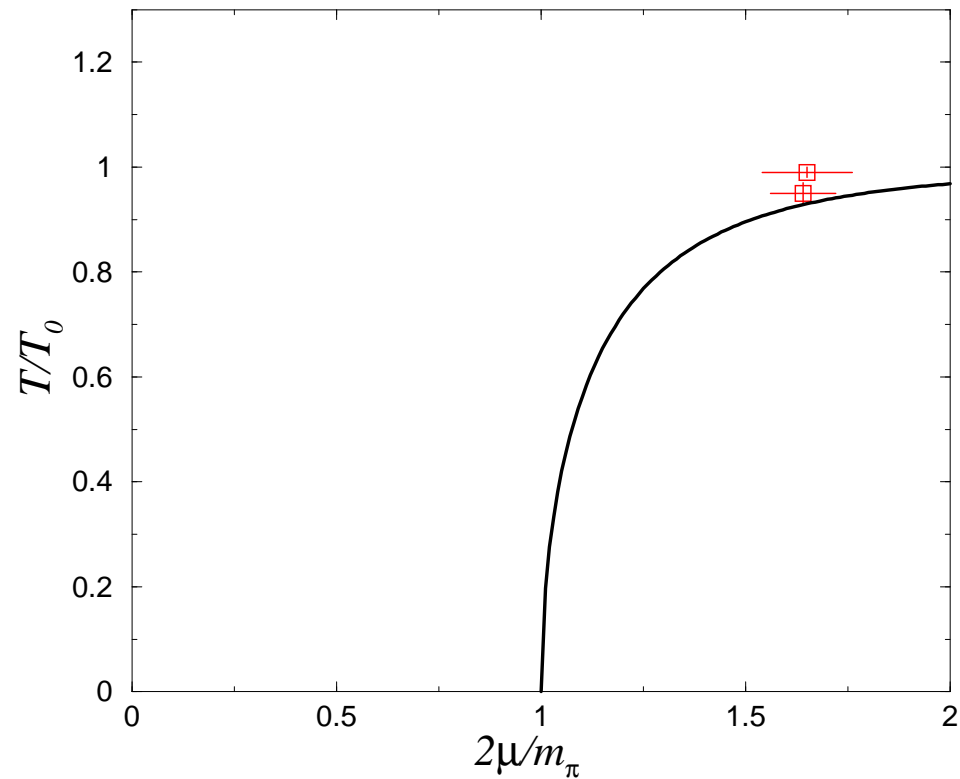


Compared to the previous finding, the light quark masses were reduced by a factor three, while the largest volume has been increased by a factor three.

This simulation is still **far from the continuum limit** ($N_t = 4$) :

$$a = \frac{1}{4T_c} \sim \mathcal{O}(0.25 \text{ fm}) \tag{1}$$

Doubts are still allowed : The critical endpoint lies too close to the critical line for pion condensation (in phase-quenched simulations).
from Splittorff hep-lat/0505001



D. Taylor expansion in μ_q , from points along the β -axis

- The chemical potential enters always in the combination μ_q/T .
- Reweighting gives μ_q -dependence (in principle, at least).
- In fact, reweighting is **restricted to small μ_q/T and small V** .
- The error analysis of results of reweighting is difficult, a breakdown might even not be noticed (Glasgow method).

Rescue : Observables can be obtained as power series in μ_q/T .

By now has become the “bread and butter method”.

Only by Taylor expansion a reliable $V \rightarrow \infty$ behavior can be determined giving access to intensive quantities like p .

$$p(T, \mu_q) = p(T, 0) + \Delta p(T, \mu_q)$$

Δp is an even function of μ_q/T (since $Z(\mu_q/T) = Z(-\mu_q/T)$)

$$\frac{\Delta p(T, \mu_q)}{T^4} = \sum_{k=1}^{\infty} c_{2k}(T) \left(\frac{\mu_q}{T}\right)^{2k}$$

The Taylor coefficients stem from derivatives w.r.t. μ_q of the determinant, more precisely

$$\frac{\partial \ln \det D(\mu_q)}{\partial \mu_q} = \text{tr} \left[D^{-1} \frac{\partial D}{\partial \mu_q} \right]$$

and higher derivatives. Only even derivatives are non-vanishing. Therefore

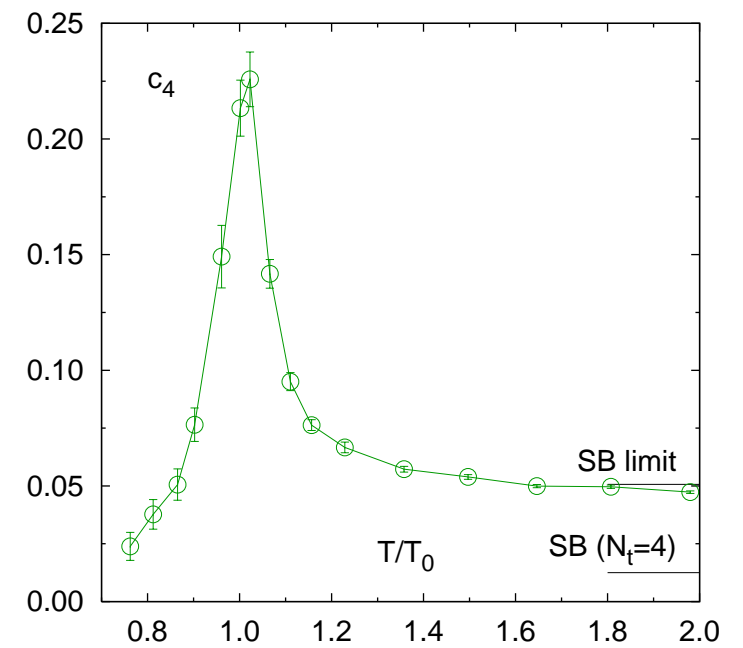
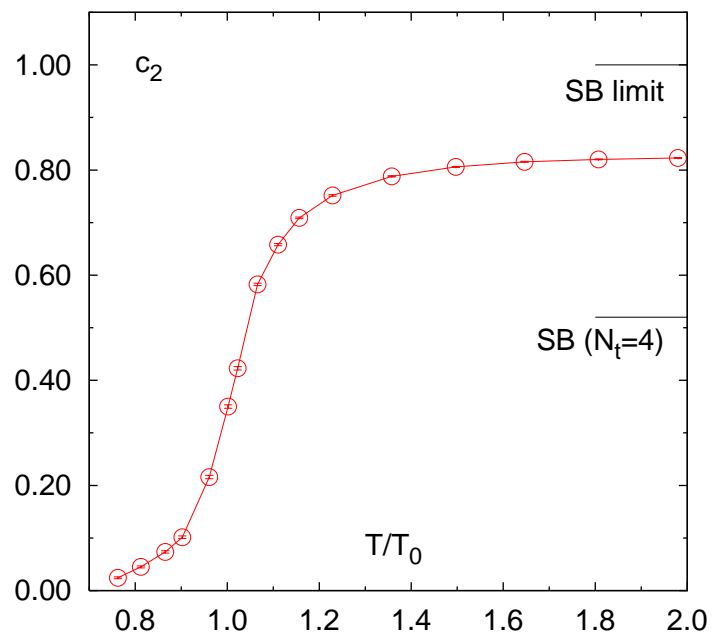
$$c_{2k} = \left\langle \text{tr} \left(\text{polynomial of order } 2k \text{ in } D^{-1} \text{ and } \frac{\partial D}{\partial \mu_q} \right) \right\rangle_{|\mu_q=0}$$

Taylor coefficients are easily calculable (in principle !) in simulations at $\mu_q = 0$, practically obtained by means of stochastic estimators.

These observables become increasingly noisy with larger k .

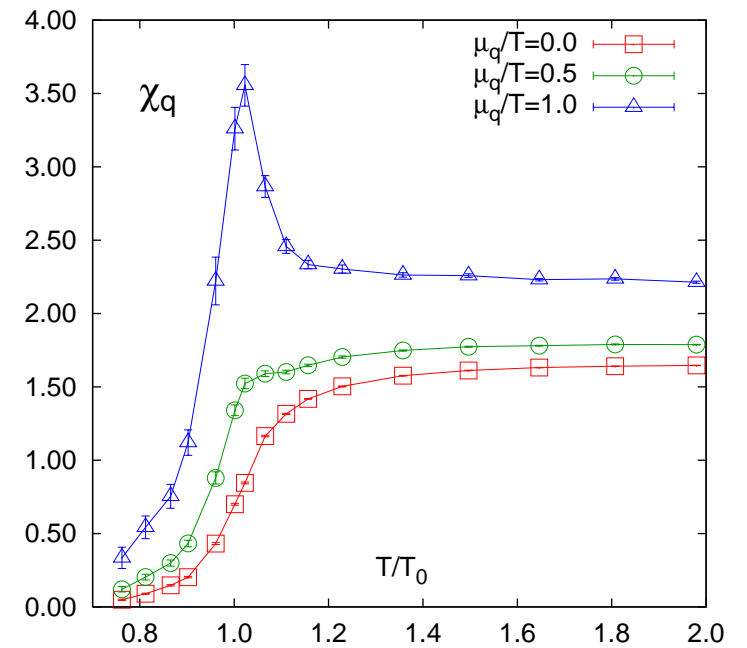
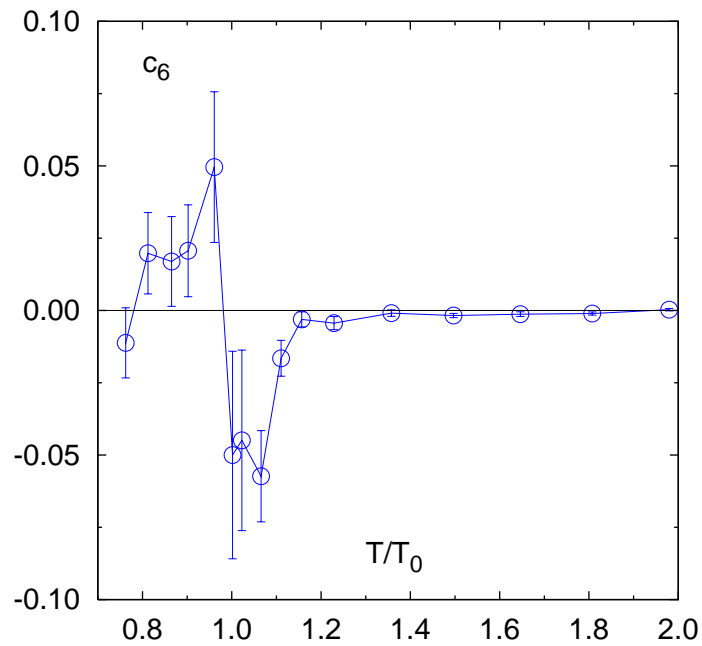
The first two Taylor coefficients c_2 and c_4 as functions of temperature look very nice.

from Ch. Schmidt hep-lat/0610116



The Taylor coefficient c_6 and the quark number susceptibility χ_q (for three values of μ_q), all as functions of temperature.

from Ch. Schmidt hep-lat/0610116



In principle, **knowledge of c_{2k} should give all thermodynamics :**

- The equation of state (EoS)
- The transition line $T_c(\mu_q)$
- The critical endpoint (μ_c^E, T_c^E)

For **all bulk quantities similar** series expansions exist :

$$\frac{n_q}{T^3} = 2c_2 \frac{\mu_q}{T} + 4c_4 \left(\frac{\mu_q}{T}\right)^3 + 6c_6 \left(\frac{\mu_q}{T}\right)^5 + \dots$$
$$\frac{\chi_q}{T^2} = 2c_2 + 12c_4 \left(\frac{\mu_q}{T}\right)^2 + 30c_6 \left(\frac{\mu_q}{T}\right)^4 + \dots$$

Going to higher density (higher μ_q/T) meets difficulties :

- higher order k is required
- the coefficients become more noisy
- the computation needs large volumes

A better way by simulations at

- imaginary baryonic chemical potential ($\mu_q = i\eta_q$)
- imaginary isospin chemical potential ($\mu_I = i\eta_I$)

has been proposed/explored.

(see M. D'Elia and F. Sanfilippo arXiv:0904.1400)

For the prediction of quantum number fluctuations it is important to discriminate between different quarks:

$$\frac{p}{T^4} = \frac{1}{VT^3} \ln Z(T, \mu_u, \mu_d, \mu_s) = \sum_{ijk} \frac{1}{i!j!k!} \chi_{ijk}^{uds} \left(\frac{\mu_u}{T}\right)^i \left(\frac{\mu_u}{T}\right)^i \left(\frac{\mu_d}{T}\right)^j$$

$$\chi_{ijk}^{uds} = \frac{\partial^{i+j+k} p/T^4}{\partial(\mu_u/T)^i \partial(\mu_d/T)^j \partial(\mu_s/T)^k}$$

or

different charges (baryon charge, strangeness, electric charge) ;

$$\frac{p}{T^4} = \frac{1}{VT^3} \ln Z(T, \mu_B, \mu_S, \mu_Q) = \sum_{ijk} \frac{1}{i!j!k!} \chi_{ijk}^{uds} \left(\frac{\mu_u}{T}\right)^i \left(\frac{\mu_u}{T}\right)^i \left(\frac{\mu_d}{T}\right)^j$$

$$\chi_{ijk}^{BQS} = \frac{\partial^{i+j+k} p/T^4}{\partial(\mu_B/T)^i \partial(\mu_Q/T)^j \partial(\mu_S/T)^k}$$

Meaning of the first two expansion coefficients for some charge X :

$$2c_2^X = \frac{1}{VT^3} \langle N_X^2 \rangle$$
$$24c_4^X = \frac{1}{VT^3} (\langle N_X^4 \rangle - 3\langle N_X^2 \rangle^2)$$

This is variance and kurtosis.

Intensively discussed in experimental searches for the critical endpoint.

8. Deep inside the phase diagram : Properties of dense matter

Results of two collaboration for the Equation of State (EoS)

1) MILC and hotQCD collaborations,

light and strange quarks at almost physical quark masses μ_l and μ_s

Temporal extent $N_t = 4$ and 6 (distance from continuum limit):
differences are visible

Calculations up to $\mathcal{O}(\mu^6)$ (up to c_6)

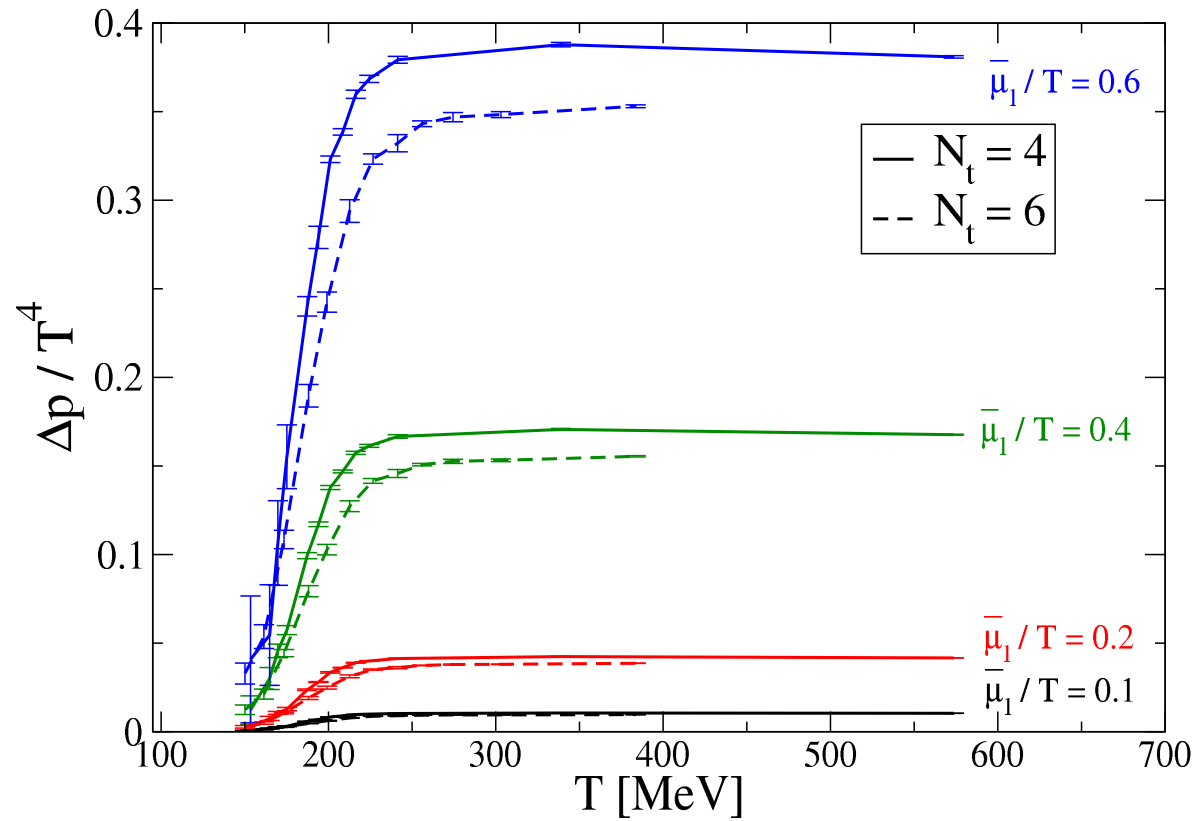
Comparison with HRG (Hadron Resonance Gas, taking the empirical hadron masses [to several GeV] with their baryonic charge into account)

2) BMW collaboration, light and strange quarks

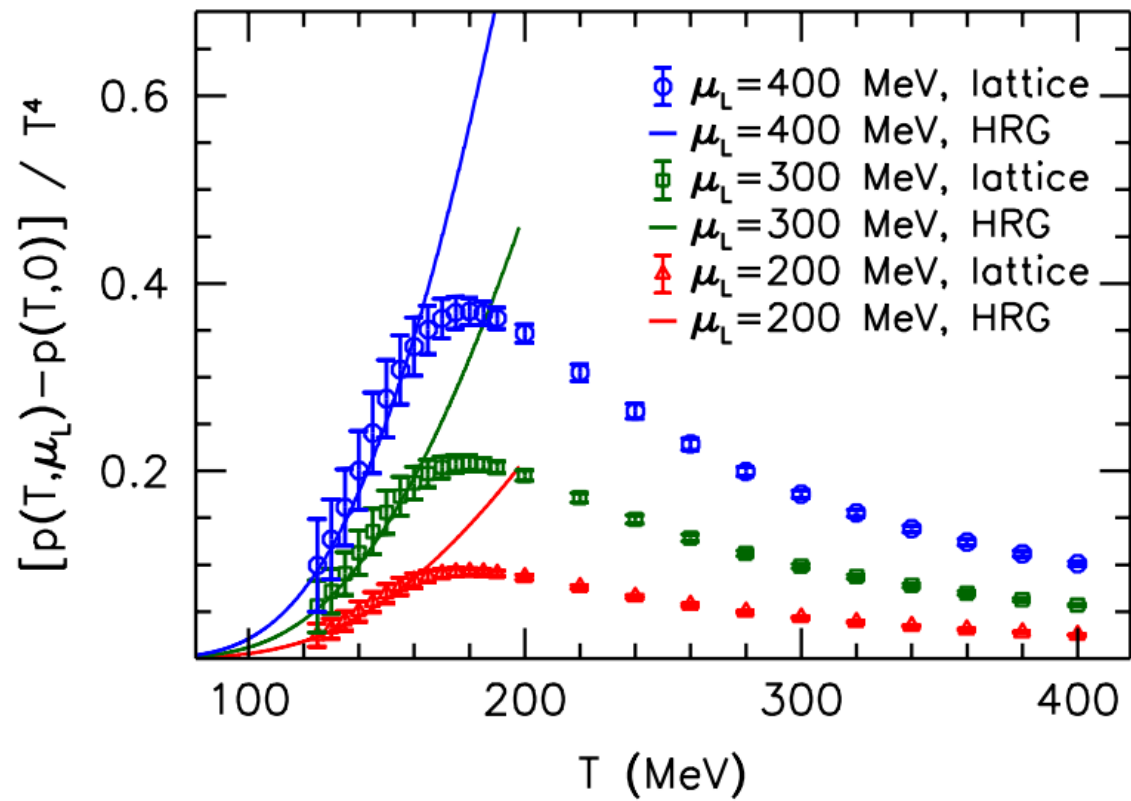
Calculations up to $\mathcal{O}(\mu^2)$ (up to c_2)

Data for $N_t = 6, 8, 10, 12$, quantities can be extrapolated to continuum limit

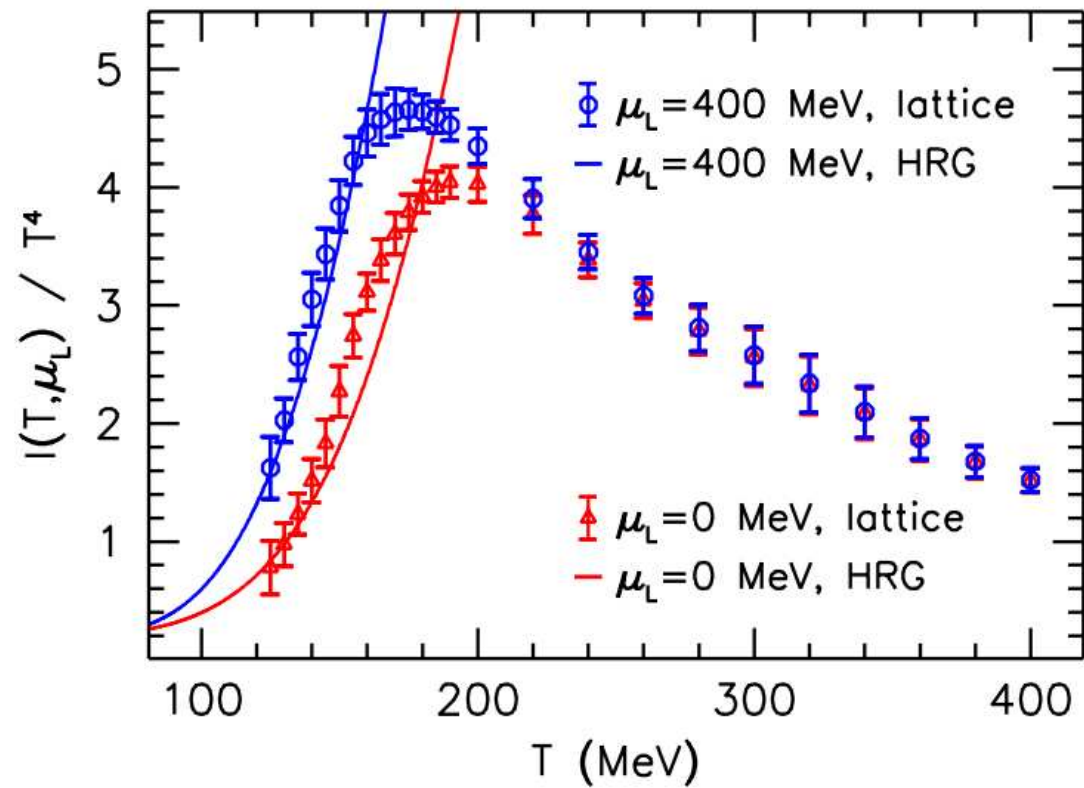
Change in the pressure due to $\mu \neq 0$ (MILC+hotQCD)



Difference between the pressure at $\mu > 0$ and $\mu = 0$ (BMW)



The trace anomaly for non-zero μ_L (BMW, compared with HRG)



What else might be interesting ?

For the hadronization process on top of the freeze-out curve (inside the “hadronic phase”) the following observables will be of large interest:

- screening lengths
- quark condensate $\langle \bar{q}q \rangle$, other condensates ...
- hadron masses
- hadron radii

see: A. Hart, M. Laine, and O. Philipsen,

hep-lat/0010008 hep-ph/0004060

9. Outlook

Much more should be said about properties of the quark-gluon plasma :

- input for hydrodynamics : EoS under construction, velocity of sound
- many applications of Kubo-type formulae, like ...
- viscosity : an ideal fluid ?
- heat conductivity
- electric conductivity
- other transport coefficients
- di-lepton spectral function
- heavy quark diffusion
- jet quenching